WIRELESS VLF/ELF MINE COMMUNICATION

by

ANUP KUMAR GOGOI

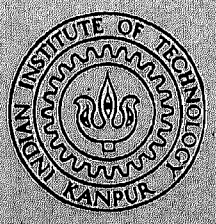

DEPARTMENT OF ELECTRICAL ENGINEERING

INDIAN INSTITUTE OF TECHNOLOGY, KANPUR

JUNE, 1990

WIRELESS VLF/ELF MINE COMMUNICATION

A Thesis Submitted
in Partial Fulfilment of the Requirements
for the Degree of
DOCTOR OF PHILOSOPHY

by

ANUP KUMAR GOGOI

to the

DEPARTMENT OF ELECTRICAL ENGINEERING
INDIAN INSTITUTE OF TECHNOLOGY, KANPUR

JUNE, 1990

EE-1990-D-GOG-WIR

CERTIFICATE

Certified that this thesis "**Wireless VLF/ELF Mine Communication**" submitted by Mr. Anup Kumar Gogoi (Roll No. 8410461) towards partial fulfillment of the requirements for the award of Ph. D. degree has been done under our supervision. It, to our knowledge, has not been submitted elsewhere for a degree.

Dr. A. Mahanta
Asst. Professor

Dr. R. Raghuram
Professor

Department of Electrical Engineering
Indian Institute of Technology
Kanpur, India.

ACKNOWLEDGEMENT

I express my deep sense of gratitude to Dr. R. Raghuram and Dr. A. Mahanta for their invaluable guidance and encourgement throughout the course of my thesis work.

I am thankful to the authorities of the Assam Engineering College for sponsoring me under QIP scheme. I am highly obliged to Assam Electronic Development Corporation for providing me the necessary support in the final stage of my thesis work. I am very thankful to my friend Dr. A.K. Nayak for his untiring help in the final preparation of my thesis.

Finally, I thank Mr. J.P. Gupta for his efficient typing work.

ANUP KUMAR GOGOI

SYNOPSIS

Name of Student : Anup Kumar Gogoi Roll No. 8410461

Degree for which submitted : Ph.D.

Department : Electrical Engineering

Thesis Title: WIRELESS VLF/ELF MINE COMMUNICATION

Name of thesis supervisors : Dr. R. Raghuram & Dr. A. Mahanta

Month and year of thesis submission : June, 1990

Communication between personnel on the ground surface and people working in underground mine is very important for normal operational work as well as for emergency rescue operations. Cables are prone to get damaged in the event of a mine disaster. A wireless communication system which can transmit and receive signals through the earth region over the underground mine area plays a crucial role for rescue operations. Normal radio frequency electromagnetic (EM) waves get attenuated very rapidly in the earth medium, while a very low frequency EM wave can propagate sufficient distance with moderate power requirement. This makes VLF/ELF systems attractive for mine communication.

For transmitting voice or other signals from the surface of the earth to underground mining area, a wire loop antenna may be laid on the earth surface. The loop should be sufficiently large

to cover a wide mine area. In such a case there may be considerable variation of current distribution in the loop.

A receiver operating at VLF/ELF is subjected to atmospheric noise which is very much impulsive in nature. Besides, various machineries used in mining operation introduce strong interfering signals which adversely affect the receiver performance.

The objective of this thesis is (a) to analyse loop antennas on the earth surface, and (b) to study performance of PSK receivers in mine environment. A brief description of the work follows.

Chapter 1 gives a brief account of the work in the areas of wire antennas for through the earth wireless communication, and performance study of receivers in mine environment.

Chapter 2 describes the derivation of vector (magnetic) and scalar potential, due to a horizontal current element radiating over the lossy earth. Fourier transform technique has been used for obtaining integral representation for the magnetic vector potential. The magnetic vector potential has both horizontal and vertical components. By applying Larentz gauge to the vector potential, the scalar potential for a charge doublet is obtained from which the scalar potential for a point charge associated with the current element is derived. Both the vector and the scalar potentials are represented as Sommerfeld type integrals. The horizontal component of vector potential for the special case of the source and the observation points being located on the

air/earth interface has been obtained in a closed form. This component of the vector potential and the scalar potential due to a point charge are the necessary potentials for analysing wire antennas on the earth surface.

Chapter 3 describes the formulation of the antenna problem. A mixed potential integral equation formulation has been employed. The scalar potential does not lend to a closed form representation we have used a quasi static approach to obtain a closed form expression for the scalar potential. The method of moments has been used for obtaining current distribution in the loop antenna. From the current distribution in the surface loop, the field inside the earth has been computed.

Chapter 4 describes the derivation of a closed form expression for the self impedance of a circular loop antenna on the earth surface by considering an uniform current distribution for the whole loop. Neumann's formula which is usually used for inductance computation has been suitably modified for the computation of the self impedance.

In chapter 5 a method has been presented for studying performance of PSK receivers in atmospheric noise which contains an impulse-like component superimposed on a homogeneous background. This noise has been modelled as a two component random process. One component is Gaussian in nature which represents the background noise. The other component is assumed to be a stationary Poisson arrival process of pure impulses.

A conventional PSK receiver can not perform satisfactorily in presence of strong interfering signals which may be generated from different machineries. The effectiveness of spread spectrum receiver for such situation has been studied by considering an interfering tone at the carrier frequency in addition to atmospheric noise.

CHAPTER 1

INTRODUCTION

1.1 THROUGH THE EARTH WIRELESS COMMUNICATION

Communication to and from miners located deep underground is necessary to achieve co-ordinated work as well as for emergency rescue operations. The use of electromagnetic waves for underground mine communication, remained almost unexplored till late 1960s. The main problem is the earths finite conductivity due to which high frequency radio waves cannot propagate through the earth beyond a few metres. Using very low frequencies extentive tests were carried out in the seventies at Eagle and Imperial Coal Mines in USA. These showed successful voice communication from the surface to the mine, and coded interrupted continuous wave transmission from mine to surface [1,2].

A downlink (surface to subsurface) transmitter for voice communication needs a considerable amount of power, to achieve a sufficiently high signal to noise ratio. Since the power requirement for surface equipment can be obtained from the mains supply, this is not a very serious handicap. On the other hand an uplink (subsurface to surface) transmitter should be light, and the power requirement has to be met from the miner's Cap-lamp battery. In the event of a disaster, the transmitter should be able to continue transmitting signals for sufficiently long time,

which can even be two to three days long. To conserve power, interrupted continuous wave transmission is usually used. For example, every second the transmitter may transmit a pulse for a duration of 100 millisecond and remain off for the rest of the period. In addition to such "beeps" a set of low bandwidth coded messages can also be incorporated in the uplink transmitter. A miner receives voice messages from the surface personnel and he responds via these coded messages.

1.2. WIRE ANTENNAS FOR MINE COMMUNICATION

Both linear and loop wire antennas have been used for voice and coded continuous wave transmissions. Linear antenna has been experimentally shown to be effective for both downlink [3,4] and uplink [5] transmission. The main disadvantage of a linear antenna is that it requires some type of grounding at the wire ends to provide a continous path for the current. Farstad [5] has demonstrated the use of roof bolts for grounding of uplink linear antennas.

Wire loops are easy to implement and can be used both as receiving and transmitting antennas. For uplink communication, Wait and Spies [6] have suggested the use of a small wire loop that can be excited by a portable transmitter. The loop may be implemented by laying a wire around a pillar or on the mine floor. They obtain the magnetic fields on the surface of the earth due to a small horizontal loop inside the earth by representing the loop

as a vertical magnetic dipole. When the loop is not very small the analysis cannot be carried out by treating it as a vertical dipole. Wait and Hill [7] have computed field due to a horizontal filamentary current loop in stratified earth, by allowing the loop to be of any size, but carrying a constant current. However, it is not permissible to assume a constant current in a loop antenna when the loop diameter is large. For downlink transmission a loop may be laid on the earth surface and it should be sufficiently large to cover a wide area inside the mine. In such a loop there may be a considerable variation of current distribution.

In addition to the computation of field, it is also important to know the input impedance for the wire loops. Wait [8] has computed the self impedance of a rectangular loop on the earth surface by considering an uniform current distribution for the whole loop. Circular wire loop antennas embedded in a dissipative medium have been analysed by King [9]. Comparison of the values for input impedance of a small loop obtained assuming constant current, and that given by actual analysis, shows that the resistive parts differ by an order of magnitude, while the reactive parts agree closely. A similar situation is expected when the loop is located on a dissipative half space.

1.3 ELECTROMAGNETIC NOISE IN MINE ENVIRONMENT

To have a communication link between surface and subsurface we have to use ELF or VLF band of frequencies. The performance of a communication system at these frequency bands is affected by

atmospheric noise which is non-Gaussian in nature. A wide band observation of ELF/VLF atmospheric noise reveals the presence of a non overlapping impulse like component superimposed over a homogeneous background noise [10,12]. The impulsive component is caused by local thunderstorm activities while the background component is due to the numerous unresolved pulses from distant world-wide lightning flashes. In addition to the atmospheric noise, machineries used for normal mining operations create intense electromagnetic interference which is usually dominant at the harmonic frequencies of the mains supply. The interference is usually much stronger than the desired signal.

Two approaches are usually taken to develop an atmospheric noise model depending upon the bandwidth of the receiver. At VLF the ratio of bandwidth to centre frequency is usually small and therefore the received noise may be considered as a narrow band process. At ELF this ratio is not small, and so the noise should be treated as a wideband process. Omura and Shaft [11] considered VLF atmospheric noise as a narrowband process with a log-normal envelope. Receiver performance with this noise model was obtained by both intutive and rigorous methods. The rigorous method is very difficult to implement. Field and Lewinstein [12] modelled the atmospheric noise as a two component random process. For ELF a wide band approach, and for VLF a narrow band approach were taken. The model can be used for receivers with envelope detection. However, the methodology for evaluation of receiver performance with coherent detection as in PSK has not been discussed by the authors.

1.4 PRESENT INVESTIGATION

(a) Loop antenna on the earth surface

We consider a loop antenna on the earth surface for downlink transmission. Fig. 1.1 depicts a downlink communication system. The earth is considered to be a homogeneous lossy half space. A mixed potential integral equation formulation has been employed for the antenna problem. The method of moments has been used for obtaining current distribution in the antenna. The potentials are obtained from a horizontal current element radiating over a dissipative earth, and they appear as Sommerfeld type integrals. These infinite integrals are highly oscillatory and are difficult to evaluate numerically [13,14]. When the current element is located at the air/earth interface, the Sommerfeld type integral which represent the horizontal component of the magnetic vector potential can be evaluated in a closed form. In a mixed potential formulation only the horizontal component of magnetic vector potential is necessary. The scalar potential is also obtained in a closed form, following a quasi-static approach. These potentials have been used to obtain current distribution in the loop antenna. Magnetic field components inside the earth have been computed for the current distribution in the surface loop. We also derive a closed form expression for self impedance of a small circular loop antenna on the earth surface by considering an uniform current distribution for the whole loop. A comparison has been made for the input impedance values obtained by the method of moments and those given by this expression.

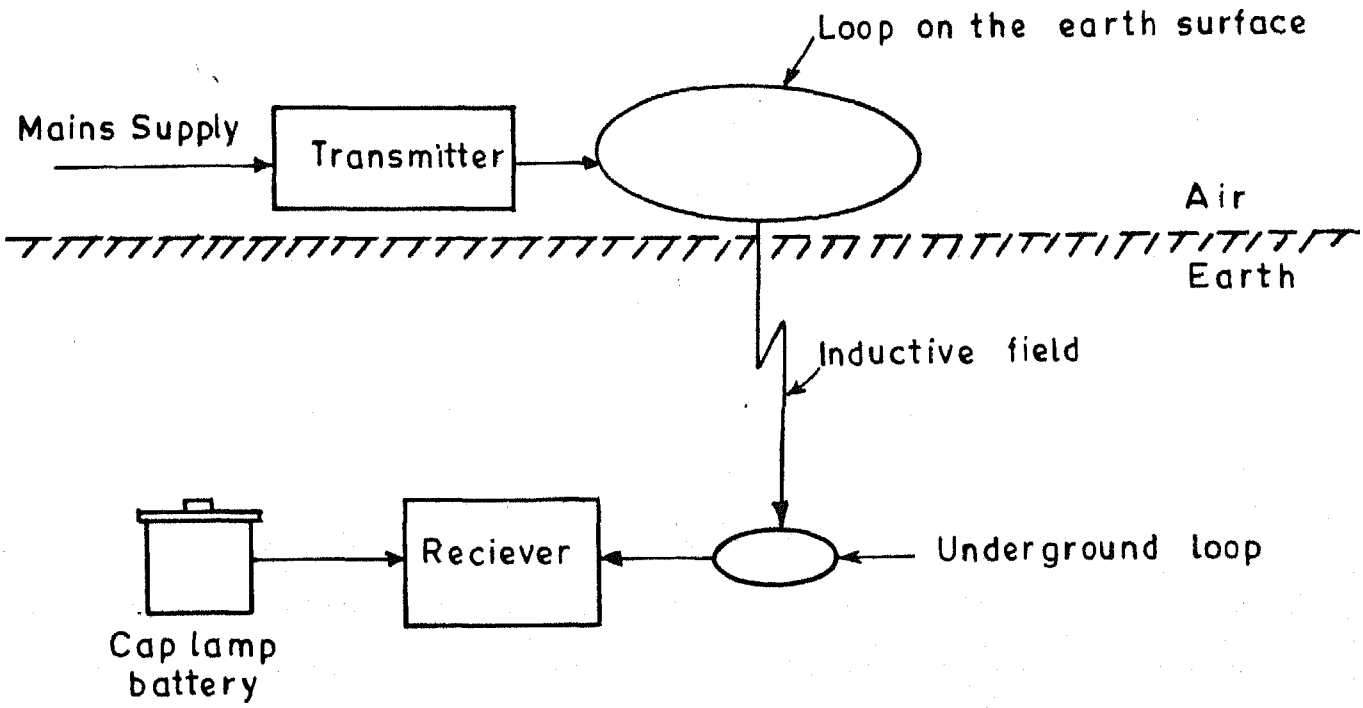

Fig. 1.1 A down link communication system .

(b) A model for atmospheric noise

We consider atmospheric noise as a two component random process and follow the wide band approach. One component is the background noise due to distant and numerous lightning flashes. This component can be described as a zero-mean Gaussian process [10,12]. The other component is due to the local thunderstorm activities which gives rise to non-overlapping large spiky pulses. The arrival of these pulses is assumed to be a stationary Poisson process of pure impulses.

This noise model is used to evaluate the performance of a coherent PSK receiver. A conventional PSK receiver can not perform satisfactorily in the presence of strong interfering signals, for example the harmonic interferences in the mine environment. To effectively suppress the interfering affect, spread spectrum communication technique can be employed [15,16,17]. The performance of a direct sequence spread spectrum receiver in the presence of a tone interference at the carrier frequency besides the atmospheric noise,has also been studied in this investigation.

CHAPTER 2

HORIZONTAL CURRENT ELEMENT OVER DISSIPATIVE EARTH

2.1 INTRODUCTION

This chapter describes the derivation of vector (magnetic) and scalar potential for a time harmonic electric dipole source located over a dissipative half space. Fourier transform technique [18,19,20] is employed for obtaining an integral representation for the magnetic vector potential. From the magnetic vector potential, the scalar potential of a point charge associated with the horizontal dipole is obtained. These potentials are used in Chapters 3 and 4 for the analysis of a loop antenna laid on the surface of the earth.

The effect of finitely conducting earth on the electromagnetic field excited by a time harmonic dipole was first analysed by Sommerfeld [21]. Banos [22] follows an unified approach irrespective of the dipole being electric or magnetic, vertical or horizontal, located in the air region or embeded in the conducting medium. Special features such as nonisotropic and stratified medium have been discussed in the literature [23, 24]. Hertz vector potential has traditionally been used to express the fields [22,23,24]. We express the electric field in terms of the magnetic vector potential and the scalar potential due to a point charge associated with the current element. By using the vector and the scalar potentials, the electric field due to the current element can be expressed in a two component from, each component

being identified separately with the current and the charge. In Chapter 3 we analyse a loop antenna on the earth surface by using a mixed-potential (vector and scalar) integral equation formulation. In this integral equation only horizontal component of the vector potential is necessary, although the vector potential has both horizontal and the vertical components. It will be shown in the present chapter, that the horizontal component can be expressed in a closed form. In Chapter 3 the scalar potential is expressed in a closed form by using a quasi-static approach. The quasi-static approximation is defered to Chapter 3, since it depends on loop dimension. In this chapter we consider only an isolated current element.

2.2 HELMHOLTZ EQUATIONS

A time harmonic horizontal current element over a dissipative half space is shown in Fig. 2.1. The dipole is oriented in the direction of positive x axis and is located at a height z_o. The source is restricted to be in the air region only, and in the limiting case, z_o is allowed to be zero when the dipole is located at the interface. For a horizontal electric dipole, the boundary conditions cannot be satisfied with only the x component of magnetic vector potential unless the dipole is in unbounded space or above a perfectly conducting surface. It is necessary to include a z component of the vector potential to satisfy the boundary conditions. For a x directed current element of dipole moment $\rho(\rho=I\overline{dl})$, with a delta function distribution one can write

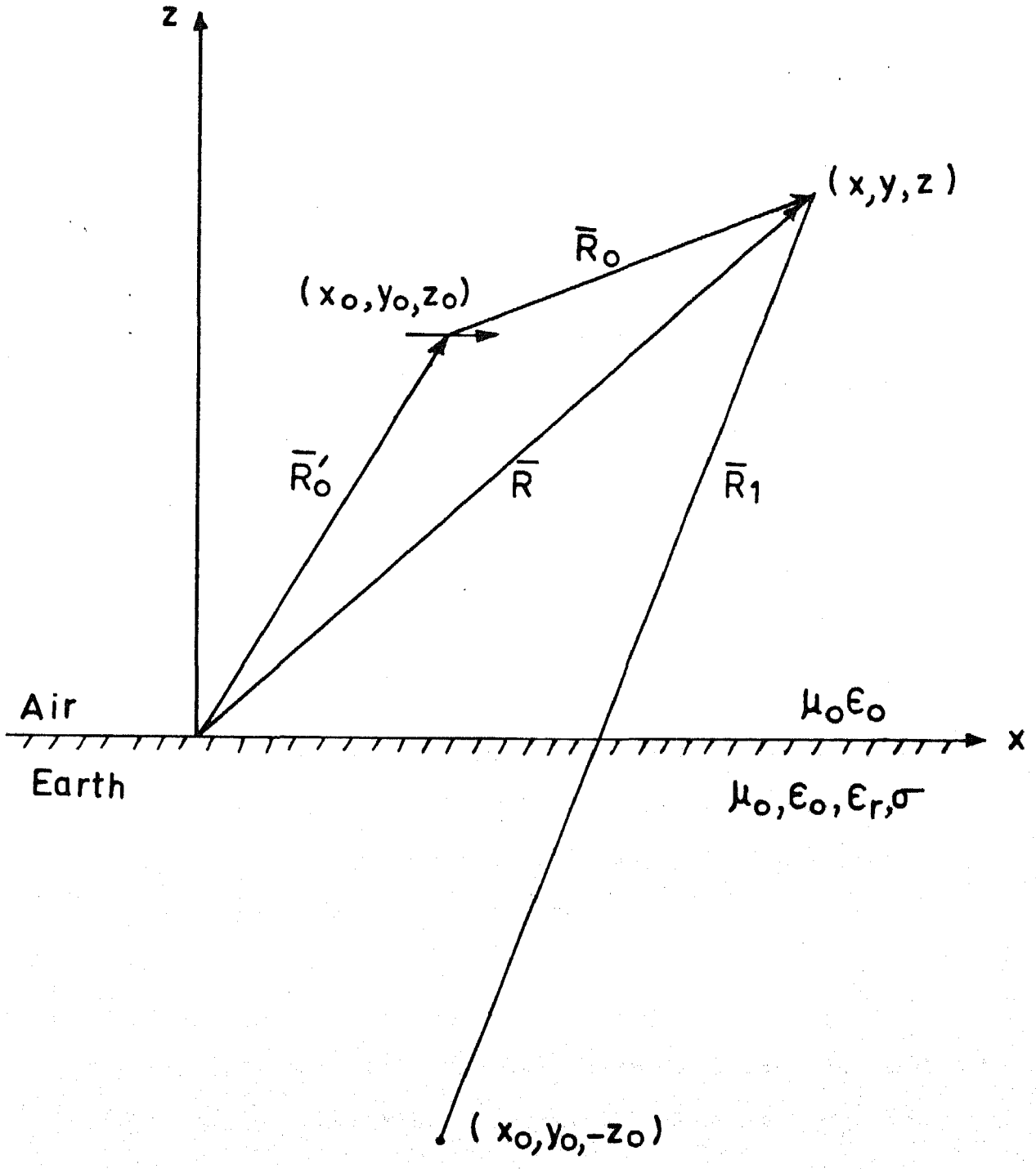

Fig. 2.1 A current element over lossy earth.

$$
\begin{aligned}
(\nabla^2+k_o^2)\ A_{xo}(\bar{R}) &= -\rho\mu_o\delta\ (\bar{R}-\bar{R}_o'), && z \geq 0 \\
(\nabla^2+k_o^2)\ A_{zo}(\bar{R}) &= 0\ , && z \geq 0 \\
(\nabla^2+k_1^1)\ A_{x1}(\bar{R}) &= 0\ , && z \leq 0 \\
(\nabla^2+k_1^2)\ A_{z1}(\bar{R}) &= 0\ . && z \leq 0
\end{aligned}
\qquad (2.1)
$$

Time dependence of $e^{j\omega t}$ is assumed. The position vectors $\bar{R}$ and $\bar{R}_o'$ represent the field point co-ordinate (x,y,z) and source point co-ordinate (x_o,y_o,z_o) respectively. The propagation constants k_o and k_1 are given by

$$
\begin{aligned}
k_o^2 &= \omega^2\mu_o\varepsilon_o \\
k_1^2 &= \omega^2\mu_o\varepsilon_1
\end{aligned}
\qquad (2.2)
$$

where permeabilities (μ_o and μ_1) of the two regions have been assumed to be same, and ε_i $(i = 0,1)$, and ω denote the permitivities and angular frequency respectively. The permitivity ε_1 of the lossy half space can be written as

$$\varepsilon_1 = \varepsilon_o\varepsilon' \qquad (2.3)$$

where ε' is the relative complex effective dielectric constant and can be written in terms of relative dielectric constant ε_r and conductivity σ as

$$\varepsilon' = \varepsilon_r - j\,\frac{\sigma}{\omega\varepsilon_o}\ . \qquad (2.4)$$

The field components in terms of the vector potentials are given by the following relations.

$$H_x = \frac{1}{\mu_o} \frac{\partial}{\partial y} A_z \qquad (2.5a)$$

$$H_y = \frac{1}{\mu_o} \left(\frac{\partial}{\partial z} A_x - \frac{\partial}{\partial x} A_z\right) \qquad (2.5b)$$

$$H_z = - \frac{1}{\mu_o} \frac{\partial}{\partial y} A_x \qquad (2.5c)$$

$$E_x = - j\omega A_x + \frac{1}{j\omega\mu_o\varepsilon} \frac{\partial}{\partial x} \nabla.\bar{A} \qquad (2.5d)$$

$$E_y = \frac{1}{j\omega\mu_o\varepsilon} \frac{\partial}{\partial y} \nabla.\bar{A} \qquad (2.5e)$$

$$E_z = - j\omega A_z + \frac{1}{j\omega\mu_o\varepsilon} \frac{\partial}{\partial z} \nabla.\bar{A} \qquad (2.5f)$$

where for air $\varepsilon = \varepsilon_o$, and for the lower half space $\varepsilon = \varepsilon_1$.

The following Fourier transform pair is defined.

$$\tilde{f}(\alpha_1,\alpha_2,z) = \frac{1}{2\pi} \int_{-\infty}^{\infty}\int_{-\infty}^{\infty} f(x,y,z)\, e^{-j(\alpha_1 x+\alpha_2 y)}\, dxdy \qquad (2.6a)$$

$$f(x,y,z) = \frac{1}{2\pi} \int_{-\infty}^{\infty}\int_{-\infty}^{\infty} \tilde{f}(\alpha_1,\alpha_2,z)\, e^{j(\alpha_1 x+\alpha_2 y)}\, d\alpha_1 d\alpha_2 \qquad (2.6b)$$

where f and $\tilde{f}$ represent any component of the vector potential in the space and the transform domain respectively. Application of Fourier transform to the set of Helmholtz equations given by (2.1) leads to a new set of Helmholtz equations, but having only one independent variable, namely the z co-ordinate. They are as follows.

$$\left[\frac{d^2}{dz^2}+\gamma_o^2\right]\tilde{A}_{xo}(\alpha_1,\alpha_2,z) = \frac{-\rho\mu_o}{2\pi}\, e^{-j(\alpha_1 x_o+\alpha_2 y_o)}\,\delta(z-z_o), \quad z \geq 0 \tag{2.7a}$$

$$\left[\frac{d^2}{dz^2}+\gamma_o^2\right]\tilde{A}_{zo}(\alpha_1,\alpha_2,z) = 0\ , \quad z \geq 0 \tag{2.7b}$$

$$\left[\frac{d^2}{dz^2}+\gamma_1^2\right]\tilde{A}_{x1}(\alpha_1,\alpha_2,z) = 0\ , \quad z \leq 0 \tag{2.7c}$$

$$\left[\frac{d^2}{dz^2}+\gamma_1^2\right]\tilde{A}_{z1}(\alpha_1,\alpha_2,z) = 0\ , \quad z \leq 0 \tag{2.7d}$$

where $\gamma_o = \sqrt{k_o^2 - \alpha_1^2 - \alpha_2^2}$

$\gamma_1 = \sqrt{k_1^2 - \alpha_1^2 - \alpha_2^2}$ (2.7e)

with $\mathrm{Re}(\gamma_i) \geq 0$ and $\mathrm{Im}(\gamma_i) \leq 0$, $(i = 0,1)$.

The solutions for magnetic vector potentials in transform domain can be written as

$$\tilde{A}_{xo}(\alpha_1,\alpha_2,z) = A\, e^{-j\gamma_o z}\ , \quad z \geq z_o \tag{2.8a}$$

$$\tilde{A}_{xo}(\alpha_1,\alpha_2,z) = B\, e^{j\gamma_o z} + C\, e^{-j\gamma_o z}, \quad 0 \leq z \leq z_o \tag{2.8b}$$

$$\tilde{A}_{zo}(\alpha_1,\alpha_2,z) = D\, e^{-j\gamma_o z} \quad , z \geq 0 \tag{2.8c}$$

$$\tilde{A}_{x1}(\alpha_1,\alpha_2,z) = E\, e^{j\gamma_1 z} \quad , z \leq 0 \tag{2.8d}$$

$$\tilde{A}_{z1}(\alpha_1,\alpha_2,z) = F\, e^{j\gamma_1 z} \quad , z \leq 0 \ . \tag{2.8e}$$

2.3 BOUNDARY CONDITIONS

The boundary conditions at the interface (z=0) in the space as well as in the transform domains are as follows.

At z = 0 :

(a) E_y is continuous, hence from (2.5e) one gets

$$\frac{\nabla.\bar{A}_o}{\varepsilon_o} = \frac{\nabla.\bar{A}_1}{\varepsilon_1} \tag{2.9a}$$

$$\text{or} \quad \varepsilon_1\left(\frac{\partial}{\partial x} A_{xo} + \frac{\partial}{\partial z} A_{zo}\right) = \varepsilon_o\left(\frac{\partial}{\partial x} A_{x1} + \frac{\partial}{\partial z} A_{z1}\right) \tag{2.9b}$$

which can be written in transform domain as

$$\frac{d}{dz}\left(\varepsilon_1\tilde{A}_{zo} - \varepsilon_o\tilde{A}z_1\right) = j\alpha_1(\varepsilon_o\tilde{A}_{x1} - \varepsilon_1\tilde{A}_{xo}). \tag{2.9c}$$

(b) E_x is continuous, hence from (2.9a) and (2.5d) one can write

$$A_{xo} = A_{x1} \tag{2.9d}$$

$$\text{or} \quad \tilde{A}_{xo} = \tilde{A}_{x1} \ . \tag{2.9e}$$

(c) Continuity of H_x and (2.5a) gives

$$A_{zo} = A_{z1} \tag{2.9f}$$

or $$\tilde{A}_{zo} = \tilde{A}_{z1} \ . \tag{2.9g}$$

(d) From continuity of H_y and (2.5b) one gets

$$\frac{\partial}{\partial z} A_{xo} - \frac{\partial}{\partial x} A_{zo} = \frac{\partial}{\partial z} A_{x1} - \frac{\partial}{\partial x} A_{z1} \tag{2.9h}$$

From (2.9f) and (2.9h) one can write

$$\frac{\partial}{\partial z} A_{xo} = \frac{\partial}{\partial z} A_{x1} \tag{2.9i}$$

or $$\frac{d}{dz} \tilde{A}_{xo} = \frac{d}{dz} \tilde{A}_{x1} \ . \tag{2.9j}$$

Besides these boundary conditions at the interface, the following conditions are to be satisfied at the source location $z = z_o$.

At $z = z_o$:

(e) E_x is continuous, and hence from (2.9e) one can write

$$\tilde{A}_{xo}\Big|_{\overset{+}{z}_o} = \tilde{A}_{xo}\Big|_{\overset{-}{z}_o} \tag{2.9k}$$

(f) Integrating left and right hand sides of (2.7a) from $\bar{z}_o$ to $\overset{+}{z}_o$ one gets

$$\frac{d}{dz}\tilde{A}_{xo}\Big|_{\overset{+}{z}_o} - \frac{d}{dz}\tilde{A}_{xo}\Big|_{\bar{z}_o} = \frac{-\rho\mu_o}{2\pi} e^{-j(\alpha_1 x_o+\alpha_2 y_o)} \quad . \qquad (2.91)$$

2.4 IMPOSITION OF BOUNDARY CONDITIONS

By imposing the boundary conditions, a set of equations for the unknowns A, B, C, D, E and F can be obtained as follows.

At z = 0 :

From (2.9e), (2.8b) and (2.8d)

$$B + C = E \quad . \qquad (2.10a)$$

From (2.9g), (2.8c) and (2.8e)

$$D = F \quad . \qquad (2.10b)$$

From (2.9c), (2.8b), (2.8c), (2.8d) and (2.8e) one can write

$$-j\gamma_o\varepsilon_1 D - j\gamma_1\varepsilon_o F = j\alpha_1\left\{\varepsilon_o E - \varepsilon_1(B+C)\right\} \quad . \qquad (2.10c)$$

From (2.10a), (2.10b) and (2.10c) one obtains

$$D = -\frac{\alpha_1(\varepsilon_0-\varepsilon_1)E}{\varepsilon_1\gamma_o + \varepsilon_o\gamma_1} \quad . \qquad (2.10d)$$

From (2.9j), (2.8b) and (2.8d) one gets

$$E = \frac{\gamma_o}{\gamma_1}(B-C) \quad . \qquad (2.10e)$$

At $z = z_o$:

From (2.9k), (2.8a) and (2.8b)

$$Ae^{-j\gamma_o z_o} = Be^{j\gamma_o z_o} + Ce^{-j\gamma_o z_o} \quad . \tag{2.10f}$$

From (2.9L), (2.8a) and (2.8b) one can write

$$Ae^{-j\gamma_o z_o} + Be^{j\gamma_o z_o} - Ce^{j\gamma_o z_o} = \frac{\rho\mu_o}{j2\pi\gamma_o} e^{-j(\alpha_1 x_o + \alpha_2 y_o)} \quad . \tag{2.10g}$$

From the equations (2.10a), (2.10b), (2.10d), (2.10e), (2.10f) and (2.10g), A, B, C, D, E and F can be obtained. They are given as follows.

$$A = \frac{\rho\mu_o}{j4\pi\gamma_o} M \left(e^{j\gamma_o z_o} + R\, e^{-j\gamma_o z_o}\right)$$

$$= \frac{\rho\mu_o}{j4\pi} M \left[\frac{e^{j\gamma_o z_o}}{\gamma_o} - \frac{e^{-j\gamma_o z_o}}{\gamma_o} + \frac{2}{\gamma_o+\gamma_1} e^{-j\gamma_o z_o}\right] \tag{2.11a}$$

$$B = \frac{\rho\mu_o}{j4\pi\gamma_o} Me^{-j\gamma_o z_o} \tag{2.11b}$$

$$C = \frac{\rho\mu_o}{j4\pi\gamma_o} RMe^{-j\gamma_o z_o} \tag{2.11c}$$

$$D = \frac{2\rho\mu_o\alpha_1}{j4\pi k_o^2} \frac{\gamma_1-\gamma_o}{\varepsilon'\gamma_o+\gamma_1} M\, e^{-j\gamma_o z_o} \tag{2.11d}$$

$$E = \frac{\rho\mu_o}{j2\pi} \frac{1}{\gamma_o+\gamma_1} M\, e^{-j\gamma_o z_o} \tag{2.11e}$$

$$F = D \tag{2.11f}$$

where $$R = \frac{\gamma_o - \gamma_1}{\gamma_o + \gamma_1} \tag{2.11g}$$

and $$M = e^{-j(\alpha_1 x_o + \alpha_2 y_o)} \quad . \tag{2.11h}$$

2.5 MAGNETIC VECTOR POTENTIALS IN SPACE DOMAIN

Taking Fourier inverse transform of the set of equations (2.8a) to (2.8d), the vector potentials in space domain are obtained. They can be written as

$$A_{xo}(x,y,z) = \frac{1}{2\pi} \iint_{-\infty}^{\infty} N\,(A^i_{xo}+A^r_{xo}+A^c_{xo})\,e^{-j\gamma_o z}\, d\alpha_1 d\alpha_2, \quad z \geq 0 \tag{2.12a}$$

$$A_{x1}(x,y,z) = \frac{1}{2\pi} \iint_{-\infty}^{\infty} N\,E\,e^{j\gamma_1 z}\, d\alpha_1 d\alpha_2, \quad z \leq 0 \tag{2.12b}$$

$$A_{zo}(x,y,z) = \frac{1}{2\pi} \iint_{-\infty}^{\infty} N\,D\,e^{-j\gamma_o z}\, d\alpha_1 d\alpha_2, \quad z \geq 0 \tag{2.12c}$$

$$A_{z1}(x,y,z) = \frac{1}{2\pi} \iint_{-\infty}^{\infty} N\,F\,e^{j\gamma_1 z}\, d\alpha_1 d\alpha_2. \quad z \leq 0 \tag{2.12d}$$

In (2.12a) A_{xo} has been written in the form

$$A_{xo} = A^i_{xo} + A^r_{xo} + A^c_{xo} \tag{2.13a}$$

where

$$A^{i}_{xo} = \frac{\rho\mu_o}{j8\pi^2} \iint_{-\infty}^{\infty} \frac{N}{\gamma_o} e^{-j\gamma_o|(z-z_o)|} d\alpha_1 d\alpha_2 , \qquad (2.13b)$$

$$A^{r}_{xo} = \frac{-\rho\mu_o}{j8\pi^2} \iint_{-\infty}^{\infty} \frac{N}{\gamma_o} e^{-j\gamma_o(z+z_o)} d\alpha_1 d\alpha_2 , \qquad (2.13c)$$

$$A^{c}_{xo} = \frac{\rho\mu_o}{j4\pi^2} \iint_{-\infty}^{\infty} \frac{N}{\gamma_o+\gamma_1} e^{-j\gamma_o(z+z_o)} d\alpha_1 d\alpha_2 , \qquad (2.13d)$$

with

$$N = e^{j(\alpha_1(x-x_o) + \alpha_2(y-y_o))} . \qquad (2.13e)$$

Using the identity [19]

$$\frac{e^{-jk_oR}}{R} = \frac{+j}{2\pi} \iint_{-\infty}^{\infty} \frac{N}{\gamma_o} e^{-j\gamma_o|(z-z_o)|} d\alpha_1 d\alpha_2 , \qquad (2.13f)$$

where $R^2 = (x-x_o)^2 + (y-y_o)^2 + (z-z_o)^2$

one can write A^{i}_{xo} and A^{r}_{xo} in the following form :

$$A^{i}_{xo} = \frac{\rho\mu_o}{4\pi} \frac{e^{-jk_oR}}{R}$$

$$A^{r}_{xo} = \frac{-\rho\mu_o}{4\pi} \frac{e^{-jk_oR_1}}{R_1} \qquad (2.13g)$$

where $R_1^2 = (x-x_o)^2 + (y-y_o)^2 + (z+z_o)^2$.

A^{i}_{xo} and A^{r}_{xo} can be identified as the direct and the image fields when the dipole is located over a perfectly conducting plane. A^{c}_{xo} can be identified as the necessary correction term for an imperfect ground. Combining A^{i}_{xo}, A^{r}_{xo} and A^{c}_{xo} and substituting D, E and F from equations (2.11d), (2.11e) and (2.11f), the magnetic vector potentials i.e., equations (2.12a) to (2.12d) can be rewritten as follows :

$$A_{xo}(x,y,z) = \frac{\rho\mu_o e^{-jk_oR}}{4\pi R} - \frac{\rho\mu_o e^{-jk_oR_1}}{4\pi R_1} + \frac{\rho\mu_o}{j4\pi^2}\iint_{-\infty}^{\infty} \frac{N}{\gamma_o+\gamma_1} e^{-j\gamma_o(z+z_o)}\, d\alpha_1 d\alpha_2,$$

$$z \geq 0 \qquad (2.14a)$$

$$A_{x1}(x,y,z) = \frac{\rho\mu_o}{j4\pi^2}\iint_{-\infty}^{\infty} \frac{N}{\gamma_o+\gamma_1} e^{j(\gamma_1 z-\gamma_o z_o)}\, d\alpha_1 d\alpha_2 \;,\; z \leq 0 \qquad (2.14b)$$

$$A_{zo}(x,y,z) = \frac{\rho\mu_o}{j4\pi^2}\iint_{-\infty}^{\infty} \frac{(\gamma_1-\gamma_o)\, N\, e^{-j\gamma_o(z+z_o)}}{k_1^2\gamma_o + k_o^2\gamma_1}\, \alpha_1\, d\alpha_1 d\alpha_2,$$

$$z \geq 0 \qquad (2.14c)$$

$$A_{z1}(x,y,z) = \frac{\rho\mu_o}{j4\pi^2}\iint_{-\infty}^{\infty} \frac{(\gamma_1-\gamma_o)N\, e^{j(\gamma_1 z-\gamma_o z_o)}}{k_1^2\gamma_o + k_o^2\gamma_1}\, \alpha_1\, d\alpha_1 d\alpha_2,$$

$$z \leq 0 \qquad (2.14d)$$

where N is given by (2.13e).

The integrals in the expressions (2.14) to (2.17) are in the form of surface integrals over the entire (α_1, α_2) plane. These integrals are basically of the same form, excpet (2.16) and

(2.17) which contain the additional term α_1. The term α_1 can be removed by defining the following relations.

$$A_{zo} = \frac{\partial}{\partial x} W_{zo}$$

$$A_{z1} = \frac{\partial}{\partial x} W_{z1} \qquad (2.15)$$

where W_{zo} and W_{z1} do not contain α_1 and are given by

$$W_{zo} = \frac{-\rho\mu_o}{4\pi^2} \iint_{-\infty}^{\infty} \frac{(\gamma_1-\gamma_o)N\ e^{-j\gamma_o(z+z_o)}}{k_1^2\gamma_o + k_o^2\gamma_1}\ d\alpha_1 d\alpha_2 \quad , \qquad (2.16)$$

$$W_{z1} = \frac{-\rho\mu_o}{4\pi^2} \iint_{-\infty}^{\infty} \frac{(\gamma_1-\gamma_o)N\ e^{j(\gamma_1 z-\gamma_o z_o)}}{k_1^2\gamma_o + k_o^2\gamma_1}\ d\alpha_1 d\alpha_2 \ . \qquad (2.17)$$

The surface integrals can be expressed in form of cylindrical co-ordinates both in the space and the transform domains using the relations

$$\begin{aligned} (x-x_o) &= r\cos\phi \\ (y-y_o) &= r\sin\phi \\ r^2 &= (x-x_o)^2 + (y-y_o)^2 \end{aligned} \qquad (2.18a)$$

for the space co-ordinates x and y, and

$$\begin{aligned} \alpha_1 &= \lambda\cos\beta \\ \alpha_2 &= \lambda\sin\beta \\ \lambda^2 &= \alpha_1^2 + \alpha_2^2 \end{aligned} \qquad (2.18b)$$

for the transform variables α_1 and α_2.

From (2.7e) and (2.18b), γ_o and γ_1 can be written as

$$\gamma_o = \sqrt{k_o^2 - \lambda^2}$$

$$\gamma_1 = \sqrt{k_1^2 - \lambda^2} \qquad (2.19)$$

with $Re(\gamma_i) \geq 0$ and $Im(\gamma_i) \leq 0$, $(i = 0,1)$.

The area $d\alpha_1 d\alpha_2$ can be written as $\lambda d\lambda d\beta$ in polar co-ordinates. With these transformations N can be written as

$$N = e^{j(\alpha_1(x-x_o) + \alpha_2(y-y_o))}$$

$$= e^{j(\lambda r\cos\phi \cos\beta + \lambda r\sin\phi \sin\beta)}$$

$$= e^{j\lambda r\cos(\beta-\phi)} . \qquad (2.20)$$

From (2.16) and (2.20) one can write

$$W_{zo}(r,z) = \frac{-\rho\mu_o}{4\pi^2} \int_0^{\infty} \frac{(\gamma_1-\gamma_o)\, e^{-j\gamma_o(z+z_o)}}{k_1^2\gamma_o + k_o^2\gamma_1} \lambda d\lambda \int_0^{2\pi} e^{j\lambda r\cos(\beta-\phi)}\, d\beta .$$

(2.21)

Using the identity for the Bessel function of zero order [19],

$$J_o(\lambda r) = \frac{1}{2\pi} \int_0^{2\pi} e^{j\lambda r\cos(\beta-\phi)}\, d\beta \qquad (2.22)$$

one can write

$$W_{zo}(r,z) = \frac{-\rho\mu_o}{2\pi}\int_0^\infty \frac{(\gamma_1-\gamma_o)\, e^{-j\gamma_o(z+z_o)}}{k_1^2\gamma_o + k_o^2\gamma_1} J_o(\lambda r)\lambda d\lambda \ . \qquad (2.23)$$

A_{zo} can be obtained from (2.23) by taking the x derivative as defined by (2.15). Doing similar exercises one obtains the magnetic vector potentials as follows.

$$A_{xo}(r,z) = \frac{\rho\mu_o e^{-jk_oR}}{4\pi R} - \frac{\rho\mu_o e^{-jk_1R_1}}{4\pi R_1} + \frac{\rho\mu_o}{j2\pi}\int_0^\infty \frac{e^{-j\gamma_o(z+z_o)}}{\gamma_o+\gamma_1} J_o(\lambda r)\lambda d\lambda \ ,$$

$$z \geq 0 \qquad (2.24)$$

$$A_{zo}(r,z) = \frac{\rho\mu_o}{2\pi}\frac{\partial}{\partial x}\int_0^\infty \frac{(\gamma_o-\gamma_1)e^{-j\gamma_o(z+z_o)}}{k_1^2\gamma_o+k_o^2\gamma_1} J_o(\lambda r)\ \lambda d\lambda, \quad z \geq 0$$

$$(2.25)$$

$$A_{x1}(r,z) = \frac{\rho\mu_o}{j2\pi}\int_0^\infty \frac{e^{j(\gamma_1 z-\gamma_o z_o)}}{\gamma_o+\gamma_1} J_o(\lambda r)\ \lambda d\lambda, \qquad z \leq 0 \qquad (2.26)$$

$$A_{z1}(r,z) = \frac{\rho\mu_o}{2\pi}\frac{\partial}{\partial x}\int_0^\infty \frac{(\gamma_o-\gamma_1)\, e^{j(\gamma_1 z-\gamma_o z_o)}}{k_1^2\gamma_o + k_o^2\gamma_1} J_o(\lambda r)\ \lambda d\lambda \ , \quad z \leq 0.$$

$$(2.27)$$

These integrals, which are of the Sommerfeld type, in general, can not be evaluated in a closed form.

2.6 CLOSED FORM EXPRESSION FOR A_{xo} ($z = z_o = 0$)

When the source and the observation points are located at the interface the horizontal component of the vector potential has a closed form expression which can be obtained as follows. From (2.24) and (2.26) when $z = z_o = 0$, one can write

$$A_{xo}(r,o) = A_{x1}(r,o)$$

$$= \frac{\rho\mu_o}{j2\pi} \int_0^\infty \frac{J_o(\lambda r)\lambda d\lambda}{\gamma_o+\gamma_1} \quad . \tag{2.28}$$

Multiplying the numerator and denominator of (2.28) by $(\gamma_1-\gamma_o)$ one can write (noting that $\gamma_i = \sqrt{k_i^2 - \lambda^2}$)

$$A_{xo}(r,o) = \frac{\rho\mu_o}{j2\pi} \int_0^\infty \frac{(\gamma_1-\gamma_o)\ J_o(\lambda r)\lambda d\lambda}{k_1^2 - k_o^2} \tag{2.29}$$

$$= \frac{\rho\mu_o}{2\pi(k_1^2-k_o^2)} \left\{U+V\right\}$$

where $$U = \int_0^\infty j\gamma_o\ J_o(\lambda r)\ \lambda d\lambda \tag{2.30}$$

$$V = -\int_0^\infty j\gamma_1\ J_o(\lambda r)\ \lambda d\lambda \quad . \tag{2.31}$$

The integrals (2.30) and (2.31) are of the similar form and hence only one of them will be treated for closed form derivation. Differentiating (2.30) w.r.t. k_o one obtains

$$\frac{d}{dk_o}\int_0^\infty j\gamma_o\, J_o(\lambda r)\,\lambda d\lambda \;=\; j\int_0^\infty \frac{k_o J_o(\lambda r)\lambda d\lambda}{\gamma_o} \quad . \tag{2.32}$$

The r.h.s of (2.32) has a closed form expression [19] which gives

$$\frac{d}{dk_o}\int_0^\infty j\gamma_o\, J_o(\lambda r)\,\lambda d\lambda \;=\; -\frac{k_o e^{-jk_o r}}{r} \quad . \tag{2.33}$$

Integration of (2.33) w.r.t. k_o gives

$$\int_0^\infty j\gamma_o\, J_o(\lambda r)\,\lambda d\lambda \;=\; -\int \frac{k_o e^{-jk_o r}}{r}\, dk_o$$

$$= -\frac{e^{-jk_o r}}{r^2}\,(jk_o + \frac{1}{r}) \quad . \tag{2.34}$$

Since,

$$\frac{1}{r}\frac{\partial}{\partial r}\,(\frac{e^{-jk_o r}}{r}) \;=\; -\frac{e^{-jk_o r}}{r^2}\,(jk_o + \frac{1}{r}) \tag{2.35}$$

one can write

$$\int_0^\infty j\gamma_o J_o(\lambda r)\,\lambda d\lambda \;=\; \frac{1}{r}\frac{\partial}{\partial r}\,(\frac{e^{-jk_o r}}{r}) \quad . \tag{2.36}$$

Doing similar exercises one gets from (2.31)

$$\int_0^\infty -j\gamma_1 J_o(\lambda r)\,\lambda d\lambda \;=\; -\frac{1}{r}\frac{\partial}{\partial r}\,(\frac{e^{-jk_1 r}}{r}) \quad . \tag{2.37}$$

Hence from (2.36), (2.37), (2.30), (2.31) and (2.29Ø) one can write the final closed form expression for A_{xo} as

$$A_{xo}(r,o) = \frac{\rho\mu_o}{2\pi(k_1^2-k_o^2)} \frac{1}{r} \frac{\partial}{\partial r} \left(\frac{e^{-jk_o r}}{r} - \frac{e^{-jk_1 r}}{r}\right) . \qquad (2.38)$$

2.7 SCALAR POTENTIAL DUE TO A POINT CHARGE

From the magnetic vector potential $\bar{A}_o$, a scalar potential ϕ_o can be obtained by using Lorentz gauge. The potential ϕ_o is the scalar potential associated with the dipole (current element). The scalar potential ϕ_o^+ due to a point charge q associated with the current element can be obtained from ϕ_o by the relation [26]

$$\phi_o = \frac{\partial}{\partial x_o} (\phi_o^+) \qquad (2.39)$$

where the derivative is to be taken at the source point along the direction of the current element. Using Lorentz gauge one can write

$$\phi_o = \frac{j\omega}{k_o^2} \nabla.\bar{A}_o . \qquad (2.40)$$

For the horizontal current element the vector potential $\bar{A}_o$ has x and z components, and hence from (2.39) and (2.40) one can write

$$\frac{\partial}{\partial x_o} \phi_o^+ = \frac{j\omega}{k_o^2} \left\{\frac{\partial}{\partial x} A_{xo} + \frac{\partial}{\partial z} A_{zo}\right\} . \qquad (2.41)$$

By integrating (2.41) w.r.t. source variable x_o one obtains

$$\phi_o^+ = \phi_x^+ + \phi_z^+ \tag{2.42}$$

where $$\phi_x^+ = \frac{j\omega}{k^2} \int (\frac{\partial}{\partial x} A_{xo}) \, d_{xo} \tag{2.43}$$

$$\phi_z^+ = \frac{j\omega}{k_o^2} \int (\frac{\partial}{\partial z} A_{zo}) \, d_{xo} \quad . \tag{2.44}$$

Using (2.43) and (2.13a), ϕ_x^+ can be written as follows :

$$\phi_x^+ = \phi_{x1}^+ + \phi_{x2}^+ + \phi_{x3}^+ \tag{2.45}$$

where $$\phi_{x1}^+ = \frac{j\omega}{k_o^2} \int (\frac{\partial}{\partial x} A_{xo}^i) \, dx_o \quad , \tag{2.46}$$

$$\phi_{x2}^+ = \frac{j\omega}{k_o^2} \int (\frac{\partial}{\partial x} A_{xo}^r) \, dx_o \quad , \tag{2.47}$$

$$\phi_{x3}^+ = \frac{j\omega}{k_o^2} \int (\frac{\partial}{\partial x} A_{xo}^c) \, dx_o \quad . \tag{2.48}$$

Using (2.13b) one can write r.h.s. of (2.46) as

$$\frac{j\omega}{k_o^2} \int (\frac{\partial}{\partial x} A_{xo}^i) \, dx_o =$$

$$\frac{j\omega}{k_o^2} \int \left[\frac{\partial}{\partial x} \left\{ \frac{\rho\mu_o}{j8\pi^2} \iint_{-\infty}^{\infty} \frac{e^{-j\gamma_o|(z-z_o)|}}{\gamma_o} e^{j(\alpha_1(x-x_o)+\alpha_2(y-y_o))} d\alpha_1 d\alpha_2 \right\} \right] dx_o \tag{2.49}$$

The derivative w.r.t. x introduces a term $j\alpha_1$ while the integration w.r.t. x_o introduces the term $-\frac{1}{j\alpha_1}$. This gives

$$\frac{j\omega}{k_o^2}\int\left(\frac{\partial}{\partial x}A^i_{xo}\right)dx_o = -\frac{j\omega}{k_o^2}A^i_{xo} \quad . \tag{2.50}$$

Similarly one gets

$$\frac{j\omega}{k_o^2}\int\left(\frac{\partial}{\partial x}A^r_{xo}\right)dx_o = -\frac{j\omega}{k_o^2}A^r_{xo} \quad , \tag{2.51}$$

$$\frac{j\omega}{k_o^2}\int\left(\frac{\partial}{\partial x}A^c_{xo}\right)dx_o = -\frac{j\omega}{k_o^2}A^c_{xo} \quad . \tag{2.52}$$

Using the set of equations (2.45) to (2.48), and (2.50) to (2.52) one can write

$$\phi^+_x = -\frac{j\omega}{k_o^2}A_{xo} \quad . \tag{2.53}$$

Substituting for A_{xo} from (2.24), one can write (2.53) in the form

$$\phi^+_x = \frac{qdle^{-jk_oR}}{4\pi R\varepsilon_o} - \frac{qdle^{-jk_oR_1}}{4\pi R_1\varepsilon_o} + \frac{qdl}{j2\pi\varepsilon_o}\int_0^\infty \frac{e^{-j\gamma_o(z+z_o)}}{\gamma_o+\gamma_1}J_o(\lambda r)\lambda d\lambda \tag{2.54}$$

where use of the continuity equation $I=j\omega q$ and the relation $\frac{\omega^2\mu_o}{k_o^2} = \frac{1}{\varepsilon_o}$ have been made.

From (2.14c), the derivative $\frac{\partial}{\partial z} A_{zo}$ can be written as

$$\frac{\partial}{\partial z} A_{zo} = \frac{\rho\mu_o}{j4\pi^2} \iint_{-\infty}^{\infty} \frac{-j\gamma_o(\gamma_1-\gamma_o)Ne^{-j\gamma_o(z+z_o)}}{k_1^2\gamma_o+k_o^2\gamma_1} \alpha_1 d\alpha_1 d\alpha_2 \qquad (2.55)$$

where N is given by (2.13e). Integration of (2.55) w.r.t. x_o gives

$$\int(\frac{\partial}{\partial z} A_{zo})dx_o = \frac{\rho\mu_o}{j4\pi^2}\iint_{-\infty}^{\infty} \frac{\gamma_o(\gamma_1-\gamma_o)Ne^{-j\gamma_o(z+z_o)}}{k_1^2\gamma_o+k_o^2\gamma_1} d\alpha_1 d\alpha_2. \qquad (2.56)$$

The double integral in (2.56) can be transformed into cylindrical co-ordinates as described in section (2.5). Multiplying (2.56) by $\frac{j\omega}{k_o^2}$ and comparing with (2.44) one gets

$$\phi_z^+ = \frac{qdl}{j2\pi\varepsilon_o}\int_0^{\infty} \frac{\gamma_o(\gamma_o-\gamma_1)\, e^{-\gamma_o(z+z_o)}}{k_1^2\gamma_o + k_o^2\gamma_1} J_o(\lambda r)\, \lambda d\lambda \,. \qquad (2.57)$$

Substituting for ϕ_x^+ and ϕ_z^+ from equations (2.54) and (2.57), respectively, one gets

$$\phi_o^+ = \frac{qdl\ e^{-jk_oR}}{4\pi R\varepsilon_o} - \frac{qdl\ e^{-jk_oR_1}}{4\pi R_1\varepsilon_o} + \frac{qdl}{j2\pi\varepsilon_o}\int_0^{\infty} \psi_o e^{-j\gamma_o(z+z_o)} J_o(\lambda r)\lambda d\lambda \qquad (2.58)$$

where $$\psi_o = \frac{1}{\gamma_o+\gamma_1} + \frac{\gamma_o(\gamma_o-\gamma_1)}{k_1^2\gamma_o + k_o^2\gamma_1} \,. \qquad (2.59)$$

Using the relation $\gamma_i = \sqrt{k_i^2 - \lambda^2}$, ψ_o can be written as

$$\psi_o = \frac{\gamma_o - \gamma_1}{k_o^2 - k_1^2} + \frac{\gamma_o(\gamma_o - \gamma_1)}{k_1^2\gamma_o + k_o^2\gamma_1}$$

$$= (\gamma_o - \gamma_1)\left\{\frac{k_o^2(\gamma_o + \gamma_1)}{(k_o^2 - k_1^2)(k_1^2\gamma_o + k_o^2\gamma_1)}\right\}$$

$$= \frac{k_o^2}{k_1^2\gamma_o + k_o^2\gamma_1} . \qquad (2.60)$$

Substituting for ψ_o from (2.60) in (2.58) we get

$$\phi_o^+ = \frac{qdl\ e^{-jk_oR}}{4\pi R\varepsilon_o} - \frac{qdl\ e^{-jk_oR_1}}{4\pi R_1\varepsilon_o} + \frac{qdl\omega^2\mu_o}{j2\pi}\int_0^\infty \frac{e^{-j\gamma_o(z+z_o)}}{k_1^2\gamma_o + k_o^2\gamma_1} J_o(\lambda r)\lambda d\lambda .$$

(2.61)

which is an exact expression for the scalar potential ϕ_o^+. In Chapter 3, this expression is used to arrive at a closed form expression for the Green's function for a point charge associated with a loop antenna located on the earth surface by employing a quasistatic approximation.

CHAPTER 3

LOOP ANTENNA ON THE EARTH SURFACE FOR UNDERGROUND MINE COMMUNICATION

3.1 INTRODUCTION

High frequency wireless communication through the earth is not feasible due to strong attenuation of electromagnetic fields while propagating through the conducting earth. By using base-band modulation voice communication can be achieved for downlink, i.e., surface to subsurface communication [2]. A downlink transmitter needs a considerable amount of power, which can be provided by the mains supply. A loop antenna may be laid on the surface of the earth to provide a communication link from surface to underground mine area. The loop should be sufficiently large to cover a wide area inside the mine. In such a loop there may be considerable variation of current distribution along the loop periphery.

To analyse wire antenna over the dissipative earth both rigorous [27] and approximate techniques [28,29,30,31] have been employed. The approximate techniques break down when the distance between the antenna and the earth surface is much smaller than the wavelength at the operating frequency. The rigorous method is based on Sommerfeld-integral formulation, however, the integral is to be evaluated numerically and it is very time consuming. In the present investigation the problem of a loop antenna on the earth surface (Fig. 3.1) has been formulated in terms of Sommerfeld-type integrals. The analysis is carried out by the method of moments. A

A mixed potential integral equation formulation has been employed [27,32]. For the magnetic vector potential we shall use the closed form expression given by (2.38). The scalar potential is also obtained in a closed form following a quasi-static approach. These potentials are used to obtain current distribution in the loop antenna. Magnetic field components inside the earth have been computed due to the current distribution in the surface loop.

3.2 FORMULATION OF THE ANTENNA PROBLEM

To analyse a horizontal wire antenna over an imperfectly conducting ground, first the formulation of the problem is carried out assuming the antenna to be in free space. Necessary modifications are then incorporated in this formulation to allow the presence of the dissipative half space. Fig. 3.2 depicts a horizontal antenna of arbitrary shape situated at a height h from the ground surface.The wire is assumed to be a perfect conductor.

3.2.1. Wire antenna in free space

For an incident electric field $\overline{E}_i$, the scattered field $\overline{E}_s$ from the conductor can be written as

$$\overline{E}_s = -j\omega\overline{A} - \nabla\phi \qquad (3.1)$$

where, the magnetic vector potential $\overline{A}$ and the scalar potential ϕ are due to the current and charge distributions on the surface of the conductor. Since, the wire radius is much smaller than the wavelength, thin wire approximations can be made according to

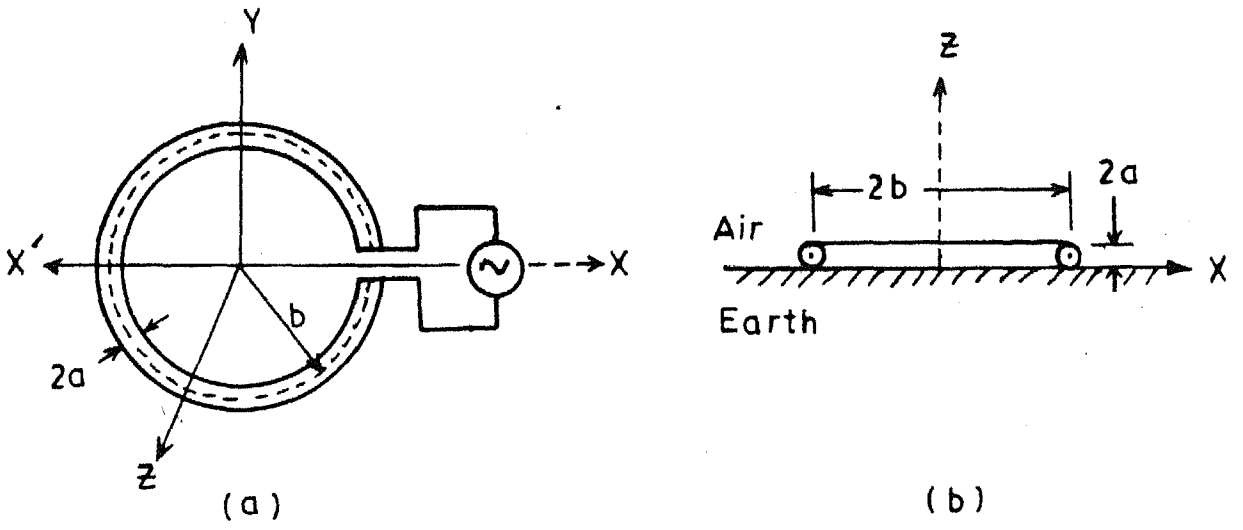

Fig.3.1 Circular wire loop on the surface of the earl
(a) Top view
(b) Sectional view at X'-X

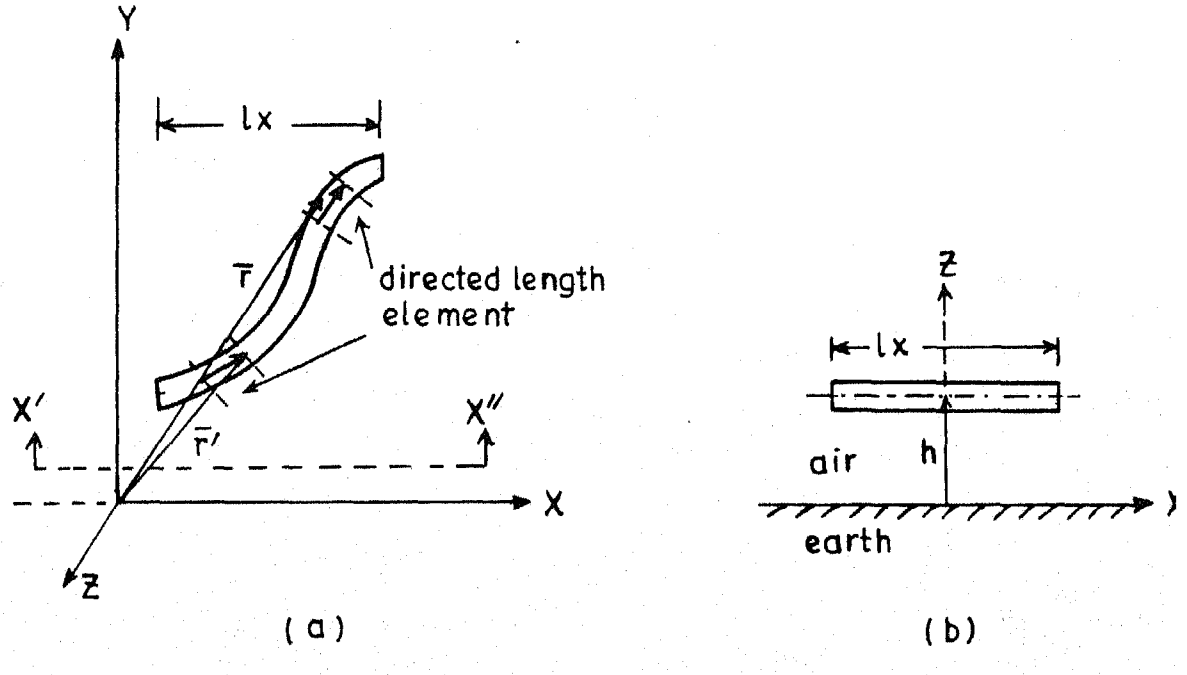

Fig.3.2 A horizontal wire segment above the ear
(a) Plan view on the earth surface.
(b) Side view at x'-x''.

which the current and charge distributions can be assumed to be located along the wire axis, and the boundary conditions can be applied on the surface of the wire.

At the surface of the conductor the sum of incident electric field and scattered field is zero. Hence,

$$E_1^s(\bar{s}) = - E_1^i(\bar{s}) , \quad (\bar{s}) \text{ on wire surface,} \tag{3.2}$$

where subscript 1 means that the component is in the direction of the wire axis. From (3.1) and (3.2) one can write

$$E_1^i(\bar{s}) = j\omega A_1(\bar{s}) + \frac{\partial}{\partial l} (\phi(\bar{s})) \tag{3.3}$$

where

$$A_1(\bar{s}) = \int_{axis} I_1(l') \cos\theta \; G_A^a (\bar{s}/\bar{l}')dl' , \tag{3.4}$$

$$\phi(\bar{s}) = \int_{axis} q(l') \; G_\phi^a(\bar{s}/\bar{l}')dl' . \tag{3.5}$$

In (3.4) and (3.5) the Green's function G_A^a and G_ϕ^a are given by

$$G_A^a (\bar{s}/\bar{l}') = \frac{\mu_o e^{-jk_o R_s}}{4\pi R_s} \tag{3.6}$$

$$G_\phi^a (\bar{s}/\bar{l}') = \frac{e^{-jk_o R_s}}{4\pi R_s \varepsilon_o} \tag{3.7}$$

$$\text{where} \quad R_s = |\bar{s} - \bar{l}'| . \tag{3.8}$$

The current $I_1(l')$ and charge density $q(l')$ are related by the equation of continuity,

$$q(\bar{l}') = \frac{-1}{j\omega} \frac{d}{dl'} [I_1(\bar{l}')] \quad . \tag{3.9}$$

θ is the angle between the directed length elements (axial directions) at the source and the observation points as shown in Fig.3.2. The source point l' lies on the axis, and the field point $\bar{s}$ is on the surface of the conductor.

Equation (3.3) is an integral equation for the potentials $A_1(\bar{s})$ and $\phi(\bar{s})$. This is a mixed potential integral equation formulation in terms of current and charge distributions. In a mixed potential integral equation formulation a derivative of first order is present while in a single potential formulation a second order derivative is necessary. This gives the former numerical advantage over the latter. Since, charge and current are related by (3.9) the equation can be solved for current distribution in the wire antenna. The same solution procedure is applicable whether the antenna is in free space or it is above a lossy ground, the only difference being in the use of appropriate Green's functions. In the next section the Green's functions for the wire antenna in the presence of the dissipative half space are discussed.

3.2.2. Wire antenna over lossy earth

For a x directed horizontal current element over lossy earth, the x component of the magnetic vector potential in the air region is given by (2.24). The scalar potential is given by (2.61). Hence, the Green's functions $G_A(\bar{r}/\bar{r}')$ and $G_\phi(\bar{r}/\bar{r}')$ for the vector and the scalar potentials, respectively, can be written as

$$G_A(\bar{r}/\bar{r}') = \frac{\mu_o e^{-jk_o R}}{4\pi R} - \frac{\mu_o e^{-jk_o R_1}}{4\pi R_1} + \frac{\mu_o}{j2\pi}\int_0^\infty \frac{e^{-j2\gamma_o h}}{\gamma_1+\gamma_o} J_o(\lambda r)\lambda d\lambda \tag{3.10}$$

$$G_\phi(\bar{r}/\bar{r}') = \frac{e^{-jk_o R}}{4\pi R\varepsilon_o} - \frac{e^{-jk_o R_1}}{4\pi R_1\varepsilon_o} + \frac{\omega^2\mu_o}{j2\pi}\int_0^\infty \frac{e^{-j2\gamma_o h}}{k_1^2\gamma_o+k_o^2\gamma_1} J_o(\lambda r)\lambda d\lambda \ . \tag{3.11}$$

In (3.10) and (3.11) R and R_1 are the distances to the field point from the source and the image points respectively, and r is given by

$$r = (x - x_o)^2 + (y - y_o)^2 . \tag{3.12}$$

The points $\bar{r}$ and $\bar{r}'$ are respectively on the surface and on the axis of the wire. Further, it can be identified that $\bar{r}$ and $\bar{r}'$ respectively stand for the points $\bar{s}$ and $\bar{I}'$ in expressions (3.2) to (3.9).

From the Green's functions given by (3.10) and (3.11), in principle any horizontal wire antenna above or on the ground can be analysed. However, numerical evaluation of these integrals is difficult and time consuming as the Bessel functions are highly oscillatory and converge very slowly. An accurate method for evaluating these Sommerfeld-type integrals is necessary as one has to compute these integrals repeatedly, for solving antenna current in frequency domain. For transient analysis the computation is to be repeated for many frequencies which makes it even more time consuming. Efforts to develop new, more efficient and more widely applicable methods for evaluation of these integrals are continuing [13,14,33,34,35].

Green's functions with h = 0

In the present investigation, our interest is about a loop antenna which is laid on the surface of the earth and hence, h the height of the antenna on the ground surface is zero. By putting h = 0 in Eqn. (3.10), the Green's function for magnetic vector potential can be written as

$$G_A(\bar{r}/\bar{r}')\Big|_{h=0} = \frac{\mu_o}{j2\pi}\int_0^\infty \frac{J_o(\lambda r)}{\gamma_1+\gamma_o}\,\lambda d\lambda \ . \qquad (3.13)$$

This integral has been obtained in a closed form in Chapter 2, and is given by (2.38). Writing $g_A(\bar{r}/\bar{r}')$ for Green's function for this special case (h = 0) one can write

$$g_A(\bar{r}/\bar{r}') = \frac{\mu_o}{2\pi r(k_1^2-k_o^2)} \frac{\partial}{\partial r}\left[\frac{e^{-jk_o r}}{r} - \frac{e^{-jk_1 r}}{r}\right] . \qquad (3.14)$$

From (3.11) the Green's function for the scalar potential for h=0 becomes

$$G_\phi(\bar{r}/\bar{r}')\Big|_{h=0} = \frac{\omega^2\mu_o}{j2\pi} \int_0^\infty \frac{J_o(\lambda r)\lambda d\lambda}{k_1^2\gamma_o + k_o^2\gamma_1} . \qquad (3.15)$$

The integral in (3.15) does not have a closed form expression. However, by putting $k_o = 0$, the integral can be evaluated. Doing this amounts to obtaining fields in the air region by Laplace's equation instead of Maxwell's equation. This is permissible if the distance between the source and the observation point is very small in comparison to the free space wavelength, or $k_o r << 1$. This is a quasi-static approach and will be valid for a practical sized loop antenna that may be used for underground mine communcation. In such cases it happens that $|k_1 r|$ is quite large indicating that there may be considerable variation of current distribution in the antenna, but the condition $k_o r << 1$, is still satisfied. Writing $k_\phi(\bar{r}/\bar{r}')$ for the quasi-static ($k_o=0$) counter-part of $G_\phi(\bar{r}/\bar{r}')$ with h = 0 one gets

$$k_{\phi}(\bar{r}/\bar{r}') = \frac{\omega^2\mu_o}{j2\pi}\int_0^{\infty}\frac{J_o(\lambda r)\lambda d\lambda}{-jk_1^2\lambda}$$

$$= \frac{\omega^2\mu_o}{2\pi k_1^2}\int_0^{\infty} J_o(\lambda r)d\lambda \qquad (3.16)$$

$$= \frac{\omega^2\mu_o}{2\pi k_1^2}\left(\frac{1}{r}\right) . \qquad (3.17)$$

3.3 POWER SERIES EXPANSION OF $g_A(\bar{r}/\bar{r}')$

The Green's function $g_A(\bar{r}/\bar{r}')$ given by (3.14) can be expressed in a power series form as follows.

$$\frac{e^{-jk_o r}}{r} = \frac{1}{r} - jk_o - \frac{k_o^2 r}{2!} + \frac{jk_o^3 r^2}{3!} + \frac{k_o^4 r^3}{4!} - \frac{jk_o^5 r^4}{5!} \ldots .$$

$$\frac{e^{-jk_1 r}}{r} = \frac{1}{r} - jk_1 - \frac{k_1^2 r}{2!} + \frac{jk_1^3 r^2}{3!} + \frac{k_1^4 r^3}{4!} - \frac{jk_1^5 r^4}{5!} \ldots .$$

$$\therefore \quad \frac{\partial}{\partial r}\left[\frac{e^{-jk_o r}}{r} - \frac{e^{-jk_1 r}}{r}\right] = \frac{(k_1^2-k_o^2)}{2} - \frac{j(k_1^3-k_o^3)r}{3} - \frac{(k_1^4-k_o^4)r^2}{8}$$

$$+ \frac{j(k_1^5-k_o^5)r^3}{30} \ldots . \qquad (3.18)$$

Multiplying (3.18) by $\frac{\mu_o}{2\pi r(k_1^2-k_o^2)}$ and comparing with (3.14), one gets

$$g_A(\bar{r}/\bar{r}') = \frac{\mu_o}{4\pi}\left\{\frac{1}{r} - \frac{2j(k_1^3-k_o^3)}{3(k_1^2-k_o^2)} - \frac{(k_1^4-k_o^4)r}{4(k_1^2-k_o^2)} + \frac{j(k_1^5-k_o^5)r^2}{15(k_1^2-k_o^2)} \cdots\right\}, \tag{3.19}$$

which can be expressed in the following form :

$$g_A(\bar{r}/\bar{r}') = \sum_{n=0}^{\infty} b_n\, r^{n-1}, \tag{3.20}$$

where,

$$b_n = \frac{\mu_o}{4\pi}\left\{\frac{2(-j)^n}{n!(n+2)} \cdot \frac{(k_1^{n+2}-k_o^{n+2})}{(k_1^2 - k_o^2)}\right\}. \tag{3.21}$$

The expression (3.21) is not convenient for computational purpose because when $k_1=k_o$, the numerator and the denominator both become zero. The factor (k_1-k_o) in the denominator can be removed as follows.

The term $(k_1^{n+2} - k_o^{n+2})$ appearing in the numerator of (3.21) can be factored by using the relation

$$k_1^m - k_o^m = (k_1 - k_o)\, f_{m-1} \tag{3.22}$$

where, $f_{m-1} = k_1^{m-1} + k_1^{m-2}\, k_o + k_1^{m-3}\, k_o^2 + .. k_1 k_o^{m-2} + k_o^{m-1}$.

(m terms) (3.23)

Removing the factor (k_1-k_o) from the numerator and the denominator one gets

$$b_n = \frac{\mu_o}{4\pi}\left\{\frac{2(-j)^n}{n!(n+2)} \cdot \frac{f_{n+1}}{(k_1 + k_o)}\right\} . \qquad (3.24)$$

For the special case when $k_1 = k_o$, one can write

$$f_{m-1}\Big|_{k_1=k_o} = mk_o^{m-1} . \qquad (3.25)$$

Hence, one gets

$$f_{n+1}\Big|_{k_1=k_o} = (n+2)k_o^{n+1} . \qquad (3.26)$$

From (3.24) and (3.26) one can write

$$b_n\Big|_{k_1=k_o} = \frac{\mu_o}{4\pi}\left\{\frac{2(-j)^n}{n!(n+2)} \cdot \frac{(n+2)k_o^{n+1}}{2k_o}\right\}$$

$$= \frac{\mu_o}{4\pi}\left\{\frac{(-j)^n k_o^n}{n!}\right\} . \qquad (3.27)$$

And, hence

$$g_A(\bar{r}/\bar{r}')\Big|_{k_1=k_o} = \frac{\mu_o}{4\pi}\sum_{n=0}^{\infty}\frac{(-j)^n k_o^n\, r^{n-1}}{n!} \qquad (3.28)$$

which can be identified as the power series expansion of the free space Green's function.

A few of the coefficients b_n given by (3.24) are as follows:

$$
\begin{aligned}
b_o &= \frac{\mu_o}{4\pi} \\
b_1 &= \frac{\mu_o}{4\pi} \cdot \frac{-j2}{3(k_1+k_o)} \cdot \left\{ k_1^2+k_1k_o+k_o^2 \right\} \\
b_2 &= \frac{\mu_o}{4\pi} \cdot \frac{-1}{4(k_1+k_o)} \cdot \left\{ k_1^3+k_1^2k_o+k_1k_o^2 + k_o^3 \right\} \\
b_3 &= \frac{\mu_o}{4\pi} \cdot \frac{j}{15(k_1+k_o)} \cdot \left\{ k_1^4+k_1^3k_o+ \ \ldots \ + k_o^4 \right\} \\
b_4 &= \frac{\mu_o}{4\pi} \cdot \frac{1}{72(k_1+k_o)} \cdot \left\{ k_1^5+k_1^4k_o+ \ \ldots \ + k_o^5 \right\} \\
b_5 &= \frac{\mu_o}{4\pi} \cdot \frac{-j}{420(k_1+k_o)} \cdot \left\{ k_1^6+k_1^5k_o+ \ \ldots \ + k_o^6 \right\} \\
b_6 &= \frac{\mu_o}{4\pi} \cdot \frac{-1}{2880(k_1+k_o)} \cdot \left\{ k_1^7+k_1^6k_o+ \ \ldots \ + k_o^7 \right\} \\
b_7 &= \frac{\mu_o}{4\pi} \cdot \frac{j}{22680(k_1+k_o)} \cdot \left\{ k_1^8+k_1^7k_o+ \ \ldots \ + k_o^8 \right\}
\end{aligned}
\tag{3.29}
$$

3.4 SOLUTION PROCEDURE

For obtaining numerical solution to equation (3.3), the wire antenna is divided into N equal segments along the wire axis as shown in Fig. 3.3. The nth segment is indentified by its mid point n, and two end points $\bar{n}$ and $\overset{+}{n}$. The direction of the current is from $\bar{n}$ to $\overset{+}{n}$. Each segment is sufficiently small, so that for any given segment the current can be treated as constant, with negligible error.

The total charges associated with the current $I_1(n)$ in the nth segment of length Δl_n are $\pm I_1(n)/j\omega$. The positive charge is assumed to be distributed uniformly along the axis from the point n to a point at a distance of Δl_n along the wire axis. The centre of this charge distribution is at point $\overset{+}{n}$ and the linear space which is being occupied by this distribution is identified by Δl_n^+. Likewise, for negative charge, $\bar{n}$ is the centre and the space is identified by Δl_n^-. Fig. 3.4 illustrates this model of a segment, for current and charge distributions [32, 39].

By approximating the derivative in (3.3) by a finite difference form and considering the mth segment, one can write

$$E_1^i(m) \simeq j\omega A_1(m) + \frac{V(\overset{+}{m}) - V(\bar{m})}{\Delta l_m} \tag{3.30}$$

where, $A_1(m)$ is the vector potential at point m along the direction of the axis and is due to currents in all the segements; $V(\overset{+}{m})$ and $V(\bar{m})$ are the potentials at points $\overset{+}{m}$ and $\bar{m}$ due to the charges associated with these currents. To obtain $A_1(m)$, $V(\overset{+}{m})$ and $V(\bar{m})$, the integrals (3.4) and (3.5) are to be evaluated along the entire wire axis. They are approximated as sum of integrals over N segements. Thus, one can write

$$A_1(m) = \sum_{n=1}^{N} \left\{ I_1(n) \cos\theta_{mn} \int_{\Delta l_n} g_A(m/n)dl' \right\} \tag{3.31}$$

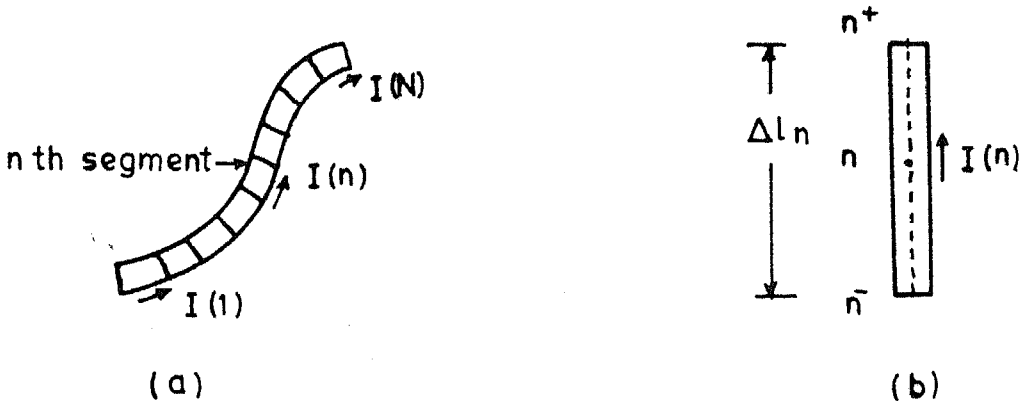

Fig. 3.3 (a) A wire divided into N segments.
(b) The nth segment.

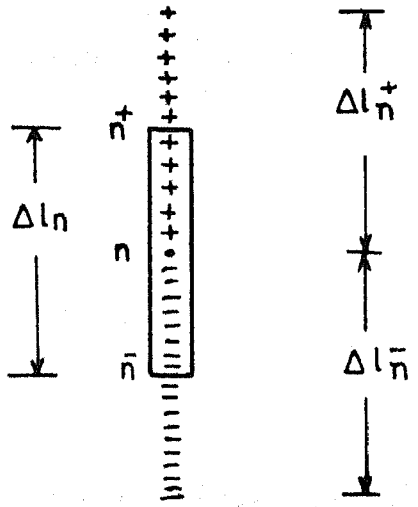

Fig. 3.4 Uniform current and charge distributions for the nth segment.

$$V(\overset{+}{m}) = \sum_{n=1}^{N} \left\{ q(\overset{+}{n}) \int_{\Delta l_n^+} k_\phi(\overset{+}{m}/\overset{+}{n})dl' + q(\overset{-}{n}) \int_{\Delta l_n^-} k_\phi(\overset{+}{m}/\overset{-}{n})dl' \right\} \tag{3.32}$$

$$V(\overset{-}{m}) = \sum_{n=1}^{N} \left\{ q(\overset{+}{n}) \int_{\Delta l_n^+} k_\phi(\overset{-}{m}/\overset{+}{n})dl' + q(\overset{-}{n}) \int_{\Delta l_n^-} k_\phi(\overset{-}{m}/\overset{-}{n})dl' \right\} , \tag{3.33}$$

where, $\cos \theta_{mn}$ is the direction consine between segements n and m, and $q(\overset{+}{n})$ and $q(\overset{-}{n})$ are the uniform charge densities with centres at $\overset{+}{n}$ and $\overset{-}{n}$ respectively. The charge density $q(\overset{+}{n})$ and $q(\overset{-}{n})$ can be expressed in terms of current $I_1(n)$ as

$$q(\overset{+}{n}) = \frac{I_1(n)}{j\omega\Delta l_n^+}$$

$$q(\overset{-}{n}) = \frac{-I_1(n)}{j\omega\Delta l_n^-} \quad . \tag{3.34}$$

Equation (3.30) can be identified as an equation for N unknown currents. By allowing m to take all the values from m=1 to m=N, a set of N equations can be obtained. These equations can be written in matrix form as

$$[V] = [Z]\,[I] \tag{3.35}$$

$$\text{where,} \quad [V] = \begin{bmatrix} E_1^i(1).\Delta l_1 \\ E_1^i(2).\Delta l_2 \\ \vdots\vdots\vdots \\ E_1^i(N).\Delta l_N \end{bmatrix} \qquad [I] = \begin{bmatrix} I_1(1) \\ I_1(2) \\ \vdots\vdots \\ I_1(N) \end{bmatrix} \tag{3.36}$$

$$[Z] = \begin{bmatrix} Z_{11} & Z_{12} & Z_{1N} \\ Z_{21} & Z_{22} & Z_{2N} \\ \cdots & \cdots & \cdots \\ \cdots & \cdots & \cdots \\ Z_{N1} & Z_{N2} & Z_{NN} \end{bmatrix} .$$

The equations defined by (3.35) can be viewed as equations for a N-port network. The matrices [V], [Z] and [I] stand for the network parameters, namely, voltage, impedance and current respectively. The element Z_{mn} of the impedance matrix [Z] can be written from (3.30) - (3.36) as

$$Z_{mn} = Z_{mn}^A + Z_{mn}^\phi \tag{3.37}$$

$$\text{where,} \quad Z_{mn}^A = j\omega\cos\theta_{mn}\Delta l_m \int_{\Delta l_n} g_A(m/n)dl' \tag{3.38}$$

$$Z_{mn}^\phi = \frac{1}{j\omega\Delta l_n^+}\int_{\Delta l_n^+} k_\phi(\overset{+}{m}/\overset{+}{n})dl' - \frac{1}{j\omega\Delta l_n^-}\int_{\Delta l_n^-} k_\phi(\overset{+}{m}/\overset{-}{n})dl'$$

$$- \frac{1}{j\omega\Delta l_n^+}\int_{\Delta l_n^+} k_\phi(\overset{-}{m}/\overset{+}{n})dl' + \frac{1}{j\omega\Delta l_n^-}\int_{\Delta l_n^-} k_\phi(\overset{-}{m}/\overset{-}{n})dl' . \tag{3.39}$$

Defining the integrals in (3.38) and (3.39) by

$$\Psi(m,n) = \frac{1}{\Delta l_n} \int_{\Delta l_n} g_A(m/n)\, dl' \qquad (3.40)$$

$$\xi(m,n) = \frac{1}{\Delta l_n} \int_{\Delta l_n} k_\phi(m/n)\, dl' \qquad (3.41)$$

one can write

$$Z_{mn} = j\omega \overline{\Delta l}_n . \overline{\Delta l}_m \Psi(m/n) + \frac{1}{j\omega} [\xi(\overset{+}{m}/\overset{+}{n}) - \xi(\overset{+}{m}/\overset{-}{n}) - \xi(\overset{-}{m}/\overset{+}{n}) + \xi(\overset{-}{m}/\overset{-}{n})] \qquad (3.42)$$

where $$\overline{\Delta l}_n . \overline{\Delta l}_m = \Delta l_n . \Delta l_m \cos \theta_{mn} \; . \qquad (3.43)$$

This result applies for self impedance (m = n) as well as for mutual impedance (m ≠ n). The integrals $\Psi(m,n)$ and $\xi(m,n)$ are evaluated in the next section.

3.5 EVALUATION OF $\Psi(m,n)$

To evaluate $\Psi(m,n)$, a local co-ordinate system with origin at n, and the y axis along the axis of the nth segment is constructed as shown in Fig. 3.5. From (3.20) and (3.40), $\Psi(m,n)$ can be written in the form

$$\Psi(m,n) = \frac{1}{\Delta l_n} \sum_{n=0}^{\infty} b_n \int_{-\Delta l_n/2}^{\Delta l_n/2} R_m^{n-1}\, dy' \qquad (3.44)$$

where, $R_m = \sqrt{\rho_m^2+(y-y')^2}$ $\quad m \neq n$

$= \sqrt{a^2+y'^2}$ $\quad m = n$. (3.45)

By making a change of variable

$$t = y - y' \tag{3.46}$$

and writing $\alpha = \frac{\Delta l_n}{2}$, the integration given by (3.44) can be rewritten as

$$\Psi(m,n) = \frac{1}{2\alpha} \sum_{n=0}^{\infty} b_n I_n \tag{3.47}$$

where, $$I_n = \int_{y-\alpha}^{y+\alpha} \left(\sqrt{t^2+\rho_m^2}\right)^{n-1} dt \ . \tag{3.48}$$

The expression (3.47) can be written as sum of two series :

$$\Psi(m,n) = \frac{1}{2\alpha} [S_o + S_1] \tag{3.49}$$

where

$$S_o = \sum_{n=2i}^{\infty} b_n I_n \tag{3.50}$$

$$S_1 = \sum_{n=1+2i}^{\infty} b_n I_n \tag{3.51}$$

with, i = 0,1,2,3....,.

Expanding the series one can write

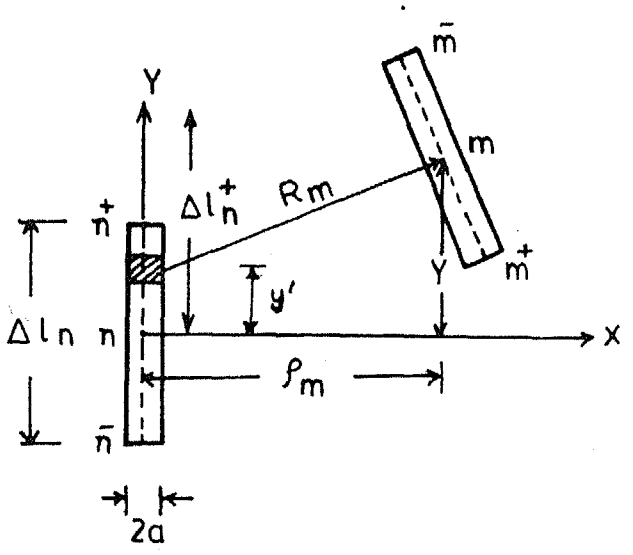

Fig.3.5 Geometry for evaluating $\psi(m, n)$

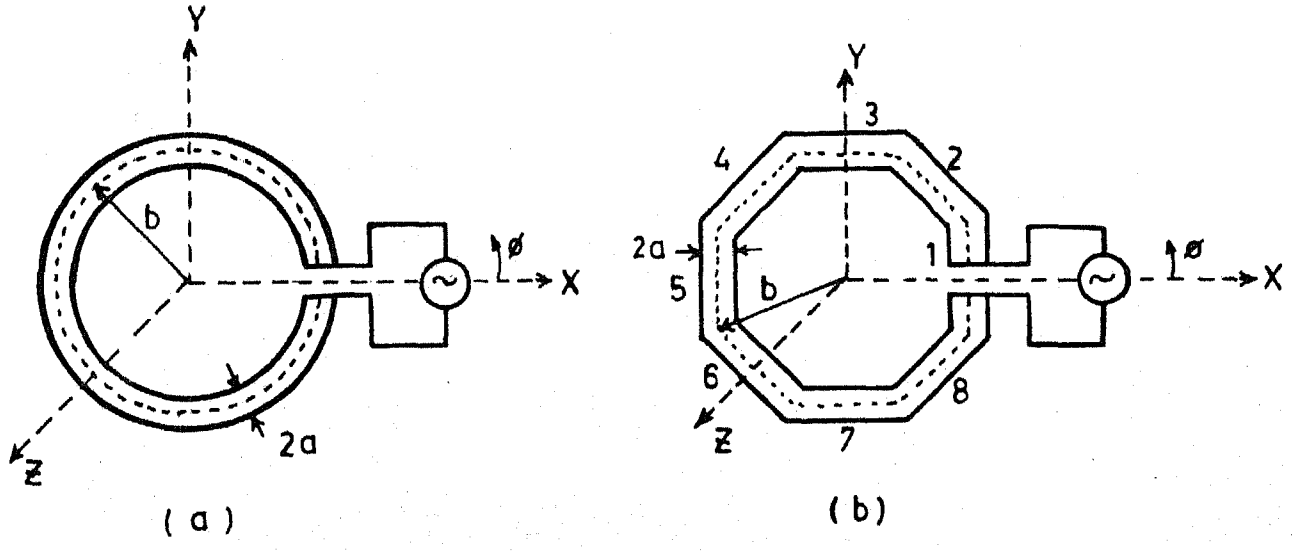

Fig.3.6 (a) Circular loop antenna with excitation at $\phi = 0^{\circ}$

(d) The reduced structure after being segmented. (Only eight segments shown).

$$S_o = b_o I_o + b_2 I_2 + b_4 I_4 + \ldots\ldots\ldots$$

$$= b_o \int_{y-\alpha}^{y+\alpha} (t^2 + \rho_m^2)^{-\frac{1}{2}}\, dt + b_2 \int_{y-\alpha}^{y+\alpha} (t^2+\rho_m^2)^{\frac{1}{2}}\, dt$$

$$+ b_4 \int_{y-\alpha}^{y+\alpha} (t^2+\rho_m^2)^{1+\frac{1}{2}}\, dt + \ldots\ldots \qquad (3.52)$$

and $S_1 = b_1 I_1 + b_3 I_3 + b_5 I_5 + \ldots\ldots\ldots$

$$= b_1 + b_3 \int_{y-\alpha}^{y+\alpha} (t^2 + \rho_m^2)\, dt + b_5 \int_{y-\alpha}^{y+\alpha} (t^2+\rho_m^2)^2\, dt + \ldots \;.$$

(3.53)

(a) Evaluation of S_o :

The integral I_o is given by

$$I_o = \int_{y-\alpha}^{y+\alpha} (t^2+\rho_m^2)^{-\frac{1}{2}}\, dt$$

$$= \log \left[\frac{y+\alpha+\sqrt{\rho_m^2+(y+\alpha)^2}}{y-\alpha+\sqrt{\rho_m^2+(y-\alpha)^2}} \right] . \qquad (3.54)$$

The other integrals of the series S_o can be obtained by using the following recursive relation [36].

$$\int (t^2+\rho_m^2)^{\eta+\frac{1}{2}}\,dt = \frac{t(t^2+\rho_m^2)^{\eta+\frac{1}{2}}}{2(\eta+1)} + \frac{(2\eta+1)\rho_m^2}{2(\eta+1)}\int (t^2+\rho_m^2)^{\eta-\frac{1}{2}} + C_i \qquad (3.55)$$

where $\eta = 0,1,2,3, \ldots,$ and C_i is an arbitrary constant.

(b) Evaluation S_1:

The integral I_n of the series S_1 can be written as

$$I_{2\eta+1} = \int_{y-\alpha}^{y+\alpha} (t^2+\rho_m^2)^{\eta}\,dt, \quad \eta = 0,1,2,\ldots . \qquad (3.56)$$

This integral can be evaluated by employing binomial expansion. One can write (for $\eta \neq 0$),

$$(t^2+\rho_m^2)^{\eta} = t^{2\eta} + {}^{\eta}C_1\rho_m^2 t^{2(\eta-1)} + {}^{\eta}C_2\rho_m^4 t^{2(\eta-2)} + \ldots + \rho_m^{2\eta}$$

$$(\eta + 1) \text{ terms} \qquad (3.57)$$

Integrating (3.57), one gets

$$\int_{y-\alpha}^{y+\alpha} (t^2+\rho_m^2)^{\eta}\,dt = \left[\frac{t^{2\eta+1}}{2\eta+1} + \frac{{}^{\eta}C_1\rho_m^2 t^{2(\eta-1)+1}}{2(\eta-1)+1} + \frac{{}^{\eta}C_2\rho_m^4 t^{2(\eta-2)+1}}{2(\eta-2)+1} + \ldots \rho_m^{2\eta}\right]_{y-\alpha}^{y+\alpha}. \qquad (3.58)$$

Following the above evaluation procedures for S_o and S_1, a few integrals I_n (given by (3.48)) are as follows :

$$I_o = \log\left[\frac{y+\alpha+\sqrt{X_m}}{y-\alpha+\sqrt{Y_m}}\right]$$

$$I_1 = 2\alpha$$

$$I_2 = \frac{y+\alpha}{2}\sqrt{X_m} - \frac{y-\alpha}{2}\sqrt{Y_m} + \frac{\rho_m^2}{2} I_o$$

$$I_3 = \frac{1}{3} Y(3) + 2\alpha\rho_m^2$$

$$I_4 = \frac{y+\alpha}{4} X_m^{1+\frac{1}{2}} - \frac{y-\alpha}{4} Y_m^{1+\frac{1}{2}} + \frac{3}{4}\rho_m^2 I_2 \qquad (3.59)$$

$$I_5 = \frac{1}{5} Y(5) + \frac{2\rho_m^2}{3} Y(3) + 2\alpha\rho_m^4$$

$$I_6 = \frac{y+\alpha}{6} X_m^{2+\frac{1}{2}} - \frac{y-\alpha}{6} Y_m^{2+\frac{1}{2}} + \frac{5}{6}\rho_m^2 I_4$$

$$I_7 = \frac{1}{7} Y(7) + \frac{3\rho_m^2}{5} Y(5) + \rho_m^4 Y(3) + 2\alpha\rho_m^6$$

where $X_m = \rho_m^2 + (y+\alpha)^2$

$$Y_m = \rho_m^2 + (y-\alpha)^2 \qquad (3.60)$$

$Y(n) = (y+\alpha)^n - (y-\alpha)^n$, n is an integer.

$\Psi(m,n)$ is to be computed by using (3.29), (3.47), (3.59) and (3.60).

Evaluation of $\zeta(m,n)$

Comparing (3.17) with (3.20), and (3.40) with (3.41), it can be seen that $\zeta(m,n)$ involves the integral I_o. One can write

$$\zeta(m,n) = \frac{\omega^2 \mu_o}{2\pi k_1^2} I_o \quad . \tag{3.61}$$

3.6 INPUT IMPEDANCE AND CURRENT DISTRIBUTION

The current in the nth segment can be obtained by solving the equation (3.35). The solution can be written in the following matrix form.

$$[I] = [Z]^{-1} [V] \tag{3.62}$$

It is assumed that the loop is excited by a unit voltage source at the gap which is located at $\phi = 0^o$, as shown in Fig. 3.6. This excitation voltage is assumed to be applied to segment number 1. The voltage matrix can be written as

$$[V] = \begin{bmatrix} 1.0 \\ 0 \\ 0 \\ \cdot \\ \cdot \\ 0 \end{bmatrix} \quad . \tag{3.63}$$

The matrix [V] is a column matrix with N entries. The input impedance Z_{in} and the input admittance Y_{in} are given by

$$Z_{in} = \frac{1}{I(1)}$$
$$Y_{in} = I(1) \qquad (3.64)$$

3.7 FIELD INSIDE THE EARTH

The closed form expressions for potentials used to obtain current distribution in a loop antenna on the earth surface, cannot be used for computation of fields inside the earth. These expressions are valid only at the air/earth interface. To compute field inside the earth Sommerfeld type integrals representing the potentials in the earth region are to be evaluated numerically. We shall be computing magnetic field components only. The magnetic fields may be picked up using a small coil, preferably wound over a ferrite core, and then fed to the miner's receiver.

For a x directed current element, Fig.2.1, the magnetic field components in terms of the magnetic vector potentials are given by (2.5a) - (2.5c). These components are denoted here as δH_{x1}, δH_{y1} and δH_{z1} to stress that these are elementary field components due to an isolated current element, and not the total field for a given antenna. These elementary field components can be obtained as follows :

From (2.5a) and (2.27) one can write

$$\delta H_{x1} = \frac{1}{\mu_o} \frac{\partial}{\partial y} (\delta A_{z1})$$

$$= \frac{\partial}{\partial y} \left[-\frac{\rho}{2\pi} \frac{\partial}{\partial x} \int_0^\infty \frac{(\gamma_1 - \gamma_o) J_o(\lambda r) \lambda \exp\{j(\gamma_1 z - \gamma_o z_o)\} d\lambda}{k_1^2 \gamma_o + k_o^2 \gamma_1} \right]$$

$$= \frac{\partial}{\partial y} \left[\frac{\rho x}{2\pi} \int_0^\infty \frac{(\gamma_1 - \gamma_o) J_1(\lambda r) \lambda^2 \exp\{j(\gamma_1 z - \gamma_o z_o)\} d\lambda}{r(k_1^2 \gamma_o + k_o^2 \gamma_1)} \right]$$

$$= \frac{\rho x}{2\pi} \int_0^\infty \frac{(\gamma_1 - \gamma_o) F_x(\lambda r) \lambda^2 \exp\{j(\gamma_1 z - \gamma_o z_o)\} d\lambda}{k_1^2 \gamma_o + k_o^2 \gamma_1} \qquad (3.65a)$$

where $F_x(\lambda r) = \frac{y}{r^2} \left\{ J_o(\lambda r) r^2 \lambda - 2 J_1(\lambda r)/r \right\}$ (3.65b)

From (2.5b) one can write

$$\delta H_{y1} = \frac{1}{\mu_o} \frac{\partial}{\partial z} (\delta A_{x1}) - \frac{1}{\mu_o} \frac{\partial}{\partial x} (\delta A_{z1}) \qquad (3.66a)$$

where the vector potentials are given by (2.26) and (2.27). From (2.26) one gets

$$\frac{1}{\mu_o} \frac{\partial}{\partial z} (\delta A_{x1}) = \frac{\partial}{\partial z} \left[\frac{\rho}{j2\pi} \int_0^\infty \frac{J_o(\lambda r) \lambda \exp\{j(\gamma_1 z - \gamma_o z_o)\} d\lambda}{\gamma_1 + \gamma_o} \right]$$

$$= \frac{\rho}{2\pi} \int_0^\infty \frac{J_o(\lambda r) \gamma_1 \lambda \exp\{j(\gamma_1 z - \gamma_o z_o)\} \, d\lambda}{\gamma_1 + \gamma_o} \qquad (3.66b)$$

From (2.27) one gets

$$\frac{1}{\mu_o}\ \frac{\partial}{\partial x}\ (\delta A_{z1}) = -\frac{\rho}{2\pi}\ \frac{\partial}{\partial x^2}\ \int_0^\infty \frac{(\gamma_1-\gamma_o)J_o(\lambda r)\lambda \exp(j(\gamma_1 z-\gamma_o z_o))d\lambda}{k_1^2\gamma_o+k_o^2\gamma_1}$$

(3.66c)

$$= \frac{\rho}{2\pi}\ \int_0^\infty \frac{(\gamma_1-\gamma_o)J_o(\lambda r)\lambda^2 F_y(\lambda r)\exp(j(\gamma_1 z-\gamma_o z_o)}{k_1^2\gamma_o+k_o^2\gamma_1}$$

(3.66d)

where $F_y(\lambda r) = \frac{J_1(\lambda r)}{r} + x^2\left\{\frac{J_o(\lambda r)\lambda}{r^2} - \frac{2J_1(\lambda r)}{r}\right\}$. (3.66e)

From (2.5c) and (2.26) one can write

$$\delta H_{z1} = -\left[\frac{\partial}{\partial y}\ (\delta A_{x1})\right]\frac{1}{\mu_o}$$

$$= \frac{\partial}{\partial y}\left[-\frac{\rho}{j2\pi}\int_0^\infty \frac{J_o(\lambda r)\lambda\ \exp(j(\gamma_1 z-\gamma_o z_o))\ d\lambda}{\gamma_1+\gamma_o}\right]$$

$$= \frac{\rho y}{j2\pi r}\int_0^\infty \frac{J_1(\lambda r)\lambda^2 \exp\{j(\gamma_1 z-\gamma_o z_o)\}d\lambda}{\gamma_1+\gamma_o}\ . \qquad (3.67)$$

These integrals for the elementary field components are oscillatory and converge very slowly. When the observation point is inside the earth the factor $\exp(j(\gamma_1 z-\gamma_o z_o))$ enhances convergence of these integrals. The convergence is quite fast when the observation point is located at a considerable depth, which is usually true for underground mines. To compute the field

components for the whole of the antenna on the earth surface, these elementary field components are to be integrated for all the current elements along the wire axis.

3.8 NUMERICAL RESULTS

Before doing actual computation it is necessary to ensure that the quasistatic approach i.e., $k_o b << 1$, is valid for the loop antenna being analysed. The purpose of these antennas, is to transmit voice signals to underground miners. For a voice grade communication the highest frequency is 3000 Hz. In the present study the maximum size of the loop is considered to be 600m. With these values we have the maximum value of $2k_o b = 0.038$. This value of $2k_o b << 1$, and hence the quasi-static formulation for the scalar potential can be used.

In figures 3.7 and 3.8 the variation of the real, $R_e(I(\phi))$, and imaginary, $I_m(I(\phi))$, parts of current $I(\phi)$ are shown. For a small loop, $I_m(I(\phi))$ remains almost constant for the whole loop; for example for the 50m loop $I_m(I(0^o)) = 165.77$ mA and $I_m(I(180^o)) = 165.63$mA. This is not true for $R_e(I(\phi))$ which can be seen from the fact that $R_e(I(0^o))=8.67$mA and $R_e(I(180^o))=-3.84$mA. This variation of $R_e(I(\phi))$ in a small loop on the earth surface or in a homogeneous lossy medium makes it different from a small loop in free space where $R_e(I(\phi))$ remains almost constant. However, since for a small loop $I_m(I(\phi)) >> R_e(I(\phi))$, the loop current can be approximated by $I_m(I(\phi))$, which is the usual criterion for identifying a small loop. As the loop diameter is

increased $R_e(I(\phi))$ becomes comparable to $I_m(I(\phi))$ and hence the magnitude and phase of the current vary considerably with ϕ, which can be seen in Figs.3.9 and 3.10. When b is considerably large the current drops very fast near the feed region of the loop. For example, for 2b = 100m, the ratio $|I(180^\circ)|/|I(0^\circ)|$ is 0.97; whereas for 2b = 200m and 300m, these values are 0.70 and 0.39 respectively. A large value of this ratio indicates that the far end section of the loop (diameterically opposite to the feed region) has practically no effect on the feed region. This effect can be seen in Fig. 3.11, where the variation of input conductance G and susceptance S, with the diameter 2b is shown. Both G and S remain almost fixed when b is large. When b is small G varies linearly with σ, and G is much smaller than |S|. When b is increased, the effect of σ becomes more and more prominant, which finally leads to the saturation for the input admittance values. Similar trends are also observed when a loop is fully embedded in a conducting medium [9]. In Tables 3.1 to 3.9 the input admittance Y_n along with $I(0^\circ)$ and $I(180^\circ)$ for different values of parameters have been tabulated. From these tables it can be seen that when |S| is at least seven times greater than G, the ratio $R_x = |I(180^\circ)/|I(0^\circ)|$ is greater than 0.95. For practical purpose, a loop antenna having greater than this value (0.95) for R_x can be considered as a small loop.

Figures 3.12 and 3.13 show the magnitude of magnetic field components inside the earth due to surface current distributions in the loops. The field strength has been obtained by normalizing

the feed point current $I(0^{o})$ to unity. Fig. 3.12 is for the case when the current distribution is almost uniform, while Fig.3.13 is for when their is a considerable variation of current distribution with ϕ. These current distributions are shown in Figs.3.7 to 3.10. The fields depend both on radial distance from the loop axis and angle ϕ. When the current distribution is almost uniform the H_z component practically does not vary with ϕ while H_r component varies to a small extent. The situation is not the same when there is a considerable variation of current distribution. In Fig. 3.13 it can be seen that when $\phi = 0^{o}$ the radial component H_r is much larger than H_r or H_z values at any other angles. This is due to the fact that current is mainly concentrated near the feed region of the antenna. The peak occurs approximately straight below the feed point.

3.8.1 DISCUSSION ON THE NUMERICAL METHOD

The formulation of the matrix equation (3.35) is based on the assumption of an uniform current for a given segment; and using a single matching point for the scattered field for each segment. This procedure is equivalent to using rectangular basis and delta test functions. Use of these simple functions requires sufficiently large number of segments to approximate the current distribution so that the current in two neighbouring segments does not change appreciably. However, the major advantage gained by using these functions in conjunction with the closed form expressions for the potentials, is that the solution procedure does not require any numerical integration for obtaining current

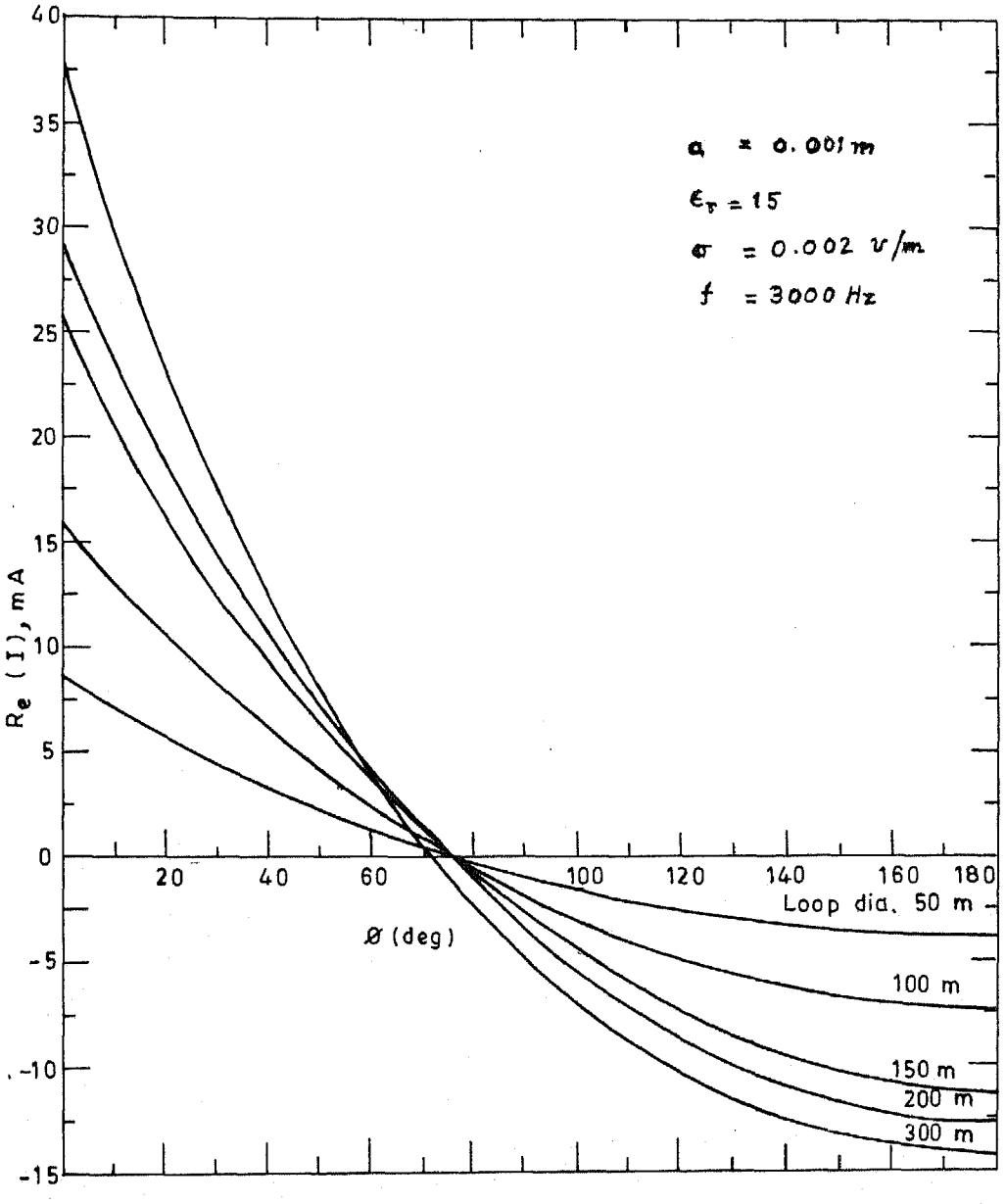

Fig.3.7 Variation of the real part ($R_e(I)$) of the loop current with Ø .

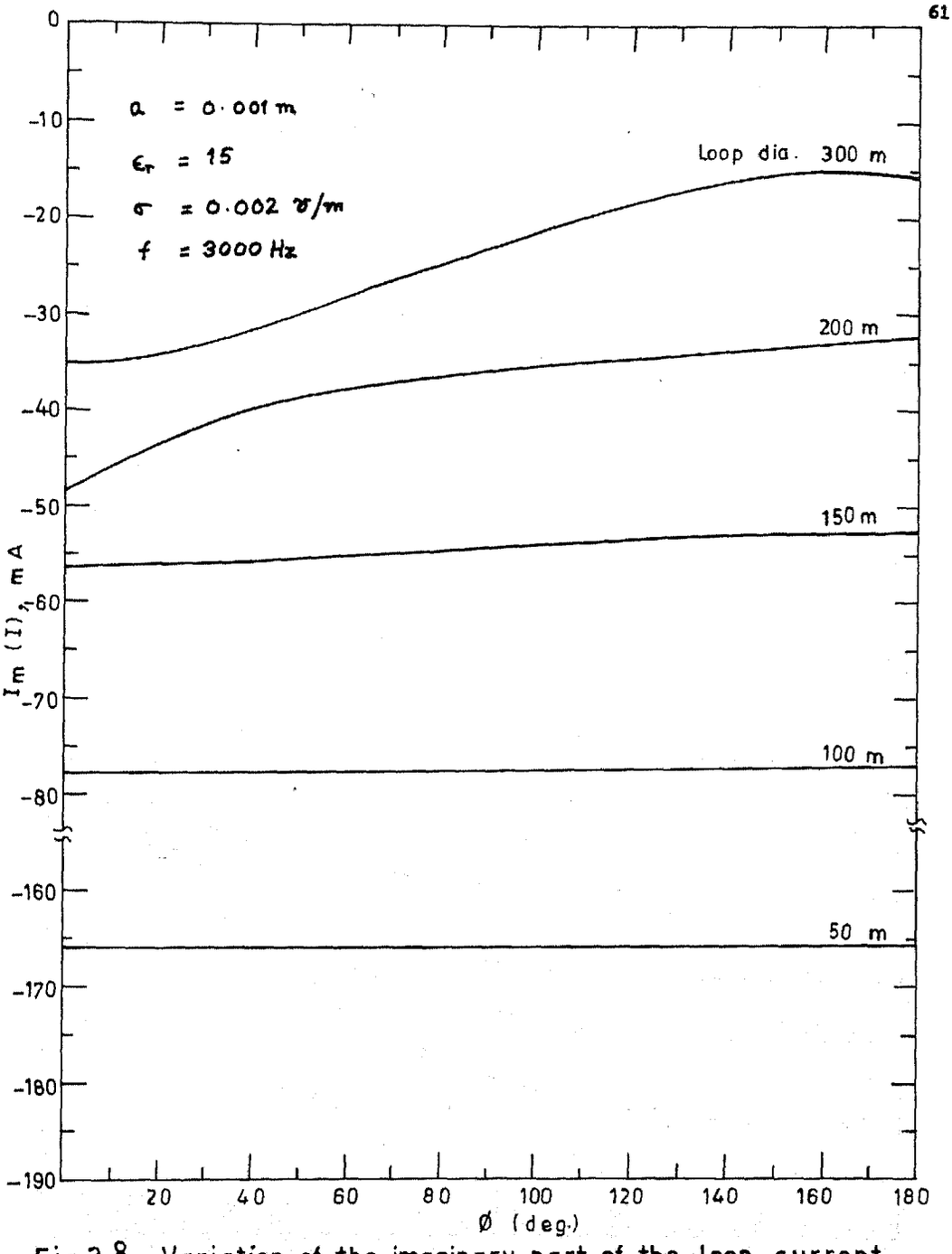

Fig.3.8 Variation of the imaginary part of the loop current $I_m(I)$ with Ø .

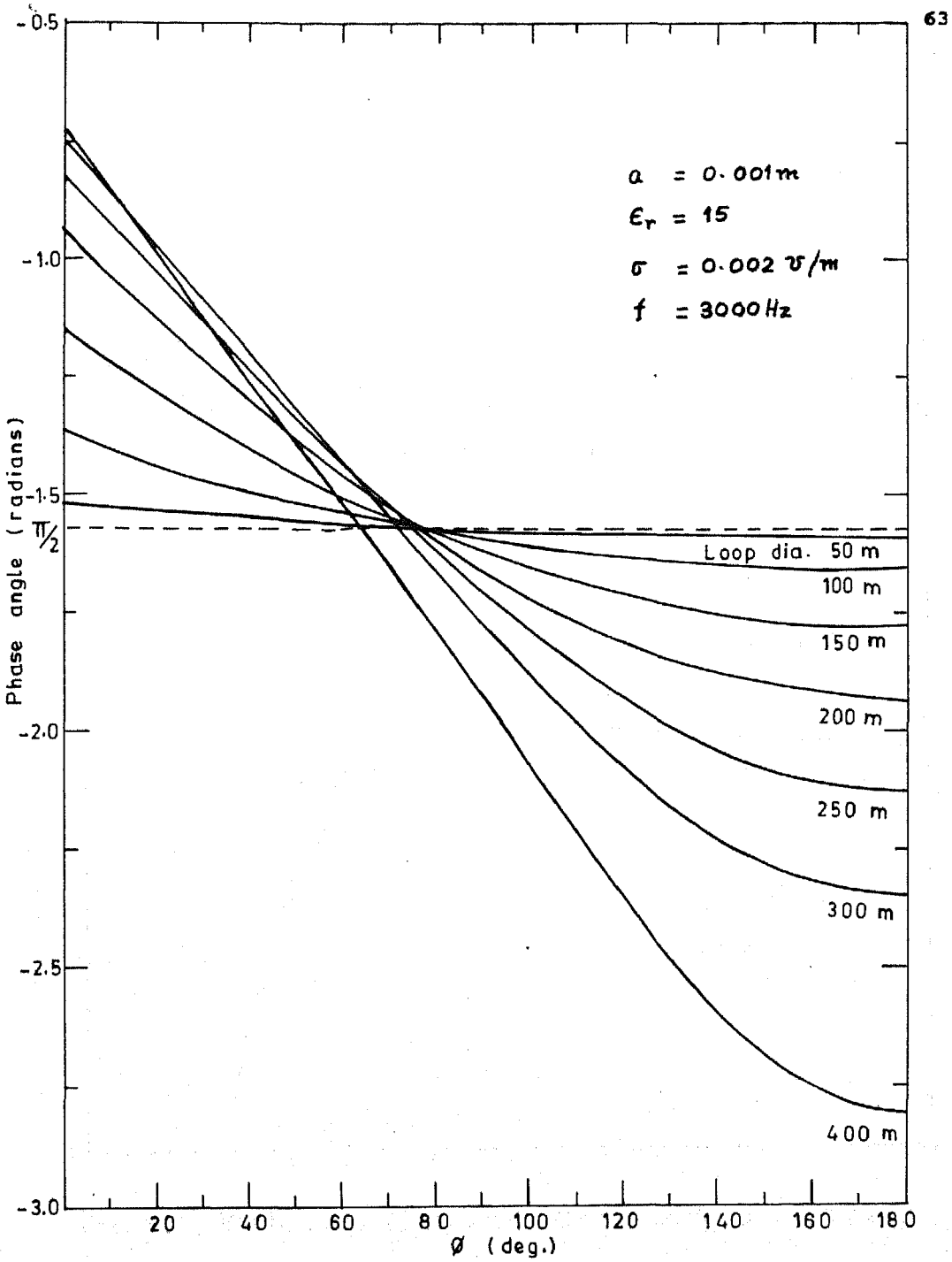

Fig. 3.10 Variation of phase angle of the loop current with Ø.

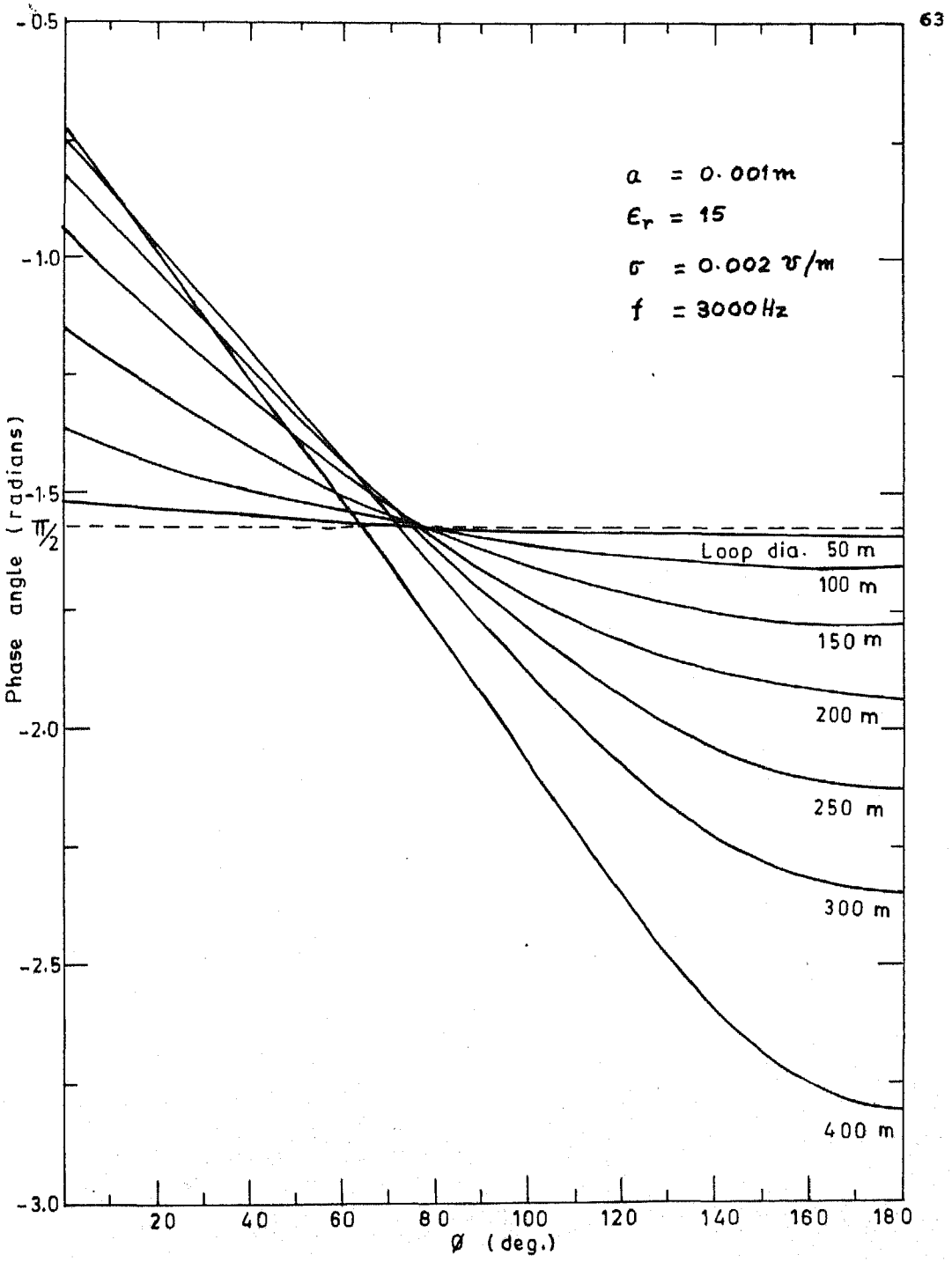

Fig. 3.10 Variation of phase angle of the loop current with ϕ.

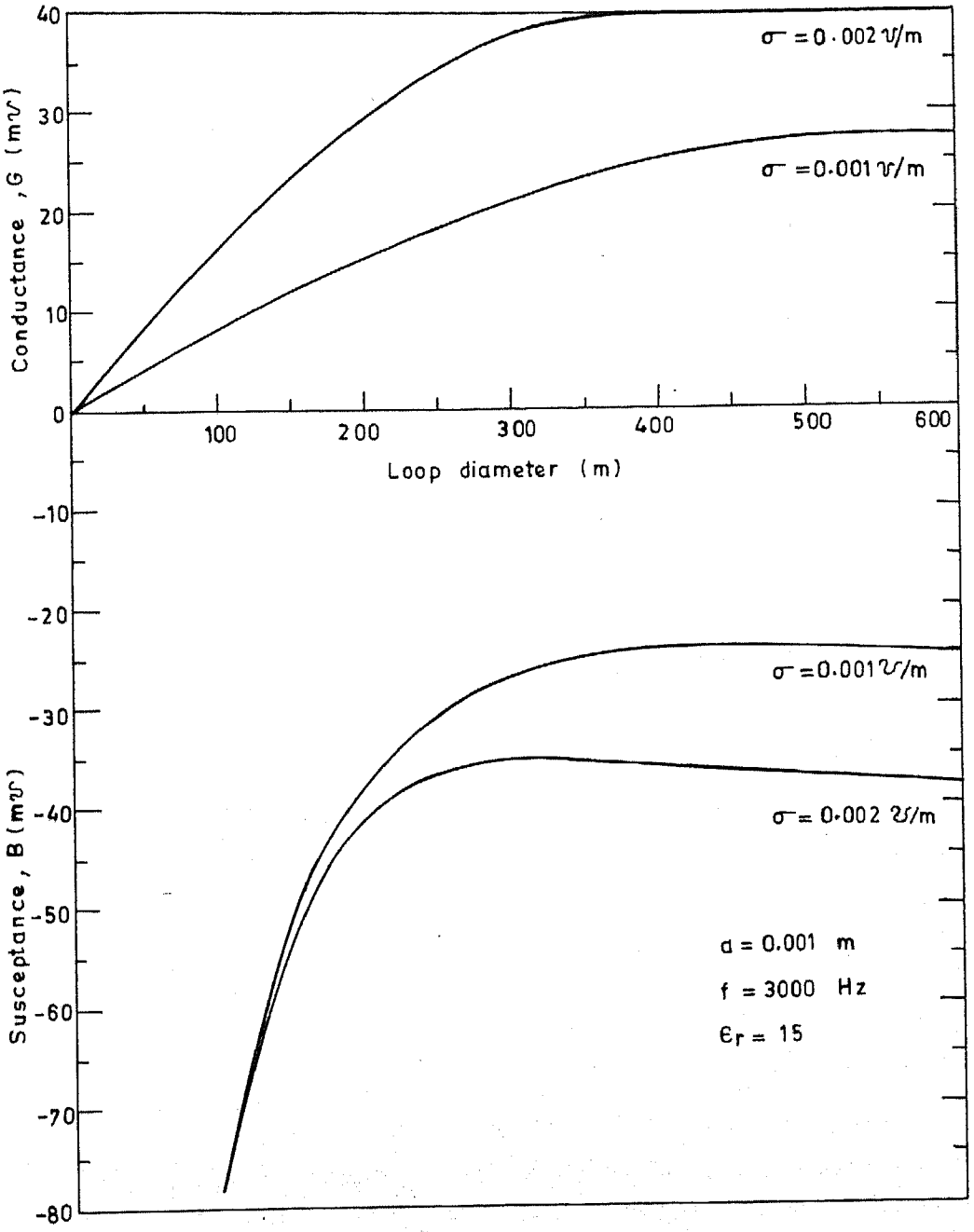

Fig. 3.11 Variation of input admittance with loop diameter.

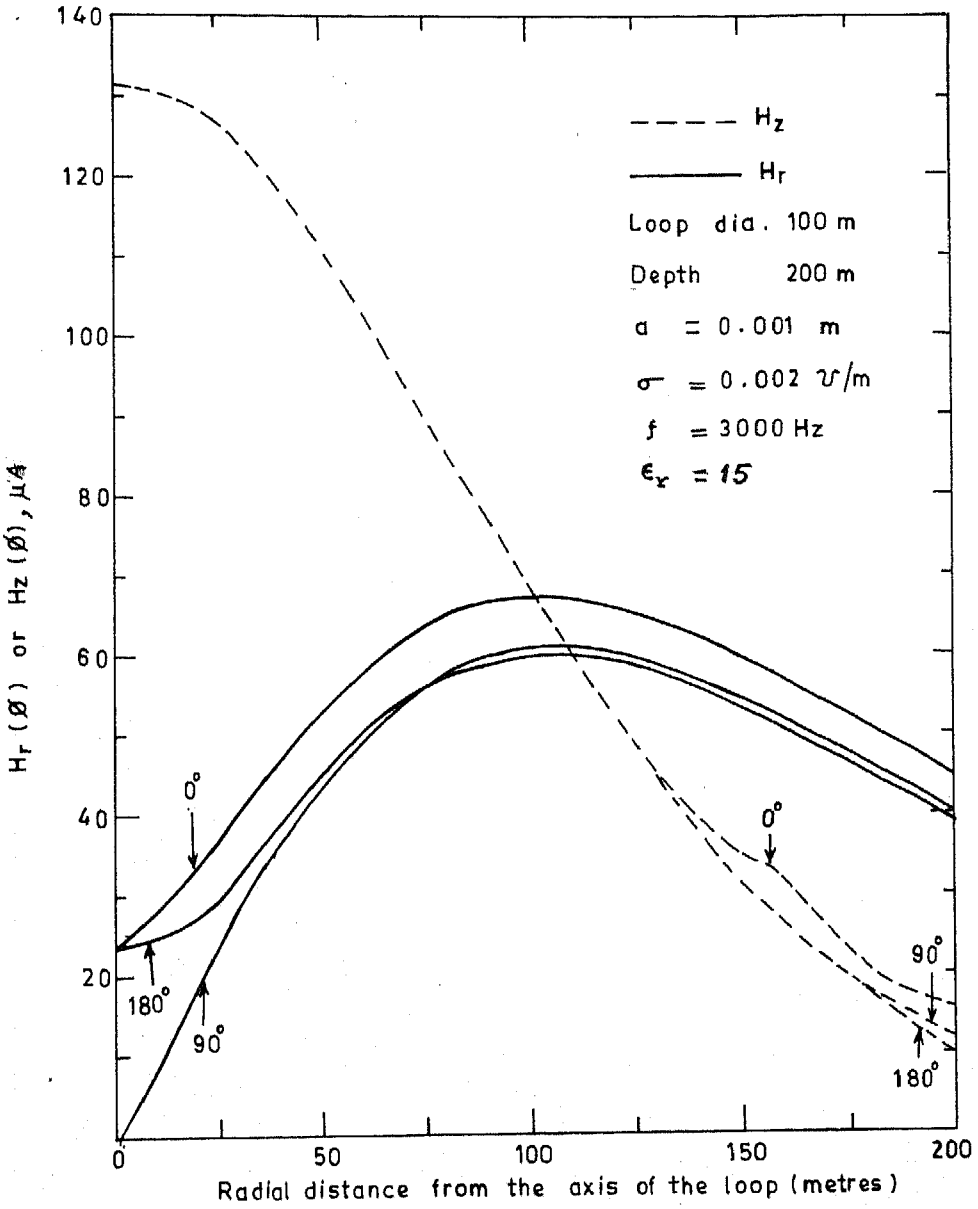

Fig. 3.12 Magnitude of magnetic field components $H_z(\phi)$ and $H_r(\phi)$ inside the earth due to current distribution in the surface loop.

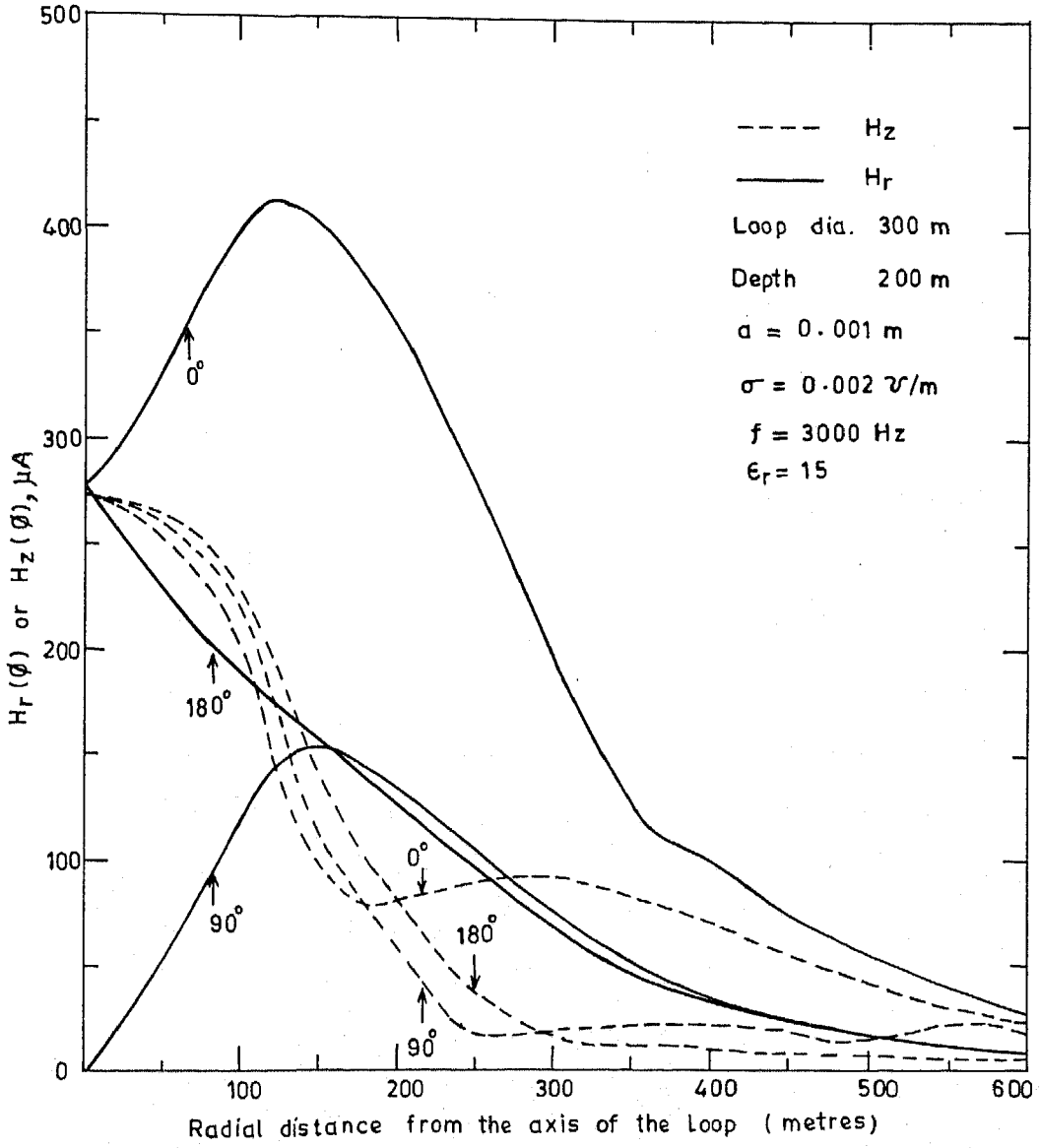

Fig. 3.13 Magnitude of magnetic field components $H_z(\phi)$ and $H_r(\phi)$ inside the earth due to current distribution in the surface loop

TABLE 3.2

Input admittance for a circular loop antenna on the earth surface

$f = 1500$ Hz, $\sigma = 0.001$ mho/m, $\varepsilon_r = 15$, $a = 0.0025$ m

Loop dia (m)	Y_{in} (milli mho)	I (0^o) *	I (180^o) *
50	4.86-j364.07	364.1 ∠-1.56	364.1 ∠ -1.58
100	8.89-j169.48	169.7 ∠-1.52	169.4 ∠ -1.59
150	12.74-j108.80	109.4 ∠-1.45	108.5 ∠ -1.62
200	16.46-j79.85	81.5 ∠-1.37	79.0 ∠ -1.66
250	20.03-j63.29	66.4 ∠-1.26	61.8 ∠ -1.72
300	23.46-j52.92	57.9 ∠-1.15	50.4 ∠ -1.78
350	26.69-j46.14	53.3 ∠-1.05	42.1 ∠ -1.85
400	29.69-j41.68	51.2 ∠-0.95	36.0 ∠ -1.94
450	32.40-j38.81	50.6 ∠-0.86	31.1 ∠ -2.03
500	34.76-j37.09	50.8 ∠-0.82	27.1 ∠ -2.13

* Magnitude in mA and phase angle in radians.

TABLE 3.2

Input admittance for a circular loop antenna on the earth surface

$f = 1500$ Hz, $\sigma = 0.001$ mho/m, $\varepsilon_r = 15$, $a = 0.0025$ m

Loop dia (m)	Y_{in} (milli mho)	I (0°) *	I (180°) *
50	4.86-j364.07	364.1 $\angle$-1.56	364.1 $\angle$ -1.58
100	8.89-j169.48	169.7 $\angle$-1.52	169.4 $\angle$ -1.59
150	12.74-j108.80	109.4 $\angle$-1.45	108.5 $\angle$ -1.62
200	16.46-j79.85	81.5 $\angle$-1.37	79.0 $\angle$ -1.66
250	20.03-j63.29	66.4 $\angle$-1.26	61.8 $\angle$ -1.72
300	23.46-j52.92	57.9 $\angle$-1.15	50.4 $\angle$ -1.78
350	26.69-j46.14	53.3 $\angle$-1.05	42.1 $\angle$ -1.85
400	29.69-j41.68	51.2 $\angle$-0.95	36.0 $\angle$ -1.94
450	32.40-j38.81	50.6 $\angle$-0.86	31.1 $\angle$ -2.03
500	34.76-j37.09	50.8 $\angle$-0.82	27.1 $\angle$ -2.13

* Magnitude in mA and phase angle in radians.

TABLE 3.3

Input admittance for a circular loop antenna on the earth surface

f = 1500 Hz, σ = 0.002 mho/m, ε_r = 15, a = 0.001 m

Loop dia (m)	Y_{in} (milli mho)	I (0°) *	I (180°) *
50	8.56-j332.84	332.9 $\angle$-1.54	332.7 $\angle$ -1.58
100	16.14-j155.48	156.3 $\angle$-1.46	155.1 $\angle$ -1.62
150	22.95-j101.20	103.8 $\angle$-1.35	99.9 $\angle$ -1.68
200	29.88-j75.28	81.0 $\angle$-1.19	72.3 $\angle$ -1.76
250	36.10-j61.60	71.4 $\angle$-1.04	56.1 $\angle$ -1.86
300	41.68-j54.05	68.3 $\angle$-0.91	45.1 $\angle$ -1.98
350	46.41-j50.18	68.4 $\angle$-0.82	37.0 $\angle$ -2.12
400	50.12-j48.61	69.8 $\angle$-0.77	30.6 $\angle$ -2.28
450	52.78-j48.42	71.6 $\angle$-0.74	25.3 $\angle$ -2.43
500	54.43-j48.93	73.2 $\angle$-0.73	20.8 $\angle$ -2.60

* Magnitude in mA and phase angle in radians.

TABLE 3.4

Input admittance for a circular loop antenna on the earth surface

$f = 1500$ Hz, $\sigma = 0.002$ mho/m, $\varepsilon_r = 15$, $a = 0.0025$ m

Loop dia (m)	Y_{in} (milli mho)	I (0°) *	I (180°) *
50	9.64-j364.11	364.2 $\angle$-1.54	364.1 $\angle$ -1.58
100	17.74-j169.75	170.7 $\angle$-1.46	169.3 $\angle$ -1.61
150	25.40-j109.67	112.6 $\angle$-1.34	108.2 $\angle$ -1.67
200	32.64-j81.76	88.0 $\angle$-1.19	78.6 $\angle$ -1.75
250	39.35-j66.80	77.5 $\angle$-1.03	60.8 $\angle$ -1.85
300	45.36-j58.56	74.1 $\angle$-0.91	48.9 $\angle$ -1.98
350	50.45-j54.31	74.1 $\angle$-0.82	40.0 $\angle$ -2.12
400	54.44-j52.56	75.7 $\angle$-0.76	33.0 $\angle$ -2.71
450	57.29-j52.31	77.6 $\angle$-0.74	27.3 $\angle$ -2.43
500	59.06-j52.83	79.2 $\angle$-0.73	22.4 $\angle$ -2.59

* Magnitude in mA and phase angle in radians.

TABLE 3.5

Input admittance for a circular loop antenna on the earth surface

$f = 3000$ Hz, $\sigma = 0.001$ mho/m, $\varepsilon_r = 15$, $a = 0.001$ m

Loop dia (m)	Y_{in} (milli mho)	I (0°) *	I (180°) *
50	4.34-j165.70	165.8 $\angle$-1.54	165.7 $\angle$ -1.58
100	8.07-j77.72	78.1 $\angle$-1.47	77.5 $\angle$ -1.62
150	11.60-j50.36	51.7 $\angle$-1.34	49.7 $\angle$ -1.68
200	14.94-j37.61	40.5 $\angle$-1.19	36.2 $\angle$ -1.76
250	18.06-j30.77	35.7 $\angle$-1.04	28.1 $\angle$ -1.86
300	20.85-j26.99	34.1 $\angle$-0.91	22.5 $\angle$ -1.98
350	23.22-j25.05	34.2 $\angle$-0.82	18.5 $\angle$ -2.12
400	25.08-j24.27	34.9 $\angle$-0.77	15.3 $\angle$ -2.28
450	26.41-j24.17	35.8 $\angle$-0.74	12.7 $\angle$-2.44
500	27.24-j24.43	36.6 $\angle$-0.73	10.4 $\angle$ -2.60

* Magnitude in mA and phase angle in radians.

TABLE 3.6

Input admittance for a circular loop antenna on the earth surface

f = 3000 Hz, σ = 0.001 mho/m, ε_r = 15, a = 0.0025 m

Loop dia (m)	Y_{in} (milli mho)	I (0^o) *	I (180^o) *
50	4.82-j182.05	182.1 $\angle$-1.54	182.0 $\angle$ -1.58
100	8.87-j84.86	85.3 $\angle$-1.47	84.7 $\angle$ -1.62
150	12.70-j54.81	56.3 $\angle$-1.34	54.1 $\angle$ -1.68
200	16.32-j40.85	44.0 $\angle$-1.19	39.3 $\angle$ -1.76
250	19.69-j33.36	38.7 $\angle$-1.04	30.4 $\angle$ -1.86
300	22.69-j29.24	37.0 $\angle$-0.91	24.4 $\angle$ -1.98
350	25.24-j27.11	37.0 $\angle$-0.82	20.0 $\angle$ -2.12
400	27.25-j26.24	37.8 $\angle$-0.77	16.5 $\angle$ -2.27
450	28.67-j26.12	38.3 $\angle$-0.74	13.7 $\angle$ -2.43
500	29.56-j26.38	39.6 $\angle$-0.72	11.2 $\angle$ -2.59

* Magnitude in mA and phase angle in radians.

TABLE 3.7

Input admittance for a circular loop antenna on the earth surface

$f = 3000$ Hz, $\sigma = 0.002$ mho/m, $\varepsilon_r = 15$, $a = 0.001$ m

Loop dia (m)	Y_{in} (milli mho)	I (0°) *	I (180°) *
50	8.67-j165.77	166.0 $\angle$-1.52	165.7 $\angle$ -1.59
100	16.09-j78.21	79.8 $\angle$-1.37	77.4 $\angle$ -1.66
150	22.96-j51.87	56.8 $\angle$-1.15	49.4 $\angle$ -1.78
200	29.08-j40.87	50.2 $\angle$-0.95	35.3 $\angle$ -1.94
250	34.07-j36.39	49.9 $\angle$-0.82	26.6 $\angle$ -2.13
300	37.58-j35.20	51.5 $\angle$-0.75	20.3 $\angle$ -2.35
350	39.59-j35.53	53.2 $\angle$-0.73	15.4 $\angle$ -2.58
400	40.37-j36.30	54.3 $\angle$-0.73	11.5 $\angle$ -2.81
450	40.41-j36.95	54.8 $\angle$-0.74	8.1 $\angle$ -3.03
500	40.11-j37.32	54.8 $\angle$-0.75	5.3 $\angle$ -3.04

TABLE 3.8

Input admittance for a circular loop antenna on the earth surface

$f = 3000$ Hz, $\sigma = 0.002$ mho/m, $\varepsilon_r = 15$, $a = 0.0025$ m

Loop dia (m)	Y_{in} (milli mho)	I (0°) *	I (180°) *
50	9.61-j182.12	182.4 $\angle$-1.52	182.0 $\angle$ -1.59
100	17.69-j85.40	87.2 $\angle$-1.37	84.5 $\angle$ -1.66
150	25.14-j56.46	61.8 $\angle$-1.15	53.7 $\angle$ -1.78
200	31.76-j44.40	54.6 $\angle$-0.95	38.4 $\angle$ -1.94
250	37.13-j39.47	54.2 $\angle$-0.82	28.8 $\angle$ -2.13
300	40.92-j38.13	55.9 $\angle$-0.75	22.0 $\angle$ -2.35
350	43.07-j38.45	57.7 $\angle$-0.73	16.7 $\angle$ -2.57
400	43.91-j39.25	58.9 $\angle$-0.73	12.3 $\angle$ -2.80
450	43.95-j39.94	59.4 $\angle$-0.74	8.7 $\angle$ -3.02
500	43.62-j40.34	59.4 $\angle$-0.75	5.6 $\angle$ -3.06

* Magnitude in mA and phase angle in radians.

TABLE 3.9

Input admittance for a circular loop antenna on the earth surface

f = 3000 Hz, σ = 0.01 mho/m, ε_r = 15.0, a = 0.0778 m

Loop dia (m)	Y_{in} (mho)	I (0^o) *	I (180^o) *
10	0.025-j1.989	1.989 $\angle$ -1.56	1.990 $\angle$ -1.57
20	0.040-j0.857	0.858 $\angle$ -1.52	0.856 $\angle$ -1.59
30	0.054-j0.529	0.531 $\angle$ -1.47	0.527 $\angle$ -1.61
40	0.068-j0.378	0.384 $\angle$ -1.39	0.375 $\angle$ -1.64
50	0.080-j0.293	0.304 $\angle$ -1.30	0.288 $\angle$ -1.68
75	0.110-j0.192	0.221 $\angle$ -1.05	0.177 $\angle$ -1.81
100	0.134-j0.153	0.203 $\angle$ -0.85	0.122 $\angle$ -2.01
125	0.152-j0.139	0.206 $\angle$ -0.74	0.088 $\angle$ -2.23

* Magnitude in ampere and phase angle in radians.

distribution in the loop. All integrations have been expressed in closed forms.

For numerical computation, the circular loop has been approximated by 36 equal and linear segments. To evaluate $\Psi(m,n)$, the first eight terms of the series (3.47) have been used. To check correctness of the numerical method, circular loop antennas in free space have been analysed using similar series expressions with eight term approximation, and these numerical results have been found to be in close agreement with the published results [9] for $k_o b \leq 1.3$.

For a very small loop which almost carries an uniform current, the computation of input impedance by this numerical method is difficult to accomplish. A small loop (electrically) can be identified by a small value of ω. When ω is very small the impedance Z^A_{mn} due to the magnetic vector potential is also very small, as $Z^A_{mn} \propto \omega$, but on the other hand, $Z^\phi_{mn} \propto \frac{1}{\omega}$. Since, for small values of ω, $Z^\phi_{mn} >> Z^A_{mn}$, the impedance matrix $[Z] = [Z^A_{mn}+Z^\phi_{mn}]$ becomes $[Z^\phi_{mn}]$ due to the limited width of memory in a computer. This matrix is singular, since an uniform current distribution does not depend on $[Z^\phi_{mn}]$ but depends on $[Z^A_{mn}]$. To have a uniform current the effect of charges are to be cancelled mutually and it requires subtracting large and almost equal numbers representing Z^ϕ_{mn}. Practically, this is difficult to accomplish in a computer. In the present investigation the computer programme has been written in FORTRAN with double precision arithmatic calculations. It has been found that a loop

of ten metre diameter for frequency 3000 Hz and σ = 0.002 mho/m can be analyzed. This corresponds to $|k_1|b \simeq 0.03$. A loop with $|k_1|b < 0.02$, does not lead to convergence. In Chapter 4 a closed form expression will be developed for self-impedance of a circular loop antenna on the earth surface.

3.9 THE LOOP ON THE EARTH SURFACE AS A HOMOGENEOUS MEDIUM PROBLEM

The loop antenna on the earth surface can be viewed as a homogeneous medium problem by using an effective propagation constant. The following effective propagation constant has been suggested by Popovic [37]:

$$k_{eff}^2 = \frac{k_o^2 + k_1^2}{2} \quad . \tag{3.68}$$

It has been found that numerical results obtained by using k_{eff}, are marginally different from the results shown in Figures 3.7 to 3.11, which have been obtained via Sommerfeld type integral representations. To understand this, a comparison of the potentials obtained from k_{eff} with the potentials used in this chapter will be useful.

The vector and the scalar potentials due to a current element of length dl, at a point at distance r from the source can be written in terms of k_{eff} as

$$\bar{A}_{eff}(r) = \frac{\mu_o I \overline{dl}\, e^{-jrk_{eff}}}{4\pi r} \tag{3.69a}$$

$$\phi_{eff}(r) = \frac{qdle^{jrk_{eff}}}{4\pi r\varepsilon_{eff}} \qquad (3.69b)$$

where, $$\varepsilon_{eff} = \frac{k_{eff}^2}{\omega^2\mu_o} \quad . \qquad (3.69c)$$

The expressions (3.69a) and (3.69b) can be written in the following series form :

$$A_{eff}(r) = \frac{\mu_o I\overline{dl}}{4\pi} f(r,k_o,k_1) \qquad (3.70a)$$

$$\phi_{eff}(r) = \frac{qdl}{4\pi\varepsilon_{eff}} f(r,k_o,k_1) \qquad (3.70b)$$

where

$$f(r,k_o,k_1) = \frac{1}{r} - j\frac{(k_1^2+k_o^2)^{1/2}}{\sqrt{2}} - \frac{r(k_1^2+k_o^2)}{4} + j\frac{r^2(k_1^2+k_o^2)^{3/2}}{12\sqrt{2}} + \frac{r^3(k_1^2+k_o^2)^2}{96} + \cdots \qquad (3.70c)$$

Expressions (3.69a) and (3.69b) can be compared with (3.19) and (3.17). Since, $k_o << |k_1|$, we can approximate these series expressions by putting $k_o=0$. With this approximation one gets

$$k_{eff} \simeq \frac{k_1}{\sqrt{2}} \quad , \qquad (3.71)$$

$$\varepsilon_{eff} \simeq \frac{k_1^2}{2\omega^2\mu_o}$$

and the expression (3.19) becomes

$$g_A(\bar{r}/\bar{r}')\Big|_{k_o=0} = \frac{\mu_o}{4\pi}\left[\frac{1}{r} - j\,\frac{2}{3}k_1 - \frac{k_1^2 r}{4} + j\,\frac{k_1^3 r^2}{15} + \frac{k_1^4 r^3}{72} + \ldots\right] . \qquad (3.72)$$

From the above one can see that

(i) the first term of the series (3.70b) is identical with the scalar potential given by (3.17) and

(ii) the series representations (3.70a) and (3.72) match closely, at least upto first few terms.

CHAPTER 4

SELF IMPEDANCE OF A SMALL LOOP ANTENNA ON THE EARTH SURFACE

4.1 INTRODUCTION

In this chapter we consider a small loop antenna on the earth surface and assume that the loop is carrying an uniform current. The self impedance (input impedance) of a small loop in free space can be computed by adding the radiation resistance with the self inductance (reactance) of the loop. The inductance can be computed using Neumann's formula. The radiation resistance is derived by integrating the radiated power over a large sphere. When the loop is on the earth surface, there will be dissipation in the body of the earth, as well as radiation to the free space. The equivalent resistance which represents these power outflows from the antenna can not be derived by taking the same approach used for radiation resistance in free space. The Neumann's formula in its basic form is expressed in terms of a d.c. magnetic vector potential. We shall replace this d.c. potential by a time varying potential for computing the self impedance for a small loop antenna on the earth surface.

4.2 NEUMANN'S FORMULA

Fig. 4.1 describes a circular loop made up of a conducting wire. The mean diameter of the loop is 2b and the radius of the wire is a. The self inductance of the loop is composed of two parts: One part is due to the magnetic flux enclosed by the

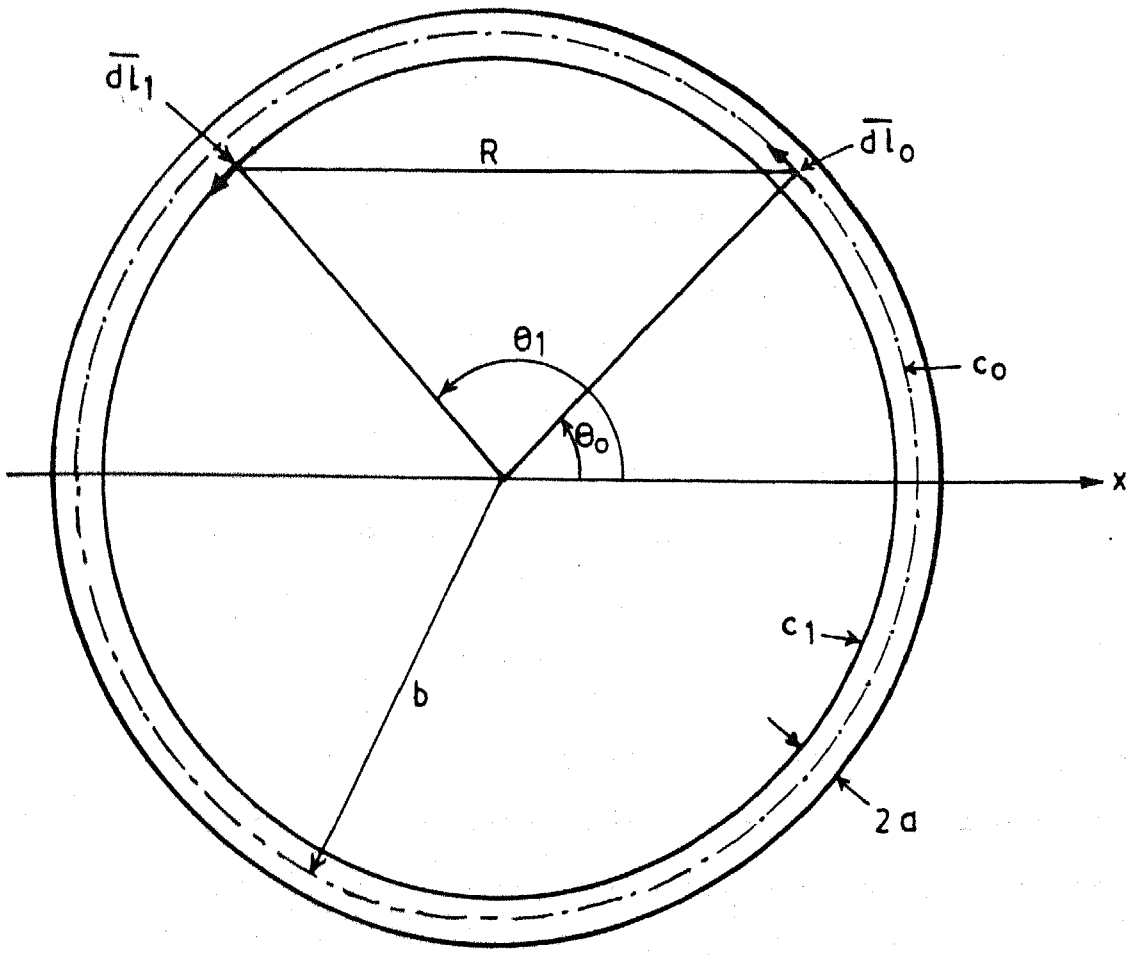

Fig. 4.1 A circular conducting loop.

contour C_1, and the other part is due to the flux inside the conductor. Let L_e is the inductance due to the flux enclosed by C_1. This inductance can be obtained by using the Neumann's formula

$$L_e = \frac{\mu_o}{4\pi} \int_{C_o} \int_{C_1} \left(\frac{1}{R}\right) \overline{dl}_o \cdot \overline{dl}_1 \quad . \tag{4.1}$$

This expression assumes that the current distribution inside the conductor can be replaced by a filamentary current defined by contour C_o to obtain the external flux enclosed by the contour C_1. Our aim is to incorporate necessary modifications to (4.1) so that it can be used for the computation of self impedance (resistance and reactance) of small antennas on the earth surface.

4.2.1 Modified Neumann's Formula

The right hand side of (4.1) can be identified as the integral of the magnetic vector potential along the contour C_1 due to an unit d.c. current flowing along the contour C_o. If the current is time varying with a small angular frequency ω, the induced e.m.f. associated with L_e is given by

$$E_{b1} = -j\omega L_e$$

$$= \frac{-j\omega\mu_o}{4\pi} \int_{C_o} \int_{C_1} \left(\frac{1}{R}\right) \overline{dl}_o \cdot \overline{dl}_1 \quad . \tag{4.2}$$

Let us assume that the wire is a perfect conductor. Then, under time varying condition there will not be any flux inside the conductor. The inductance L_e is now equal to the self inductance

of the loop. The applied voltage which must act opposite to E_{b1} is given by

$$V_i = \frac{j\omega\mu_o}{4\pi} \int_{C_o} \int_{C_1} \left(\frac{1}{R}\right) \overline{dl}_o . \overline{dl}_1 \quad . \qquad (4.3)$$

Expression (4.3) ignores the phase change experienced by the magnetic vector potential under time varying condition. To take this into account the d.c. magnetic vector potential is to be replaced by the time varying magnetic vector potential. For free space we can replace $\frac{\mu_o}{4\pi R}$ by $\mu_o e^{-jk_o R}/4\pi R$, and for a small loop on the earth surface the replacement is to be done by the magnetic vector potential given by (2.38). Self impedance Z_s of a loop is equal to the applied voltage when the loop carries an unit current. Hence Z_s for a constant current carrying loop on the earth surface can be written as

$$\begin{aligned} Z_s &= V_i / I \\ &= \frac{j\omega\mu_o}{2\pi(k_1^2 - k_o^2)} \int_{C_o} \int_{C_1} \frac{1}{R}\left[\frac{e^{-jk_o R}}{R} - \frac{e^{-jk_1 R}}{R}\right] \overline{dl}_o . \overline{dl}_1 \qquad (4.4) \end{aligned}$$

Expression (4.4) can be written in a series form by using (3.19) as

$$Z_s = \frac{j\ \omega\ \mu_o}{4\pi} \int_{C_o} \int_{C_1} \left[B_1\left(\frac{1}{R}\right) + B_2 + B_3 R + B_4 R^2 + B_5 R^3 + \ \ldots\right] \ \overline{dl}_o . \overline{dl}_1$$

(4.5a)

where $B_1 = 1$

$$B_2 = -\frac{j2}{3}\left[\frac{k_1^3 - k_o^3}{k_1^2 - k_o^2}\right]$$

$$B_3 = -\frac{1}{4}\left[\frac{k_1^4 - k_o^4}{k_1^2 - k_o^2}\right]$$

$$B_4 = \frac{j}{15}\left[\frac{k_1^5 - k_o^5}{k_1^2 - k_o^2}\right] \qquad (4.5b)$$

$$B_5 = \frac{1}{72}\left[\frac{k_1^6 - k_o^6}{k_1^2 - k_o^2}\right]$$

Retaining only the first four terms of the series, one can write

$$Z_s = \frac{j\omega\mu_o}{4\pi}\left[I_1(R) + B_2 I_2(R) + B_3 I_3(R) + B_4 I_4(R)\right] \qquad (4.6a)$$

where

$$I_1(R) = \int_{C_o}\int_{C_1}\left(\frac{1}{R}\right)\overline{dl}_o.\overline{dl}_1 \qquad (4.6b)$$

$$I_2(R) = \int_{C_o}\int_{C_1}\overline{dl}_o.\overline{dl}_1 \qquad (4.6c)$$

$$I_3(R) = \int_{C_o}\int_{C_1} R\,\overline{dl}_o.\overline{dl}_1 \qquad (4.6d)$$

$$I_4(R) = \int_{C_o}\int_{C_1} R^2\,\overline{dl}_o.\overline{dl}_1 \qquad (4.6e)$$

4.2.2 Evaluation of the integrals

First we consider the integral $I_1(R)$. The magnitude of $\overline{dl}_o$ and $\overline{dl}_1$ are given by

$$|\overline{dl}_o| = b\, d\theta_o \ , \ |\overline{dl}_1| = (b-a)\, d\theta_1 \simeq b\, d\theta_1 \quad . \tag{4.7a}$$

The angle between $\overline{dl}_o$ and $\overline{dl}_1$ is $(\theta_1-\theta_o)$, and hence

$$\overline{dl}_o . \overline{dl}_1 = b^2 \cos(\theta_1-\theta_o)\, d\theta_o d\theta_1 \quad . \tag{4.7b}$$

The distance R between $\overline{dl}_o$ and $\overline{dl}_1$ is given by

$$R^2 = b^2 + (b-a)^2 - 2b(b-a)\cos(\theta_1-\theta_o) \tag{4.7c}$$

From (4.6b) and (4.7a) - (4.7c), one can write

$$I_1(R) = b^2 \int_0^{2\pi} \int_0^{2\pi} \frac{\cos(\theta_1-\theta_o)\, d\theta_1\, d\theta_o}{\left[b^2+(b-a)^2-2b\,(b-a)\cos(\theta_1-\theta_o)\right]^{1/2}} \ . \tag{4.8a}$$

We may integrate over θ_1 first (for a fixed value of θ_o). Defining

$(\theta_1 - \theta_o) = \theta$, one gets

$$I_1(R) = b^2 \int_0^{2\pi} \int_0^{2\pi} \frac{\cos\theta\, d\theta\, d\theta_o}{\left[b^2+(b-a)^2 - 2b(b-a)\cos\theta\right]^{1/2}} \tag{4.8b}$$

This integral may be evaluated in any order. Integrating over θ_o one gets

$$I_1(R) = 2\pi b^2 \int_0^{2\pi} \frac{\cos\theta \, d\theta}{R_1} \tag{4.8c}$$

where

$$R_1 = \left[b^2 + (b - a)^2 - 2b(b - a) \cos\theta \right]^{1/2}$$

$$= \left[a^2 + 4b \, (b - a) \sin^2(\theta/2) \right]^{1/2} . \tag{4.8d}$$

The expression (4.8c) can be evaluated in terms of elliptic integrals [38]. The final result is

$$I_1(R) = 4\pi b \left[(\frac{2}{k_s} - k_s)K - \frac{2}{k_s} E \right] \tag{4.9a}$$

where $k_s^2 = 4b \, (b - a)/(2b - a)^2$ and K and E are elliptic integrals given by

$$K = \int_0^{\pi/2} \frac{dx}{(1 - k_s^2 \sin^2 x)^{1/2}} \tag{4.9b}$$

$$E = \int_0^{\pi/2} (1 - k_s^2 \sin^2 x)^{1/2} \, dx \tag{4.9c}$$

For a << b, the result of (4.9a) reduces to

$$I_1(R) = 4\pi b \left\{\ln(8b/a) - 2\right\} \qquad (4.10)$$

By going through similar exercises which were performed to arrive at (4.8c) from (4.8a), the integrals $I_1(R)$, $I_2(R)$ and $I_3(R)$ can be written as follows.

$$I_2(R) = 2\pi b^2 \int_0^{2\pi} \cos\theta \, d\theta$$

$$= 0 \qquad (4.11)$$

$$I_3(R) = 2\pi b^2 \int_0^{2\pi} \left[a^2+4b\,(b - a)\,\sin^2(\theta/2)\right]^{1/2} \cos\theta \, d\theta$$

$$= 2\pi b^2 \int_0^{2\pi} R_1 \cos\theta \, d\theta \qquad (4.12)$$

$$I_4(R) = 2\pi b^2 \int_0^{2\pi} R_1^2 \cos\theta \, d\theta \quad . \qquad (4.13)$$

Since, a<<b, R_1 in (4.12) and (4.13) can be approximated as

$$R_1 \simeq 2b \sin(\theta/2) \; . \qquad (4.14)$$

Substituting R_1 from (4.14) in (4.12) one can write

$$I_3(R) = 4\pi b^3 \int_0^{2\pi} \cos\theta . \sin(\theta/2)\, d\theta$$

$$= -\frac{16\pi b^3}{3} \quad . \tag{4.15}$$

Similarly one gets

$$I_4(R) = 8\pi b^4 \int_0^{2\pi} \cos\theta . \sin^2(\theta/2)\, d\theta$$

$$= 4\pi b^4 \int_0^{2\pi} (1 - \cos\theta)\cos\theta\, d\theta$$

$$= -4\pi^2 b^4 \quad . \tag{4.16}$$

Substituting $I_1(R)$ where (i = 1,4), in (4.6a) and using (4.5b), one can write

$$Z_s = Z_{s1} + Z_{s2} + Z_{s3} + Z_{s4} \tag{4.17a}$$

where

$$Z_{s1} = j\omega\mu_o b \left\{ \ln(8b/a) - 2 \right\} \tag{4.17b}$$

$$Z_{s2} = 0 \tag{4.17c}$$

$$Z_{s3} = j\left(\frac{1}{3}\right) \omega\mu_o b^3 \left(\frac{k_1^3 + k_1^2 k_o + k_1 k_o^2 + k_o^3}{k_1 + k_o}\right) \tag{4.17d}$$

$$Z_{s4} = \left(\frac{1}{15}\right) \pi\omega\mu_o b^4 \left(\frac{k_1^4 + k_1^3 k_o + k_1^2 k_o^2 + k_1 k_o^3 + k_o^4}{k_1 + k_o}\right) . \tag{4.17e}$$

When the loop is in a homogeneous medium (lossy or free space) with $k_1 = k_o = k$, one obtains

$$Z_{s3}\Big|_{k_1=k_o=k} = j(\tfrac{2}{3})\ \omega\ \mu_o\ k^2\ b^3 \qquad (4.18a)$$

$$Z_{s4}\Big|_{k_1=k_o=k} = (\tfrac{1}{6})\pi\ \omega\ \mu_o\ k^3\ b^4 \qquad (4.18b)$$

With this, the expression for Z_s becomes identical to the expression given in [9] for a small loop in a homogeneous medium. It can be seen that for free space, Z_{s1} and Z_{s3} are reactive, whereas Z_{s4} is resistive. The inductance associated with Z_{s1} can be identified as L_e the inductance of a loop due to the external magnetic flux. The term Z_{s4} is the radiation resistance for a small loop in free space.

For a loop antenna on the earth surface and operating at low frequencies, $|k_1| >> k_o$. This allows one to put $k_o=0$ in (4.17d) and (4.17e) without any significant error. Since $k_1^2 \simeq -j|k_1^2|$ one can write

$$Z_{s3} = j(\tfrac{1}{3})\ \omega\ \mu_o\ b^3(-j|k_1^2|)$$

$$= 40\pi k_o|k_1^2|\ b^3 \qquad (4.19a)$$

Since $k_1^2 \simeq -j\omega\mu_o\sigma$, (4.19a) can also be written as

$$Z_{S3} = \frac{1}{3}\omega^2\mu_o^2\sigma b^3 \quad . \tag{4.19b}$$

This term is resistive. The contribution from Z_{s4} is both resistive and reactive, but Z_{s3} is the dominant term. Neglecting the contribution from Z_{s4}, the self impedance can be written as

$$Z_s = R_L + jX_L \tag{4.20a}$$

where

$$R_L = 40\pi k_o |k_1^2| b^3 \tag{4.20b}$$

$$X_L = 120\pi k_o b \left\{ \ln\left(\frac{8b}{a}\right) - 2 \right\} \quad . \tag{4.20c}$$

It can be seen that for a small loop $R_L \propto b^3$. Since, $R_L << X_L$, conductance G_s, and susceptance B_s, can be written as

$$G_s = \frac{R_L}{R_L^2 + X_L^2}$$

$$\simeq \frac{R_L}{X_L^2}$$

and

$$B_s = \frac{-jX_L}{R_L^2 + X_L^2}$$

$$\simeq -j\frac{1}{X_L} \quad .$$

4.4 DISCUSSION OF RESULTS

Comparison of results obtained for small loops (where $|B_s|$ is atleast ten times greater than G_s) by using expression (4.20) and by the method of moments discussed in Chapter 3 leads to the following observations :

(i) Susceptance values are in close agreement with each other.

(ii) The conductance obtained using (4.20) is about an order of magnitude smaller than the values obtained from the method of moments. For the particular cases considered in Chapter 3 this difference has been found to be by a factor of 25 to 55.

(iii) The conductance given by (4.20) does not depend on the radius of the wire, but the values obtained by method of moments do depend on it.

The observations (i) to (iii) also hold good for loop antennas embedded in a hemogeneous dissipative medium [9]. It is useful to determine using a simple calculation procedure how large a physical loop can be treated as an electrically small loop. We consider a small loop as "small" when $\frac{G_s}{|B_s|} \leq 0.15$. When this ratio increases beyond this value the input admittance reaches saturation very rapidly. Since, B_s can be computed accurately using expression (4.20), it is desirable that the conductance G_s (or resistance R_L) is also computed accurately using a simple formula. It has been observed that if the input resistance value given by (4.19a) or (4.19b) is multiplied by factor F_c which is given by

$$F_c = \frac{2\pi}{3}\,\Omega$$

where

$$\Omega = 2\ln\left(\frac{2\pi b}{a}\right) \tag{4.21}$$

the new value agrees closely with that obtained by the method of moments within 12 percent. Using the factor F_c one can write input resistance R_{in} for a small loop antenna on the earth surface and operating at low frequency (so that $k_1^2 \simeq -j|k_1^2|$) as

$$R_{in} = \frac{2\pi}{9}\,\omega^2\mu_o^2\sigma b^3\Omega$$

$$= \frac{80\pi^2}{3}\,k_o|k_1^2|b^3\Omega\ . \tag{4.22}$$

It may be pointed out that for a small loop ($k_o b < 0.2$) in free space the radiation resistance given by (4.18b) can be used as the input resistance for a loop antenna. The disagreement observed for a loop on the earth surface is due to the fact that the real part of the current for a loop antenna on the earth surface varies to a large extent, while the imaginary part remains almost constant. Therefore, the assumption that the current is constant for a small loop on the earth surface, although can be made for the reactive part, the same does not hold good for the real part.

CHAPTER 5

PERFORMANCE OF COHERENT PSK RECEIVERS IN MINE ENVIRONMENT

5.1 INTRODUCTION

The performance of a ELF/VLF receiver operating in mine environment is strongly influenced by non-Gaussian atmospheric noise which is impulsive in nature, and the power line harmonics. The power line harmonics which are integral multiples of power frequency have strong interfering effect upto several kilohertz. In general, many approaches can be taken in evaluating receiver performance for a non-Gaussian noise, based on an appropriate noise model [10]. Two approaches are usually taken to develop a noise model at ELF/VLF, depending on the bandwidth of the receiver. At VLF the ratio of bandwidth to centre frequency is usually small and therefore the received noise may be considered as a narrow band process. At ELF this ratio is not small, and the noise should be treated as a wide band process.

Omura and Shaft [11] have considered VLF atmospheric noise as a narrow band process with a log-normal envelope of the form

$$a(t) = A\, e^{n(t)} \sin(\omega_o t + \theta)$$

where n(t) is a zero-mean real stationary Gaussian process. The exponential function emphasizes large amplitudes which have greater influence on the performance of a communication system. To evaluate receiver performance with this noise model, they

separately consider long and short integration times of the receiver. In case of long integration time the noise bursts get averaged out so that the central limit theorem can be applied. This allows one to consider the noise to be a Gaussian process. For short integration time intuitive as well as rigorous methods may be used. Though, the intuitive methods, in general, do not take into account the actual receiver structure, they can yield numerical results which are in good agreement with experimental values. However, it can not be justified on theoretical grounds. The rigorous methods are difficult to carry out by exact mathematical procedures. For example, in case of a PSK receiver with input signal $\sqrt{P}\ \sin\omega_o t$, the output is given by

$$V_o(T) = 2PT + 2\int_0^T A\, e^{n(t)} \cos(\omega_o t+\theta)\ \sqrt{2P}\ \sin\omega_o t\ dt.$$

The evaluation of this integral is very difficult due to the fact that the variables n(t) and θ may change over the integration period [0,T]. To evaluate this integral they assume T to be sufficiently small such that n(t) and θ are essentially constant over this time interval. This assumption is usually not true. However, they assume this in order to complete an otherwise extremely difficult mathematical problem. The justification for this assumption is given from the point of view of end results only, which are reasonably in good agreement with experimental values.

Field and Lewinstein [12] have modelled atmospheric noise as a two component random process. For ELF a wide-band approach and for VLF a narrow-band approach have been taken. The basis for the two component representation lies on the fact that wideband observation of ELF and VLF atmospheric noise reveals presence of intermittent, non-overlapping, large amplitude spike like pulses superimposed on a homogeneous background. These pulses are caused by local thunderstorm activity while the background is caused by large number of relatively weak, unresolved pulses from distant lightning flashes. They consider the background noise to be a zero-mean Gaussian random process, and assume a power-Rayleigh distribution for the impulsive component. The tails of the power-Rayleigh distribution falls off much more slowly as compared to a Gaussian density function. The model thus allows the relatively frequent occurence of large amplitude pulses. The two components are convolved to obtain the probability distribution function for the composite noise at the receiver input. The numerical results for noise amplitudes are in good agreement with experimental values. The amplitude density function can be directly used for receivers which employ envelope detection. However, for a non-envelope type receiver e.g., a coherent PSK receiver the probability density function at the receiver output should be known for computation of bit error rate. The methodology to accomplish this from the input density function has not been discussed by the authors. In this chapter we present a method to compute bit error rate for PSK receiver in atmospheric-type noise. We also consider the effectiveness of a direct sequence spread

spectrum receiver in presence of atmospheric noise, along with an interfering tone.

5.2 A NOISE MODEL FOR ATMOSPHERIC NOISE

We attempt to develop a model for the atmospheric noise which can reasonably describe the actual noise process, and at the same time allows to evaluate the receiver performance in a rigorous manner. The model is based on the wide band approach and it considers the atmospheric noise as a two component random process. One component is the background noise which is described by a zero-mean Gaussian process. The other component represents the non-overlapping pulses and it is considered as a discrete random process. These pulses although very spiky, have a finite width, but for convenience, these pulses are assumed to be pure impulses. The strength of an impulse is defined as the area under the finite width pulse which it replaces. The arrival of the pulses is assumed to be a stationary Poisson process. The pulses can be either positive or negative but they are assumed to be of same strength. This can be viewed as if the spikes are being clipped at a level much higher as compared to the Gaussian component. The two components are specified as follows.

Background noise

The background noise is assumed to be additive White Gaussian noise (AWGN) n_ω, with a two sided spectral density of $N_o/2$. This implies that the Gaussian noise has a spectrum that is much wider

than the bandwidth of the receiver and its spectral density is essentially constant over the receiver bandwidth.

Impulsive component

The impulsive component i(t) is represented by a sequence of impulses arriving at random points in time and can be written as

$$i(t) = \sum_{n=1}^{\infty} A_n \, \delta(t - \tau_n) \tag{5.1}$$

where $\delta(t)$ is the Dirac delta function, A_n is the amplitude of the impulse at time τ_n. A given impulse can be positive with probability P^+ and negative with probability P^-, i.e.,

$$\begin{aligned} &\text{Prob } (A_n = A_g) = P^+ \\ &\text{Prob } (A_n = -A_g) = P^- = (1-P^+) \end{aligned} \tag{5.2}$$

where A_g is the magnitude of the impulse. The Poisson arrival process for the impulses can be written as:

$$P(N) = \frac{(\lambda T)^N}{N!} \exp(-\lambda T) \quad \text{for } N = 0,1,2,.... \tag{5.3}$$

where P(N) is the probability of arrival of exactly N impulses in time duration T and λ is the average arrival rate.

This noise model is used to evaluate the performance of a coherent PSK receiver in atmospheric noise. A conventional PSK receiver can not perform satisfactorily in the presence of a strong continuous wave interference, for example, a power line harmonic tone. In such situations spread spectrum or other communication techniques have to be employed. A direct sequence spread spectrum receiver with PSK signal format can be treated as a conventional PSK receiver to evaluate the receiver performance in Gaussian as well as in atmospheric noise. A direct sequence spread spectrum transmitter with binary PSK signal format needs less bandwidth than for frequency hopped scheme. Since, power saving is a critical requirement for a trapped miner, the former has a decisive advantage over the latter from this pont of view. The following cases are considered.

(i) A coherent PSK receiver in absence of interfering tone,

(ii) Direct sequence spread spectrum receiver in presence of an interfering tone at the carrier frequency.

5.3 PSK RECEIVER

Figures 5.1a and 5.1b show a base-band data bit stream and the corresponding PSK modulated carrier wave. The base-band signal d(t) is polar and it takes the values of either 1 or -1 corresponding to the binary symbols 1 and 0 respectively. The symbols 1 and 0 are transmitted as $A_o \cos\omega_o t$ and $-A_s \cos\omega_o t$ respectively. Fig. 5.1c describes a coherent PSK receiver. The receiver multiplies the received waveform by the synchronized

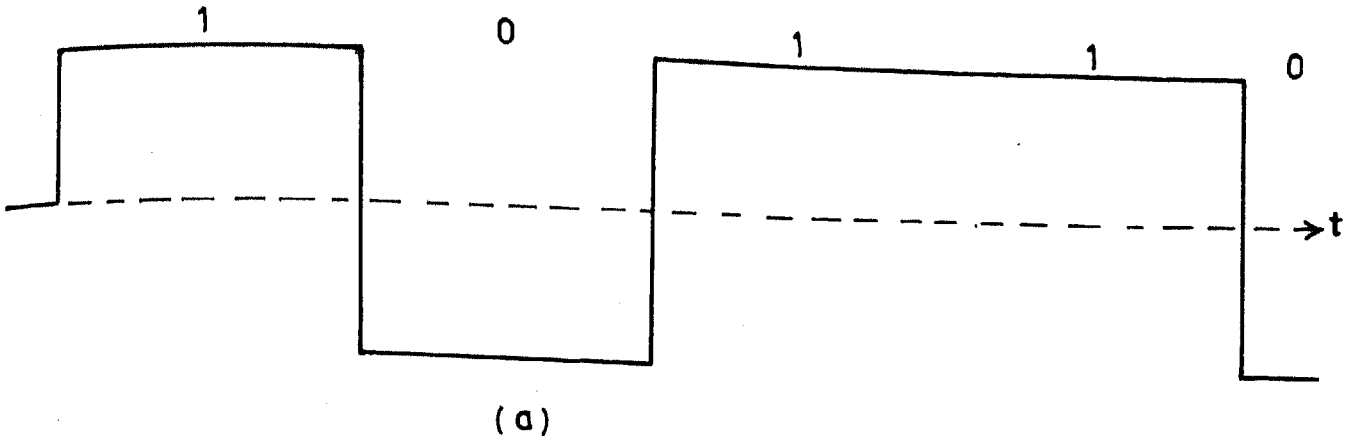

(a)

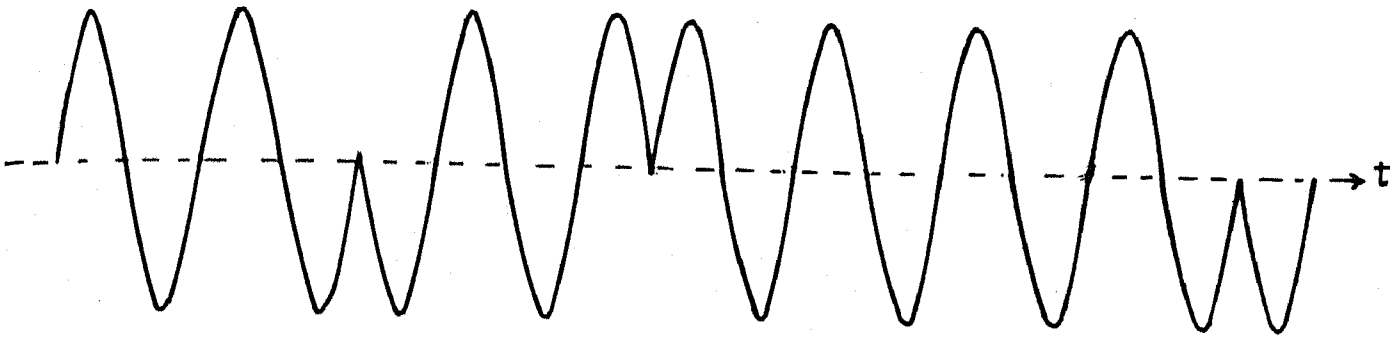

(b)

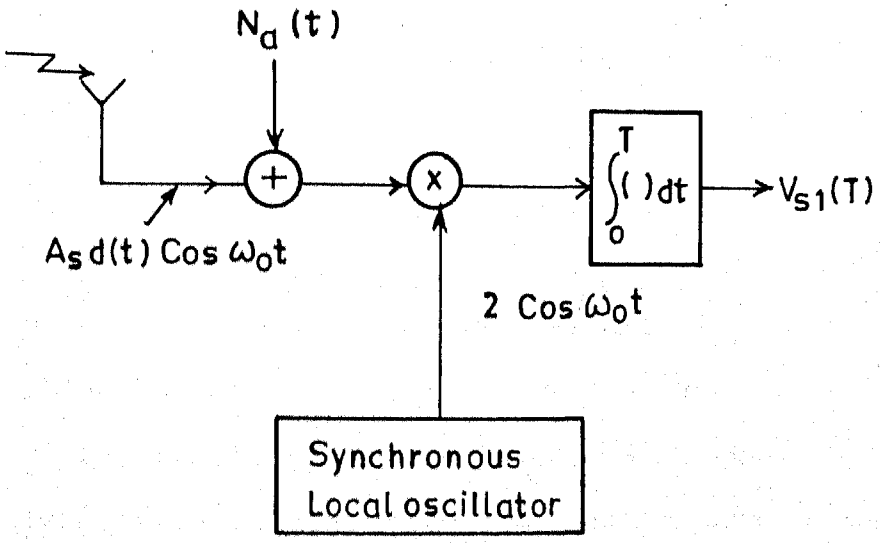

(c)

Fig.5.1 (a) Base band data bit stream.
(b) PSK modulated carrier wave.
(c) Coherent PSK receiver.

replica of the unmodulated carrier. We assume a perfect synchronization for the carrier.

Let, -1 be the transmitted data symbol. The received signal can be written as :

$$S_1(t) = -A_s \cos \omega_o t + N_a(t) \qquad (5.4)$$

where $N_a(t)$ is a random variable which represents the atmospheric noise. The receiver output $V_{s1}(T)$ is given by

$$V_{s1}(T) = -2A_s \int_0^T \cos^2 \omega_o t \, dt + N_A(T)$$

$$= -A_s \int_0^T (\cos 2\omega_o t + 1) \, dt + N_A(T)$$

$$= -A_s T + N_A(T) \qquad (5.5)$$

where the double frequency component $2\omega_o$ has been ignored. The random variable $N_A(T)$is due to the atmospheric noise. Probability density function (PDF) of $N_A(T)$ is to be known to compute the probability of bit error. Assuming a data symbol to be equally likely to be ± 1, the error probability p_{e1} can be written as :

$$p_{e1} = \text{Prob} \left[\left\{ -A_s T + N_A(T) \right\} > 0 \right] . \qquad (5.6)$$

We now consider the evaluation of the PDF of $N_A(T)$.

5.3.1 PDF for $N_A(T)$

Let $p_1(x)$ and $p_2(y)$ be the PDFs at the integrator output due to the Gaussian and the impulsive component of atmospheric noise. Convolution of $p_1(x)$ with $p_2(y)$ gives the PDF for the random variable $N_A(T)$. One can write the resulting distribution function $p_3(z)$ as :

$$p_3(z) = \int_{-\infty}^{\infty} p_1(z-y)\, p_2(y)\, dy \qquad (5.7)$$

where, z represent the random variable $N_A(T)$. The PDF $p_1(x)$ is a zero-mean Gaussian density function with variance $\sigma^2 = N_o T$ and can be written as:

$$p_1(x) = \frac{e^{-x^2/2\sigma^2}}{\sigma\sqrt{2\pi}} . \qquad (5.8)$$

Integrator output due to a single impulse

Let an impulse arrives at time t_1 during the integration period [0,T]. The integrator output V_p due to this impulse is given by

$$V_p = \int_0^T \pm A_g \delta(t-t_1) 2\cos\omega_o t \, dt$$

$$= \pm 2 A_g \cos\omega_o t_1 . \qquad (5.9a)$$

We consider the worst case situation, and replace $\cos\omega_o t$ by a rectangular wave form $C_g(t)$ as shown in Fig. 5.2. With this replacement the output due to the impulse can be either $+2A_g$ or $-2A_g$, depending on the polarity of the impulse and the polarity of the half cycle (pulse) of $C_g(t)$ during which the impulse occurs. Defining, $A_G = 2A_g$, the output due to a single impulse can be written as

$$V_p = \pm A_G \qquad (5.9b)$$

The following possibilities can happen.

(a) The impulse is positive and occurs during a positive pulse: $V_p = A_G$.

(b) The impulse is negative and occurs during a negative pulse: $V_p = A_G$.

(c) The impulse is positive and occurs during a negative pulse: $V_p = -A_G$.

(d) The impulse is negative and occurs during a positive pulse: $V_p = -A_G$.

Assuming there are equal number of positive and negative half cycles in the wave form $C_g(t)$ in the interval [0,T], it is equally likely that the impulse will occur during a positive or negative half cycle of $C_g(t)$. Given that an impulse has arrived, one can deduce the following

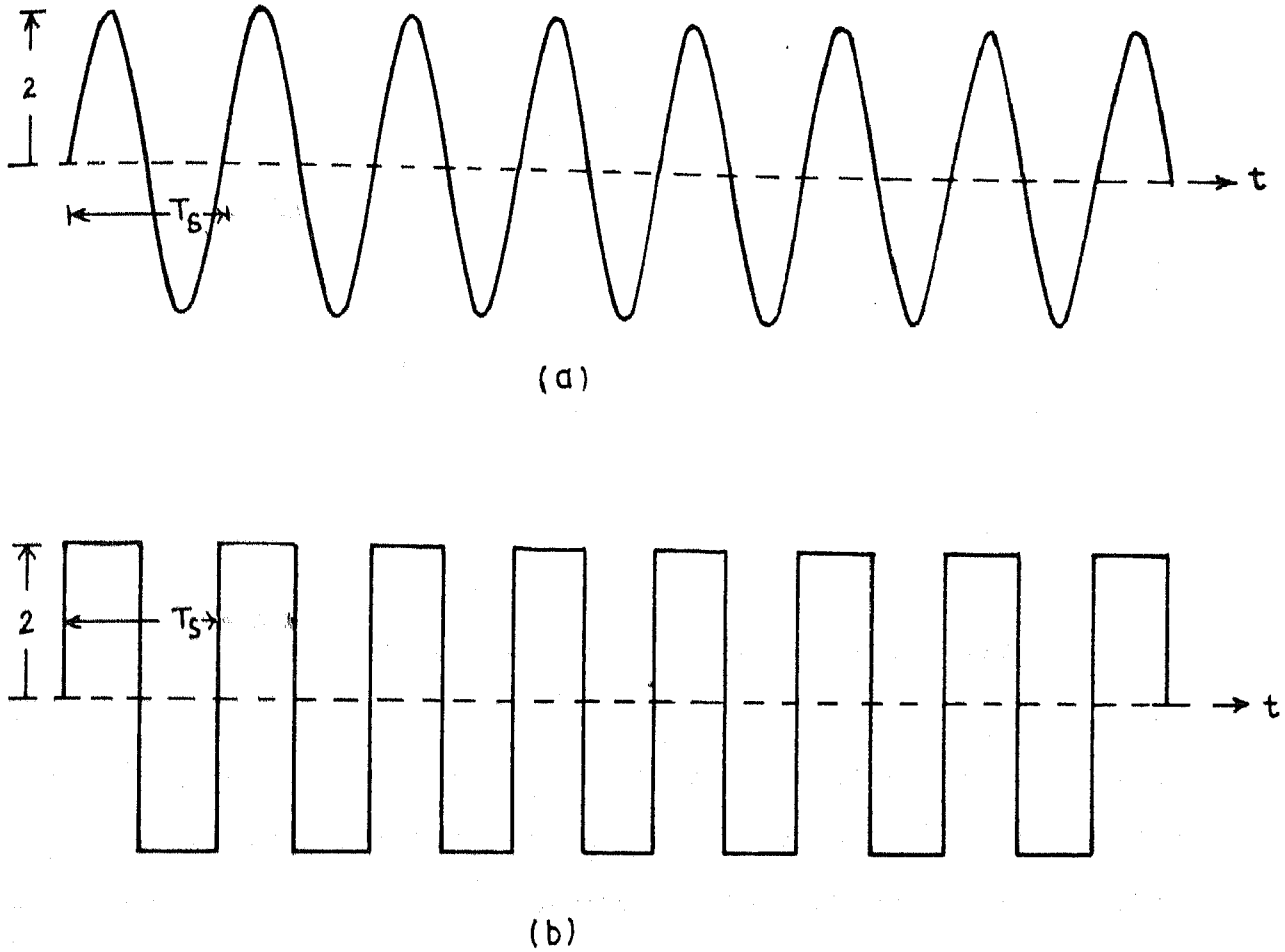

Fig.5.2 (a) Local sinusoidal carrier waveform $2\cos\omega_o t$
(b) Rectangular waveform $C_s(t)$ used in place of the local carrier sinusoid for computational purposes.

$$\text{Prob}\left[V_p = A_G\right] = \frac{1}{2} P^+ + \frac{1}{2} P^-$$

$$= \frac{1}{2} P^+ + \frac{1}{2} (1-P^+)$$

$$= \frac{1}{2} . \qquad (5.10)$$

$$\text{Prob}\left[V_p = -A_G\right] = \frac{1}{2} P^- + \frac{1}{2} P^+$$

$$= \frac{1}{2} .$$

From (5.10), it is seen that the output for a given impulse is equally likely to be $\pm A_G$, and it is independent of any probability that may be attached to the impulse being positive or negative. Thus it allows us to assume that all the impulses are of positive polarity without any loss of generality. When there are more than one impulse (during the time interval [0,T]), this argument still holds.

Integrator output due to any number of impulses

Suppose two impulses have occured during the interval [0,T]; the output can be $2A_G$, 0 and $-2A_G$, which can be illustrated by the following possible combinations :

$$\left\{(A_G, A_G) \rightarrow 2A_G\right\}, \left\{(A_G, -A_G) \rightarrow 0\right\}, \left\{(-A_G, A_G) \rightarrow 0\right\}, \left\{(-A_G, -A_G) \rightarrow -2A_G\right\}$$

The first term inside the brackets is the output due to the first impulse and the second one is due to the second impulse. Each of the above combinations takes place with probability $\frac{1}{4}$. In a similar way output for the arrival of three impulses can be obtained. When there are exactly one, two or three impulses, the conditional probabilities can be written as follows:

(a) **Number of impulses = 1**

Output V_p	A_G	0	$-A_G$
Prob	$\frac{P(1)}{2}$	0	$\frac{P(1)}{2}$

(b) **Number of impulses = 2**

Output V_p	$2A_G$	A_G	0	$-A_G$	$-2A_G$
Prob	$\frac{P(2)}{4}$	0	$\frac{P(2)}{2}$	0	$\frac{P(2)}{4}$

(c) **Number of impulses = 3**

Output V_p	$3A_G$	$2A_G$	A_G	0	$-A_G$	$-2A_G$	$-3A_G$
Prob	$\frac{P(3)}{8}$	0	$\frac{3P(3)}{8}$	0	$\frac{3P(3)}{8}$	0	$\frac{P(3)}{8}$

where P(1), P(2) and P(3) are probabilities of arrival of exactly one, two and three impulses during the interval [0,T]. The following observations can be made from these examples.

(a) Prob $(V_p = KA_G)$ = Prob $(V_p = -KA_G)$, where K = 0,1,2,3,...

(b) For N number of impulses the maximum value of K is equal to N or $K \leq N$.

(c) When N is even (odd), non-zero probabilities i.e. Prob$(V_p = KA_G)$ > 0, occur for even (odd) values of K.

For integrator output to be equal to KA_G, when N impulses have arrived, the number of impulses each contributing A_G is equal to $\frac{K+N}{2}$, where $\frac{N-K}{2}$ impulses contribute $-A_G$ (by each of them), subject to the even-even and odd-odd relationship between K and N. For example to get output equal to A_G (K=1) when there are 3 impulses, one can have the following combinations, where in each of the triplet there are two A_G and one $-A_G$.

$$\left\{(A_G, A_G, -A_G) \rightarrow A_G\right\},\ \left\{(A_G, -A_G, A_G) \rightarrow A_G\right\},\ \left\{(-A_G, A_G, A_G) \rightarrow A_G\right\}.$$

In general one can write the conditional probability for $V_p = KA_G$ when there are N impulses, as follows.

Letting $u = \frac{N+K}{2}$, one can write

$$\text{Prob}(KA_G|N) = \frac{\text{Prob}\left\{u \Rightarrow +ve,\ (N-K) \Rightarrow -ve\right\}}{\text{Prob [N arrivals]}}$$

where u => +ve means u number of impulses occur during the period of positive half cycles of $C_a(t)$. Similar is the meaning for (N-u) => -ve. Hence, one can write

$$\text{Prob}\ (KA_G|N) = \frac{\dfrac{\exp(-\lambda T/2)(\lambda T/2)^u}{u\ !} \quad \dfrac{\exp(-\lambda T/2)(\lambda T/2)^{N-u}}{(N-u)\ !}}{\exp(-\lambda T)\ (\lambda T)^N/N\ !}$$

$$= \begin{bmatrix} N \\ u \end{bmatrix} \left(\frac{1}{2}\right)^N$$

$$= \begin{bmatrix} N \\ \frac{N+K}{2} \end{bmatrix} \left(\frac{1}{2}\right)^N \quad . \qquad (5.11)$$

Hence, the unconditional probability for $V_p = KA_G$ (with $K \leq N$) is given by

$$\text{Prob}\ (KA_G) = \sum_{N=K+2i}^{\infty} P(N) \begin{bmatrix} N \\ \frac{N+K}{2} \end{bmatrix} \left(\frac{1}{2}\right)^N \qquad (5.12)$$

$$i = 0,1,2,3....$$

This is a discrete probability distribution function with the symmetry $\text{Prob}(KA_G) = \text{Prob}(-KA_G)$. The PDF defined by (5.12) was earlier denoted by $p_2(y)$ in section (5.3).

Comparing (5.7) with (5.12), the distribution function $p_3(z)$ for the random variable $N_A(T)$ at the integrator output due to atmospheric noise can be written as :

$$p_3(z) = \sum_{N=K+2i}^{\infty} \int_{-\infty}^{\infty} p_1(z-\delta(y-KA_G))\ P(N) \begin{bmatrix} N \\ \frac{K+N}{2} \end{bmatrix} (\tfrac{1}{2})^N\ dy \qquad (5.13)$$

$$i = 0,1,3.....$$

where $P_1(x)$ and $P(N)$ are given by (5.8) and (5.3) respectively. The integral (5.13) for a given value of K is equivalent to shifting the Gaussian PDF given by $p_1(x)$ to the position KA_G and multiply by the factor f_K which can be seen from (5.13) to be

$$f_K = P(N) \begin{bmatrix} N \\ \frac{K+N}{2} \end{bmatrix} \left(\frac{1}{2} \right)^N . \qquad (5.14)$$

The PDF $p_3(z)$ is an infinite summation of such weighted and shifted Gaussian shaped PDFs. The bit error rate (BER) for a PSK receiver can be computed by using (5.6). Before computing the numerical results for a PSK receiver, let us formulate for the error probability in a direct sequence spread spectrum receiver.

5.4 DIRECT SEQUENCE SPREAD SPECTRUM COMMUNICATION SYSTEM

Fig. 5.3 shows a direct sequence (DS) spread spectrum communication system with binary PSK as the modulation format. In the transmitter the carrier containing data stream is multiplied by a pseudo random or pseudo noise (PN) sequence. The PN sequence

changes its state many times during a data pulse of duration T. This leads to phase shifting of the carrier at a much higher rate than that which would have been caused by a data stream alone. The multiplication process by the PN sequence can be identified as to spread the spectrum of the signal. The receiver multiplies the received signal with a synchronized replica of the transmitter's PN sequence. This remultiplication at the receiver despreads the spectrum of the signal which now appears in the original bandwidth of the data stream. The subsequent recovery of data is identical to that of a conventional PSK receiver.

Figures 5.4a and 5.4b describe the relationship between a data bit and the PN sequence which is being generated from a four stage maximal length shift register shown in Fig.5.4c. If the register has N stages, one can write the following:

$$\begin{aligned} &\text{(i)} \quad \text{Length of the sequence} && = 2^N - 1. \\ &\text{(ii)} \quad \text{No. of ones in the sequence} && = 2^{(N-1)}. \\ &\text{(iii)} \quad \text{No. of zeros in the sequence} && = 2^{(N-1)} - 1. \end{aligned} \qquad (5.15)$$

Each state of the PN sequence is called a chip and the chip duration is denoted by T_c. If a data bit is T second long, then $T_c = \frac{T}{2^N - 1}$ seconds.

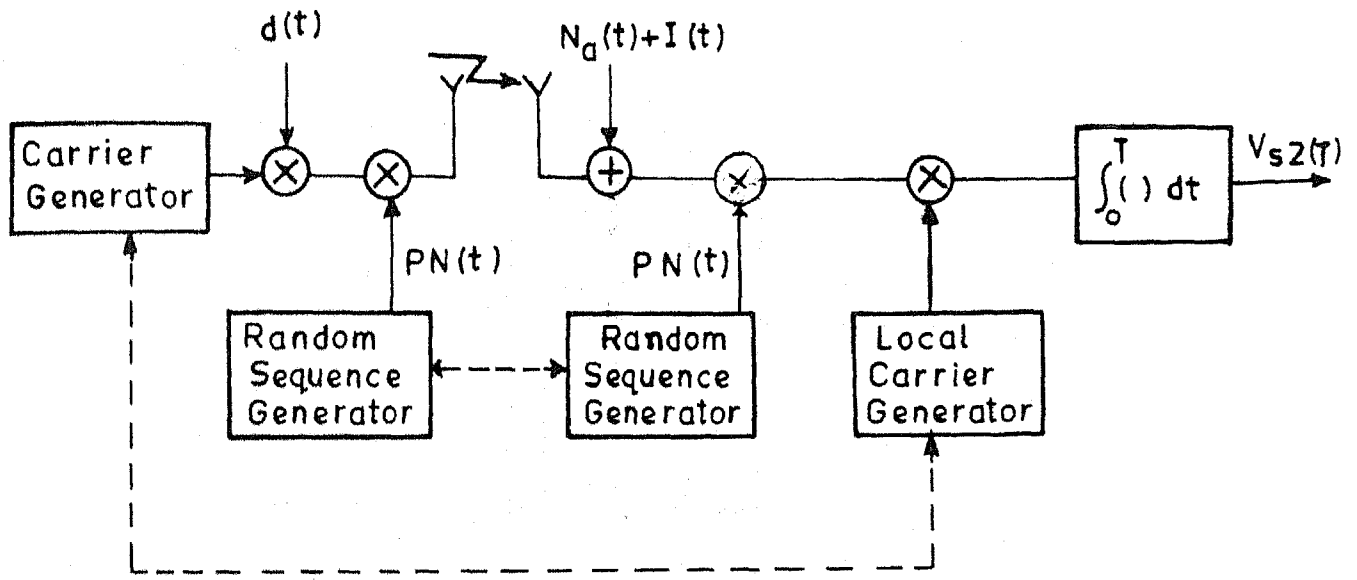

Fig.5.3 Adirect sequence spread spectrum communication system.

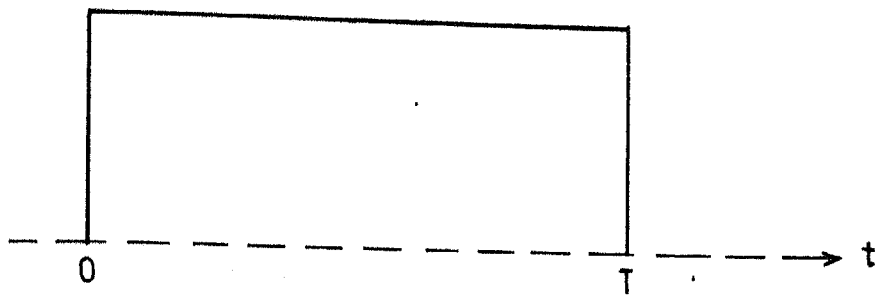

(a)

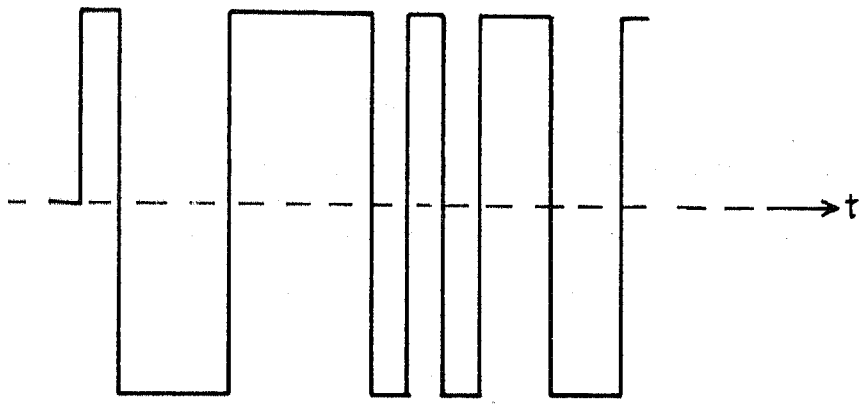

(b)

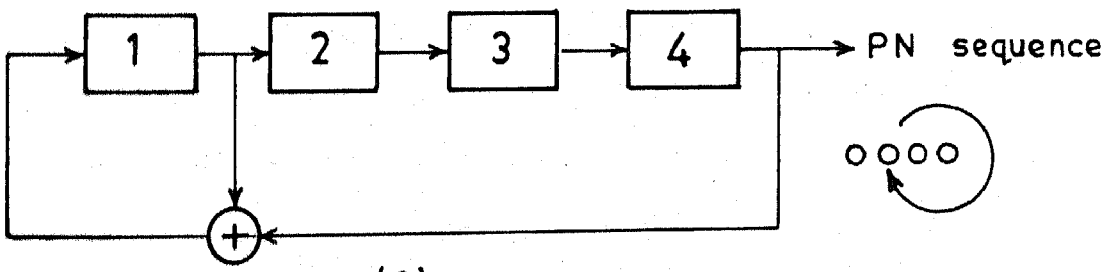

(c)

If at t = 0, the register content is 0001 (left to right) the sequence is

100011110101100

Fig.5.4 (a) Data bit. (b) PN sequence. (c) PN sequence generator.

5.4.1 Error probability :

Let, -1 be the transmitted data symbol. The received signal is given by

$$S_2(t) = -A_s\ PN(t)\ \cos\omega_o t + N_a(t) + I(t) \qquad (5.16)$$

where A_s is the amplitude of the signal and PN(t) is the pseudo noise sequence. The variables $N_a(T)$ and I(t) represent atmospheric noise and the power harmonic interfering tone respectively. The interfering signal with amplitude α_I and frequency ω_1 can be written as

$$I(t) = \alpha_I \cos(\omega_1 t + \theta_I) \qquad (5.17)$$

where θ_I is the phase angle of the interfering tone. The phase angle θ_I is a random variable which is assumed to be uniformly distributed over the range of $[0, 2\pi]$. The ratio α_I^2/A_s^2 indicates the strength of the interfering power in comparison to the signal power. In decibels (dβ) this ratio which is usually denoted by J/S, is given by

$$\frac{J}{S} = 20\log_{10}\left(\frac{\alpha_I}{A_s}\right) . \qquad (5.18)$$

Assuming a perfect synchronization for the carrier and the PN sequence, the receiver output $V_{s2}(T)$ can be written as

$$V_{s2}(T) = -A_s T + N_A(T) + g_I(T), \qquad (5.19)$$

where $-A_S T_s N_A(T)$ and $g_i(T)$ are the outputs due to the data symbol, the atmospheric noise and the interfering tone, respectively. The PDF for $N_A(T)$ is still given by (5.13), which has been obtained for a PSK receiver. In the present case, the multiplication of the received signal by the PN sequence results in phase shift keying during a data symbol, but the basic requirement that there must be equal number of positive and negative half cycles of the local carrier during the interval [0,T] remains the same as that of a PSK receiver. For a given phase angle $\theta_I = \theta$, the variable $g_i(T)$ is given by

$$g_i(T) = \alpha_I \int_0^T PN(t) \cos\left\{(\omega_1 - \omega_o)t + \theta\right\} dt$$

$$= \alpha_I B_s \sin\theta + \alpha_I B_c \cos\theta \qquad (5.20a)$$

where

$$B_s = \int_0^T PN(t) \sin(\omega_1 - \omega_o)t \qquad (5.20b)$$

$$B_c = \int_0^T PN(t) \cos(\omega_1 - \omega_o)t \ . \qquad (5.20c)$$

The variable $g_i(T)$ depends on the PN code used and the position of the interfering tone with respect to the carrier. We consider the case of $\omega_1 = \omega_o$ and hence one can write

$$B_s = 0; \quad B_c = \int_0^T PN(t)\, dt \qquad (5.21)$$

From (5.15), (5.20a) - (5.21), we get

$$g_I(T) = \alpha_I T_c \cos\theta \ . \tag{5.22}$$

The receiver output for $\theta_I = \theta$ is given by

$$V_{s2}(T)\Big|_{\theta_I = \theta} = -A_s T + N_A(T) + \alpha_I \cos\theta T_c \tag{5.23}$$

Hence, the conditional probability of error for $\theta_I = \theta$, can be written as

$$\text{Prob}\left[p_{e2}|\theta\right] = \text{Prob}\left[\left\{-A_s T + N_A(T) + \alpha_I \cos\theta\ T_c\right\} > 0\right] \tag{5.24a}$$

The unconditional probability of error p_{e2} is given by

$$p_{e2} = \frac{1}{2\pi}\int_0^{2\pi} \text{Prob}\left[p_{e2}|\theta\right]\, d\theta \tag{5.24b}$$

5.5 NUMERICAL RESULTS

For PSK receiver the bit error probability p_{e1} for a given signal to noise ratio (SNR $\triangleq E_b/N_o$, where $E_b = A_s^2\, T/2$) is computed in terms of the parameters λT and a new parameter g_x which is defined by the relation $V_p = g_x A_s T$. $A_s T$ is the receiver output due to a data bit while V_p is the output due to a single impulse. Thus g_x is a measure of the impulse strength in terms of the output due to a data bit. The parameter λT can be identified as the average number of impulses arriving during the interval [0,T].

Figures 5.5 to 5.7 give p_{e1} for different values of λT and g_x. The curve with $g_x = 0.0$ is for the case when there is no impulsive component. For g_x=0.1 and $\lambda T \leq 0.5$, the additional error rate due to the impulsive component is quite small. The performance degradation is within 0.5 dB of SNR. With this value of g_x if λT=1.0, the performance degradiation is within 1.5 dB. The amplitude g_x has much greater effect on the receiver performance than the parameter λT. This is because, if the number of pulses arriving at the receiver input increases, the output due to the pulses does not increase proportionally; there are cancellation effect. On the other hand an increase in g_x (λT fixed) does not lead to any further increase in the existing cancellation level. This can be seen by comparing different curves with same $g_x \lambda T$ product. This fact demonstrates that for a given impulse strength and arrival rate, the effect of the impulsive component on the receiver performance, can be reduced by increasing the integration time.

Fig. 5.8 describes the error probability p_{e2} for a direct sequence spread spectrum receiver in presence of an interfering tone at the carrier frequency. The PN code is derived from a maximal length shift register of 6 stages, resulting in a sequence length of 63. The receiver performance neither enhances nor deteriorates in presence of the atmospheric noise when there is no interfering signal; its performance is same as that of a PSK receiver. However, it provides strong immunity to the interfering signal. For example for J/S upto 10 dB, the peformance of the

receiver due to the intefering tone is marginally affected; the error degradation is within 0.2 dB of SNR. For J/S = 20 dB and $p_{e2} \simeq 10^{-5}$, this figure is within 1.5 dB.

5.6 A DISCUSSION ON THE ASSUMPTIONS MADE REGARDING NOISE MODEL

Two approximations have been made in this chapter for deriving the PDF for the impulsive component. These approximations are pessimistic in nature for the following reasons.

(i) The finite width pulses have been replaced by pure impulses. In the case of finite width pulses there will be cancellation effect by the oppositely polarized neighbouring half cycles of the local carrier. Because some part of the pulse may be on a positive half cycle and the remaining part on a negative half cycle, this will result in a reduced integrator output for the impulsive component.

(ii) The sinusoidal local carrier has been replaced by a rectangular wave form $C_s(t)$ to obtain the receiver output for the impulsive component in Eq. (5.9a). Since, the amplitude and frequency of $C_s(t)$ are equal to that of the original sinusoid, the receiver output values (in magnitude) are always greater or equal to those values which would have been obtained by the use of the pure sinusoid.

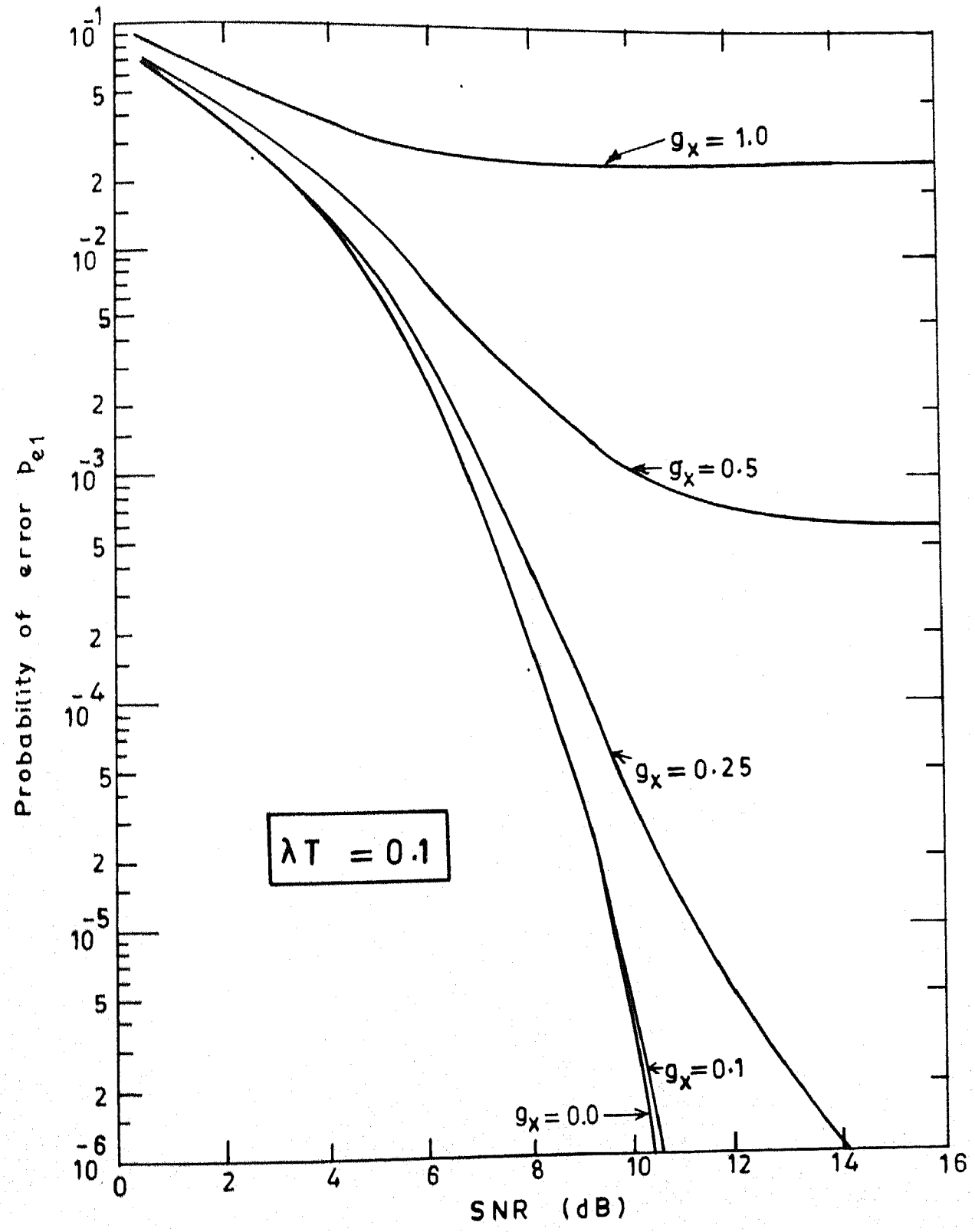

Fig.5.5 Performance of the PSK receiver in atmospheric noise

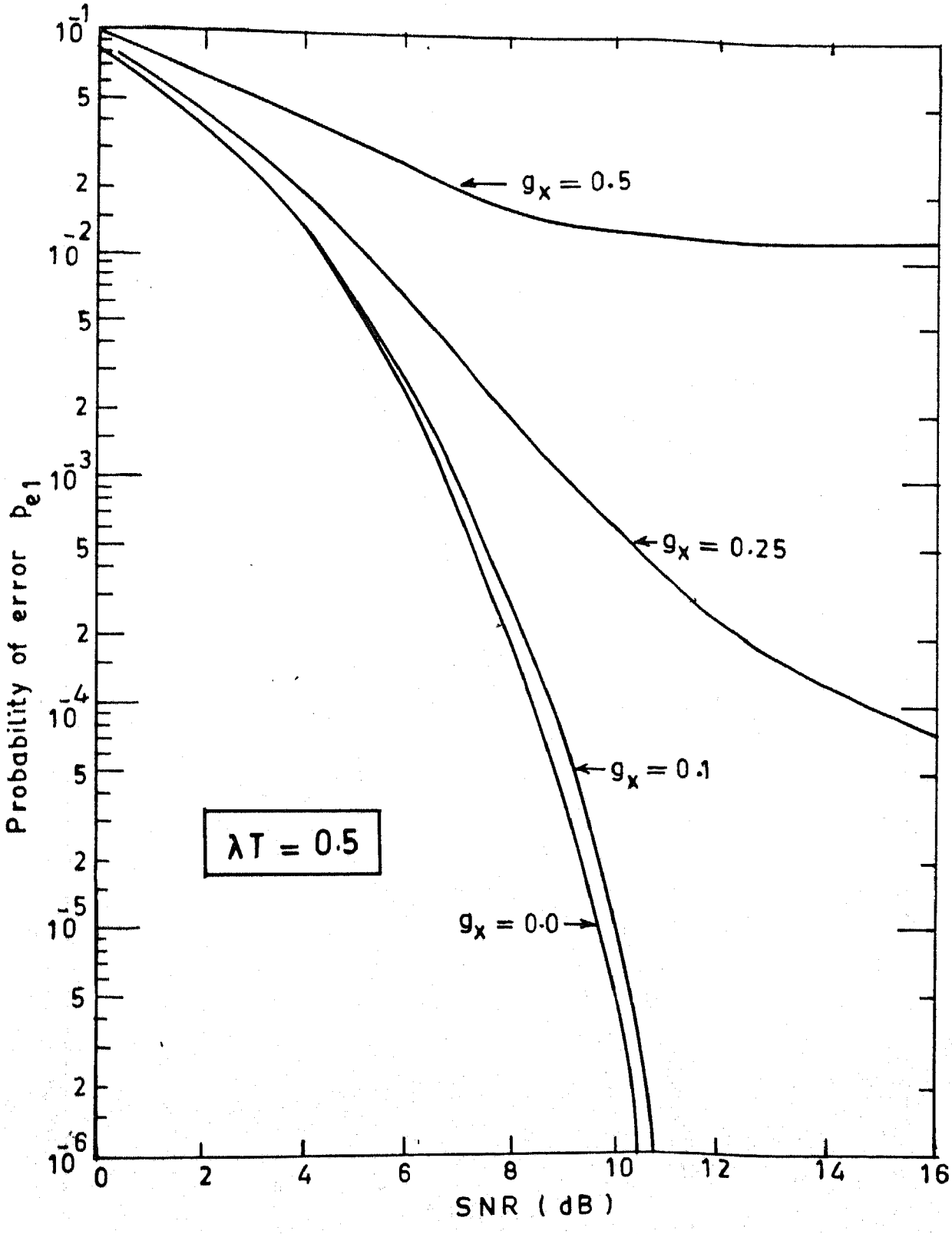

Fig. 5.6 Performance of the PSK receiver in atmospheric noise.

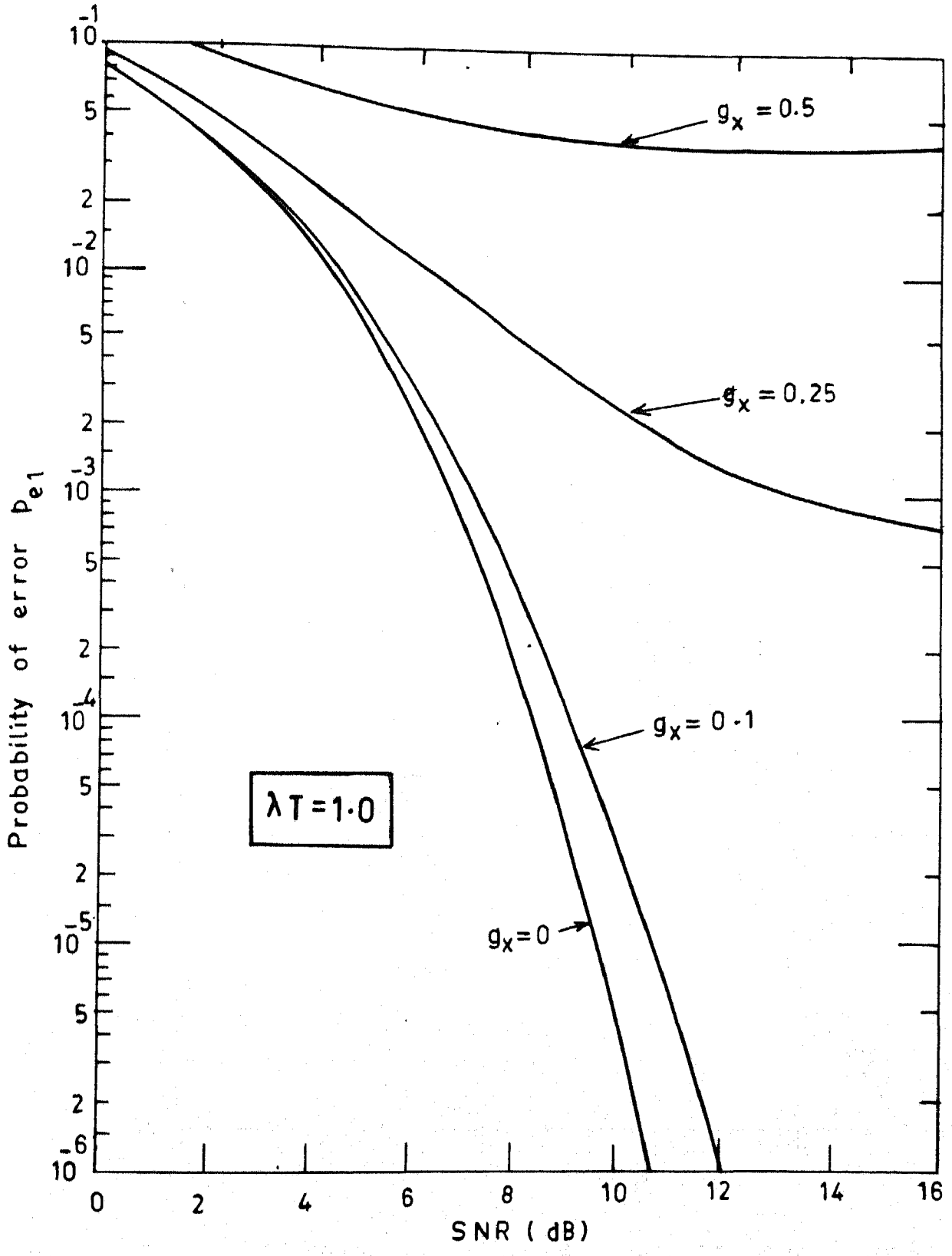

Fig.5.7 Performance of the PSK receiver in atmospheric noise.

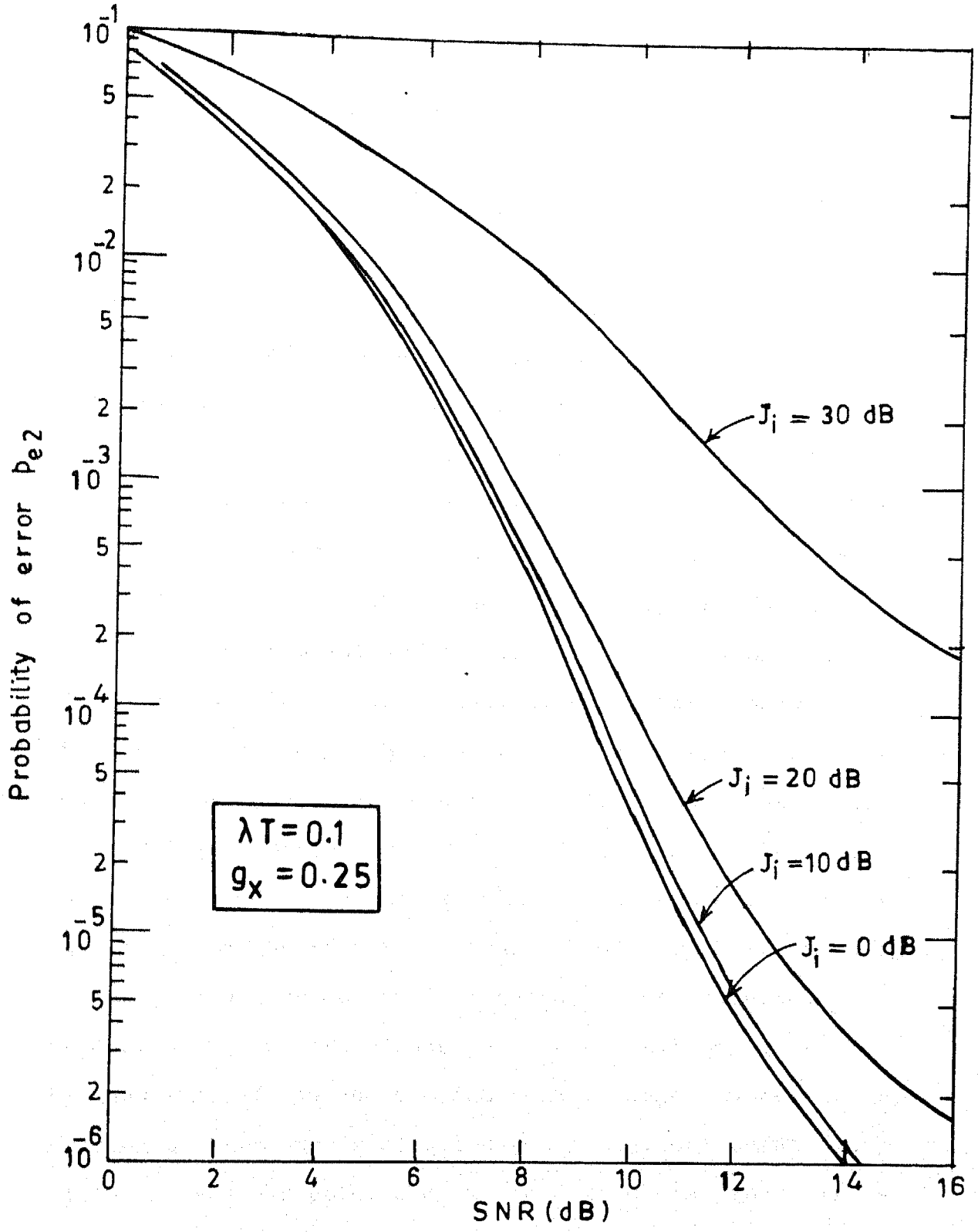

Fig. 5.8 Performance of the spread spectrum receiver in atmospheric noise and tone interference

CHAPTER 6

CONCLUSIONS

A loop antenna located on the earth surface and operating at VLF/ELF bands, used for underground mine communication, has been analysed by the method of moments. The analysis does not require any numerical integration as all integrations associated with the solution procedure have been expressed in closed forms. It has been found that as the loop diameter is increased (keeping other parameters fixed) behaviour of the loop i.e., variation of input admittance and current distribution change very rapidly when the magnitude of the input susceptance is greater than about seven times the value of the input conductance. This means, the transition from a small loop behaviour to that of a large loop is very rapid. With the change in current distributions, the field inside the earth also changes accordingly. For a small loop the vertical magnetic field component is almost independent of the relative angular position of the observation point with respect to the feed point of the antenna. For a large loop the magnitude of the fields depend both on radial distance from the loop axis and the angular position of the observation point. When there is a large variation in current distribution the radial component along the line joining the feed point and the loop axis is very large compared to radial or a vertical components of the magnetic field at any other angular positions. It is useful to predict how large a loop can be treated to be a small loop without going through the method of moments. A simple expression for this has been

developed. It is to be noted that it is possible to compute the input resistance of a small loop in free space by assuming that the loop carries an uniform current. However, it is not true for a loop antenna on the earth surface or one embedded in a dissipative medium. The reactive part of the input impedance for a small loop can be assumed to be same whether the loop is in free space or located on the earth surface.

A model for atmospheric noise which contains an impulsive component superimposed on a Gaussian background has been presented. Performance evaluation for the conventional as well as spread spectrum receiver with PSK signal format subjected to this noise has been discussed. It has been shown that same procedure is applicable for both conventional as well as spread spectrum receiver. It has been found that when the area under a pulse (impulse strength) associated with the impulsive component is less than one tenth of the area under a data bit, the performance degradation is within 0.5 dB of signal to noise ratio. This figure is based on the assumption that average arrival rate of impulses is ≤ 0.5 during the period of a data bit.

In the present investigation we have considered the earth as a homogeneous lossy half space. A better model will be to treat it as a stratified media. For a stratified medium it may not be feasible to express the potentials in a closed form. However, the potentials can be expanded in a series form by taking some approximations. There after the analysis of the antenna problem

can be carried out on similar lines as described in this investigation. Similarly, the self impedance for a small loop antenna over a stratified earth can be obtained.

In mine noise environment due to presence of strong interfering signals spread spectrum communication technique will be useful. Spread spectrum communication system can also be used for multiaccess capability using code division multiplexing. The performance analysis of the spread spectrum communication system in VLF/ELF bands will be along the usual lines as for high frequency environment, with the noise model developed in the present investigation being used in place of Gaussian noise.

REFERENCES

1. MURPHY, J.N.,and PARKINSON, H.E., "Underground mine communications", IEEE Proc., Vol.66, No.1, pp. 26-50, 1978.

2. LARGE, D.B., BALL, L., and FARSTAD, A.J., "Radio transmission to and from underground coal mines - theory and measurement", IEEE Trans., Vol. COM-21, No. 3, pp. 194-202, 1973.

3. GEYER, R.G., "Theory and experiments relating to electromagnetic fields of buried sources with consequences to communication and location", in Proc. Through-the-Earth Electromagnetics Workshop, pp. 20-33 (Colorado School of Mines, Golden, CO, Aug. 15-17, 1973) (NTIS PB 213-154/AS).

4. OLSEN, R.G., and FARSTAD, A.J., "Electromagnetic direction finding experiments for location of trapped miners", IEEE Trans., Vol. GE-11, pp. 178-185, 1973.

5. Westinghouse Georesearch Lab., "Electromagnetic location experiments in a deep hardrock mine", Bureau of Mines Contract HO242006, Sept. 1973 (NTIS PB 232-880/AS).

6. WAIT, J.R., and SPIES, K.P., "Electromagnetic fields of a small loop buried in a stratified earth", IEEE Trans., Vol. AP-21, No.5, pp. 717-718, 1971.

7. WAIT, J.R., and HILL, D.A., "Field of a horizontal loop of arbitary shape buried in two layer earth", Radio Sci., Vol. 15(5), pp. 903-912, 1980.

8. WAIT, J.R., "Electromagnetic fields of sources in lossy medium", Chapter 24 of Antenna Theory (Part 2), COLLIN, R.E., and ZUCKER, F.J., McGraw-Hill, New York, 1969.

9. KING, R.W.P., and HARRISON (Jr), C.W., "Antennas and Waves : A modern approach", MIT Press, Massachusetts, 1969.

10. KASSAM, S.A., "Signal detection in non-Gaussian noise", Springer-Verlag, New York, 1988.

11. OMURA, J.K., and SHAFT, P.D., "Modem performance in VLF atmospheric noise", IEEE Trans., Vol. COM-19, No.3, pp. 659-668, 1971.

12. FIELD (Jr), E.C., and LEWINSTEIN, M., "Amplitude-probability distribution model for VLF/ELF atmospheric noise", IEEE Trans., Vol. COM-26, No. 1, pp. 83-87, 1978.

13. PARHAMI, P., RAHMAT-SAMII, Y., and MITTRA, R., "An efficient approach for evaluating Sommerfeld integrals encountered in the problem of a current element radiating over lossy ground", IEEE Trans., Vol. AP-28, pp. 100-107, 1980.

14. MICHALSKI, K.A., "On the efficient evaluation of integrals arising in the Sommerfeld half space problem", IEE Proc., Vol. 132, Pt.H, No. 5, 1985.

15. DIXON, R.C., "Spread spectrum systems", Wiley Interscience, New York, 1976.

16. HOLMES, J.K., "Coherent spread spectrum systems", John Wiley, New York, 1982.

17. MILSTEIN, L.B., DAVIDOVICI, S., and SCHILLING, D.L., "The effect of multiple-tone interfering signals on a direct sequence spread spectrum communication system", IEEE Trans., Vol. COM-30, No. 3, pp. 436-446, 1982.

18. SNEDDON, I.N., "Fourier transform", Mc-Graw Hill, New York, 1951.

19. STINSON,D.C., "Intermediate Mathematics of Electromagnetics", Prentice Hall, New Jersey, 1976.

20. MITTRA, R., and LEE, S.W., "Analytical techniques in the theory of guided waves", Macmillan, New York, 1971.

21. SOMMERFELD, A., "Partial differential equations", pp. 24-267, Academic Press, 1949.

22. BANOS, A., "Dipole radiation in the presence of conducting half-space", Pergamon Press, New York, 1966.

23. WAIT, J.R., "Electromagnetic waves in stratified media", Pergamon Press, New York, 1962.

24. WAIT, J.R., "Wave propagation theory", Pergaman Press, New York, 1981.

25. PATRA, H.P., and MALLICK, K., "Geosounding principles : time-varying sounding, Part 2", Elsevier Scientific Pub. Company, New York, 1980.

26. MICHALSKI, K.A., "On the scalar potential of a point charge associated with a time-harmonic dipole in a layered medium", IEEE Trans., Vol. AP-35, No. 11, pp. 1299-1301, 1987.

27. MICHALSKI, K.A., SMITH, C.E., and BUTLER, C.M., "Analysis of a horizontal two-element antenna array above a dielectric half space", IEE Proc., Vol. 132, Pt. H, No. 5, 1985.

28. MILLER, E.K., POGGIO, A.J., BURKE, G.J., and SELDON, E.S., "Analysis of wire antennas in the presence of a conducting half-space, Part II. The horizontal antenna in free space", Can. J. Phys., Vol. 50, pp. 2614-2627, 1972.

29. SARKAR, T.K., "Analysis of arbitrarily oriented thin wire antennas over a plane imperfect ground", Arch. Elek. Ubertragungstech., Vol. 31, pp. 449-457, 1977.

30. MITTRA, R., PARHAMI, P., and RAHMAT-SAMII, Y., "Solving the current element problem over lossy half-space without Sommerfeld integrals", IEEE Trans., Vol. AP-27, pp. 778-782, 1979.

31. KARWOWSKI, A., "Low-frequency approach to the problem of a horizontal wire antena above an imperfect-ground," IEE Proc.H, Microwaves, Opt. & Antennas, Vol. 131, pp. 214-216, 1984.

32. HARRINGTON, R.F., "Matrix methods for field problems", IEEE Proc., Vol. 55, No.2, pp. 136-149, 1967.

33. RAHMAT-SAMII, Y., MITTRA, R., and PARHAMI, P., "Evaluation of Sommerfeld integrals for lossy half-space problems", Electromagnetics, pp. 1-28, 1981.

34. JOHNSON, W.A., and DUDLEY, D.G., "Real axis integration of Sommerfeld integrals: source and observation points in air", Radio Sci., Vol. 18, pp. 175-186, 1983.

35. LINDELL, I.V., and ALANEN, E., "Exact image theory for the Sommerfeld half-space problem, Part I : Vertical magnetic dipole", IEEE Trans., AP-32, pp. 126-133, 1984.

36. PRUDNIKOV, A.P., BRYCHKOV, Yu.A., and MARICHEV, O.I., "Integrals and series", Gordon and Breach Science Publishers, New York, 1986.

37. POPOVIC, B.D., DRAGOVIC, M.B., and DJORDJEVIC, A.R., "Analysis and synthesis of wire antennas", Wiley Interscience, New York, 1982.

38. PLONSEY, R., and COLLIN, R.E., "Principles and applications of electromagnetic fields", McGraw-Hill, New York, 1961.

39. MACLEAN, T.S.M., "Principles of antennas: wire and aperture", Cambridge University Press, London, 1986.